NTNU

Norwegian University of
Science and Technology

Sensorless Control of a 6-phase Induction Machine

Emil Hansen Mørkved

Master of Energy and Environmental Engineering
Submission date: June 2018
Supervisor: Roy Nilsen, IEL

Norwegian University of Science and Technology
Department of Electric Power Engineering

Problem Description

To increase the rating of low voltage drives, as well as increasing the redundancy of such drives, multi-phase machines are interesting alternatives. In this case a 6-phase induction machine shall be investigated.

To be able to control these drives without a position- and speed-sensor, sensorless control shall be implemented. This will require an accurate flux-model for the machine.

In the project thesis at the fall semester 2017 the candidate developed a simulation model for sensorless control of the 6-phase Induction Motor. This simulation model shall be used to analyze and possibly improve the behavior in the lower speed region. Using the voltage model for estimation of the stator flux linkage vector a correction algorithm is necessary, but combination of other models shall be investigated as well for low speed operation. The performance of the control system depends on the accuracy of the parameters of the flux model. The main focus shall be:

1. Sensorless control at low speed operation
2. Parameter sensitivity of the flux model
3. Combination of flux models

In this Master project Simulink with the Power System Library shall be used.

Preface

This master thesis was the final part of the degree MSc. in Electric Power Engineering during the spring semester of 2018 for the author under the Department of Electric Power Engineering at NTNU.

I would like to thank my supervisor Prof. Roy Nilsen for insightful discussions, thoughtful advice and quick answers whenever necessary during my work in this thesis. In addition, I would like to give a special thank to my colleague Magnus Bolstad for discussions, explanations and support during my work. Finally, I thank all my coworkers, professors and organizers to make this thesis a reality.

Abstract

The topic in this master thesis is regarding parameter sensitivity analysis for a six-phase induction motor using speed-sensorless control. Using the voltage model the inputs of the flux model are voltage and current measurements from the inverters. The flux model estimates the stator and rotor flux linkage space vectors to control the motor and follow the torque reference. The parameter sensitivity analysis is presented both for the stationary and dynamic operation in the voltage model and only for the stationary operation in the current model. The current model is not used in sensorless control, but to improve the reliability of the flux model a combination of the voltage and current model was investigated. To still operate sensorless the estimated rotor flux linkage angle was an input in the current model. It was revealed that the voltage model operates unreliably in low-speed operation if the stator resistance was estimated wrongly. This is verified in both the stationary and dynamic parameter sensitivity analysis. In the dynamic analysis, the drifting phenomenon of the flux estimations was investigated. A correction method presented first by Niemelä in his doctor thesis [5] used on a synchronous machine was explained and experimented under simulation for the six-phase induction motor. It was evident that the correction method was an improvement for the flux model, but some drawbacks were revealed. Under perfect estimated parameters the correction method functioned as a disturbance for the flux model and small stationary errors in flux amplitude and angle estimation were present when the estimated stator resistance was not correct. In addition, two improved methods for estimating the rotor flux linkage amplitude were presented, and finally, an alternative method for correcting the voltage model was developed using a closed loop observer feedback in the flux model.

Contents

1 Introduction **1**

2 Modeling of a Six-Phase Induction Machine **3**

3 Control Strategy and Simulation Method **5**
3.1 Field-Oriented Control 5
3.2 Decouple Equations for a Six-Phase Induction Motor 7
3.3 Simulation Model 7

4 Flux Models **9**
4.1 The Voltage Model 9
4.2 The Current Model 10

5 Deviation in Parameters and Measurement Errors **12**
5.1 Resistance Deviation 12
5.2 Reactance Deviation 12
5.3 Error in Measurements 12

6 Stationary Parameter Sensitivity Analysis **14**
6.1 Voltage Model 14
6.1.1 Stator Flux Linkage Estimation 14
6.1.2 Rotor Flux Linkage Estimation 20
6.1.3 Torque Estimation 29
6.2 The Current Model 31
6.2.1 Rotor Flux Linkage Estimation 31
6.2.2 Torque Estimation 34
6.2.3 Stator Flux Linkage Estimation 34

7 Dynamic Parameter Sensitivity Analysis and Drifting **38**
7.1 DC Magnetization 41
7.2 Torque/Speed Reference Change 42
7.3 Frequency Dependency 43
7.4 Crossing Zero Speed and Low-Speed Operation 45
7.5 Moment of Inertia 50
7.6 Correction Method Against Drifting 51

8 Speed-Sensorless Operation Performance **54**
8.1 Corrector block 54
8.1.1 Disturbance When Estimated Stator Resistance Is Correct . . 54

8.1.2 Stationary Error When The Stator Resistance Estimation Is Not Correct . . . 56
8.1.3 Tuning of The Corrector Block . . . 56
8.2 Improving Rotor Flux Linkage Amplitude Estimation . . . 61
8.3 Closed Loop Observer . . . 67
8.3.1 Comparing The Combination Method With Correction and The Closed Loop Observer Method . . . 68
8.3.2 Problems With The Closed Loop Observer Method . . . 71
8.4 Possible Improvements Not Investigated . . . 72

9 Summary **73**

10 Conclusion and Further Work **75**

A Machine Parameters **79**

B Base values **80**

C Control parameters **81**

D Derivation of Error-Equations in Sensitivity Analysis **82**
D.1 Voltage Model . . . 82
D.1.1 Amplitude Error Stator Flux Linkage Estimate . . . 82
D.1.2 Angle Error Stator Flux Linkage Estimate . . . 83
D.1.3 Amplitude Error Rotor Flux Linkage Estimate . . . 84
D.2 Current Model . . . 84
D.2.1 Angle Error Rotor Flux Linkage Estimate . . . 84

E Modelling from Project thesis [15] **86**
E.1 Introduction . . . 86
E.2 Modelling in Double Synchronus Reference Frame . . . 87

F Estimating the Rotor Flux Linkage Angle θ **94**

G Additional Simulations **96**

H Matlab Code Stationary Parameter Sensitivity Analysis **98**

List of Figures

2.1 Double Synchronous Frame Modeling[15] 4
3.1 The principle of field oriented control 6
6.1 Stator Flux linkage estimation with $\hat{r}_s = 1.2r_s$ 14
6.2 $\hat{\psi}_{s1}^{s1}$ and ψ_{s1}^{s1} for high speed with $\hat{r}_s = 1.5r_s$ 15
6.3 $\hat{\psi}_{s1}^{s1}$ and ψ_{s1}^{s1} for low speed with $\hat{r}_s = 1.5r_s$ 16
6.4 How the error evolves as n is approaching $-f_r$ 17
6.5 The amplitude error increases as $\hat{f}_\psi$ goes towards zero 17
6.6 How the $\hat{\psi}_{s1}^{s1}$ error variate with electrical torque for different speeds . 19
6.7 Error in the angle stator flux linkage estimation for different values of $\hat{r}_s$ at $m_e = 0.75$ pu 21
6.8 The estimated stator flux linkage around $f_\psi = 0$ 21
6.9 Rotor Flux linkage estimation with $\hat{r}_s = 1.2r_s$ 22
6.10 Rotor Flux linkage estimation with $\hat{x}_\sigma = 1.1x_\sigma$ 23
6.11 Rotor Flux linkage estimation with $\hat{x}_{s\sigma} = 1.1x_{s\sigma}$ 23
6.12 Rotor Flux linkage estimation with $\hat{x}_\sigma = 1.1x_\sigma$ and $\hat{x}_{s\sigma} = 1.1x_{s\sigma}$ . . . 24
6.13 Sensitivity to the stator resistance, r_s, for the rotor flux linkage angle estimate, $\hat{\theta}_R^{s1}$, at low speed 25
6.14 Sensitivity to the stator resistance, r_s, for the rotor flux linkage angle estimate, $\hat{\theta}_R^{s1}$, at low speed when $\hat{\xi}_{s1}^{s1} = \xi_{s1}^{s1}$ and $m_e = 0.75$ pu 27
6.15 Sensitivity to the leakage reactance, x_σ, for the rotor flux linkage angle estimate, $\hat{\theta}_R^{s1}$, and dependency of electrical torque. 27
6.16 Sensitivity of $\hat{\psi}_R$ for the parameters at low speed 28
6.17 Sensitivity of $\hat{\psi}_R$ by wrong estimation of x_σ. Here is $\hat{r}_s = r_s$ 29
6.18 Estimation of torque with $\hat{r}_s = 1.2r_s$ 30
6.19 Estimation of torque with different stator resistance estimation at low speed using the voltage model 30
6.20 Estimation of rotor flux linkage amplitude and angle with $\hat{r}_R = 1.2r_R$ using the current model 31
6.21 Estimation of rotor flux linkage amplitude and angle with $\hat{x}_H = 1.2x_H$ using the current model 32
6.22 $\hat{\theta}_R^{s1}$ error with different values of $\hat{r}_R$ vs electrical torque in motor . . . 33
6.23 Error in estimation of torque using the current model with deviation in rotor resistance and main reactance 35
6.24 Error in estimation of stator flux linkage using the current model with $\hat{r}_R = 1.2r_R$ 36
6.25 Error in estimation of stator flux linkage using the current model with $\hat{x}_H = 1.1x_H$ 36
7.1 Stator flux linkage vector measured vs estimated and drifted[15] . . . 39

7.2 The principle of drifting as consequence of a wrongly estimated stator resistance 40
7.3 DC magnetization with a wrongly estimated main reactance. 42
7.4 Step change in electrical torque reference which produces changes in the drifting of the stator flux linkage estimation 44
7.5 Frequency dependency at the dynamic start 46
7.6 Drifting of the $\hat{\psi}_{s1}$ space vector at zeros speed crossing with $\hat{r}_s = 0.5r_s$. The black circle is from the measured stator flux linkage space vector 47
7.7 Estimated stator flux linkage amplitude and angle error changes for every crossing over zero speed 47
7.8 Drifting of $\hat{\psi}_{s1}$ and $\hat{\psi}_R$ as a consequence of a wrongly estimated stator resistance. At around zero speed the error gets integrated for a long time in the same direction and the estimated stator flux linkage becomes unstable 48
7.9 Figure 7.8 shown with referenced time and speed 49
7.10 Drifting of estimated stator and rotor flux linkage space vectors as a consequence of wrongly estimated stator resistance and a change in speed 50
7.11 Speed change and causes drifting. The colors match with figure 7.10 and it is observed that a slower rise in speed causes more drifting. . . 51
7.12 Drifting with different values of moment of inertia. Here $\hat{r}_s = 0.5r_s$. . 51
7.13 Block diagram correction method against drifting[15] 53
7.14 Adaptive calculation of k_T 53
8.1 XY plot of the drifting of estimated stator flux linkage and correction. $\hat{r}_s = 1.5r_s$. 54
8.2 Amplitude and angle error vs time with and without correction. $\hat{r}_s = 1.5r_s$. 55
8.3 With and without correction block for $\hat{r}_s = r_s$ 55
8.4 Stationary error from the corrector block as a function of the estimated stator resistance 57
8.5 Tuning of corrector block 59
8.6 Tuning of $k_{corr,0}$ in corrector block 60
8.7 Using a filter solution to improve estimate of rotor flux linkage amplitude, here referred to as the filter method 61
8.8 Combination of the voltage model and current model for improving rotor flux linkage estimate, here referred to as the combination method 62
8.9 Three different estimation models for the rotor flux linkage amplitude: normal voltage model, filtered voltage model and a combined model . 63
8.10 Combination model vs filter solution with $\hat{r}_s = r_s$ and $\hat{r}_R = r_R$ 65
8.11 Combination model vs filter solution with $\hat{r}_s = 1.2r_s$ and $\hat{r}_R = 1.2r_R$. 66

8.12 Alternative method for correcting drifting using a closed loop observer feedback method 67
8.13 Closed loop feedback observer method vs Combination method with correct parameter estimation 70
8.14 Closed loop feedback observer method vs Combination method with $\hat{r}_s = 1.2r_s$ and $\hat{r}_R = 1.2r_R$ 71
E.1 Double Synchronous Frame Modelling 87
E.2 Transforming to the d-q-0 rotating reference frame 90
E.3 d axis equivalent circuit in per unit 92
E.4 q axis equivalent circuit in per unit 93
F.1 Obtaining the rotor flux linkage space vector 94
G.1 Closed loop feedback observer method with $\hat{r}_s = 0.8r_s$ and $\hat{r}_R = 0.8r_R$ 96
G.2 Closed loop feedback observer method with $\hat{r}_s = 1.5r_s$ and $\hat{r}_R = 1.5r_R$ 97

List of Tables

1 Parameters 79
2 Base values 80
3 Control Parameters 81

Acronyms

Alternating current (AC)
Artificial Neural Network (ANN)
Adaptive speed observer (ASO)
Direct Current (DC)
Dynamic Speed Estimation (DSE)
High Frequency Injection (HFI)
Model Reference Adaptive System (MRAS)
Proportional Integral (PI)
Phase-Lock Loop (PLL)
Permanent Magnet (PM)
Pulse Width Modulator (PWM)
Rotor Slot Harmonics (RSH)
Space Vector (SV)

Nomenclature

Symbol

γ	Voltage angle
ω_n	Rated angle speed, electrical
ψ	Flux linkage [pu]
σ	Conductivity $[S/m]$
θ	Rotor flux linkage angle
ε	Current angle
ξ	Stator flux linkage angle
A	Area $[m^2]$
f_r	Slip frequency [pu]
f_ψ, f_s	Synchronous frequency [pu]
i	Current [pu]
J	Total moment of inertia of drive referred to the machine side
j	Imaginary unit
k_{corr}	Correction factor
l	Length $[m]$
m_e	Electrical torque motor [pu]
m_L	load torque [pu]
n	Rotor speed [pu]
r	Resistance [pu]
T_r	Rotor time constant

T_{filter} Time constant filter

T_{samp} Sampling time $[s]$

T_{zero} Time constant zero

u Voltage [pu]

x Reactance [pu]

S_N Rated Apparent Power $[VA]$

Subscript

α α axis

β β axis

σ leakage

d direct axis

ff feed-forward

h main

MC Current model

MV Voltage model

q quadrature axis

r rotor

s stator

filt Filtered value

Superscript

$\hat{}$ Estimation

ψ_{s1} Referred to stator flux linkage axis

R Referred to rotor flux linkage axis

$s1$ Referred to s1 axis

1 Introduction

In 1972 Blasche introduced the idea of field-oriented vector control and the applications used for AC machines increased rapidly after this discovery. Earlier, due to its straightforward control strategy, DC machines were favored in most applications. Now with the field-oriented vector control one could in principle control the AC machine like the DC machine. Some decades later the performance of power electronic converters and the development of microelectronics and digital signal processing reached new higher standards. Then one started investigating the possibility to remove the speed sensor for the rotor and rely on speed estimators instead. This control strategy has been the standard the last decades and is referred sensorless control in the literature. The sensorless control's benefits compared to its counterpart speed sensor control are reduced cost due to the lack of a speed sensor, increased reliability, fewer maintenance requirements and a possibility to work in a hostile environment where speed sensor cannot[6].

Despite all its advantages, sensorless control experience some challenges that have been difficult to solve for the engineers worldwide. The problems referred to as drifting and DC offset in the open integration of Faraday's law as a result of parameter deviations and measurement errors, is still a big problem in the estimation of the flux linkages. Besides, running at low speed and especially driving through zero speed is considered an enormous challenge, and much attention is given to improve the operation at low speed. Today there exists a tremendous amount of strategies to improve this operation which is categorized in [14]: model reference adaptive-control system (MRAS) method, dynamic speed estimation (DSE) method, artificial neural networks (ANMs), adaptive speed observer (ASO) method, proportional-integral (PI) regulator method, high frequency injection (HFI) method, and rotor slot harmonic (RSH) method.

In some applications, multi-phase machines are interesting alternatives compared to the more conventional 3-phase machines. The multi-phase machines offer advantages like reduced rotor harmonic currents, improved reliability, reduced current stress for the converters without a reduction in power (the principle of power splitting)[10][11][13].

This master thesis introduces the modelling of the six-phase induction machine in section 2, the control strategy in section 3, the flux models in section 4 and the deviation in parameters in section 5. The main topic of this master thesis continues in section 6 and 7 with the parameter sensitivity analysis of the two most basic flux models: the voltage model and the current model. The sensitivity analysis is both

in steady state and during dynamics, but with extra attention on the voltage model and its parameter sensitivity to the stator resistance at low speed. The stationary parameter sensitivity analysis is investigated in section 6 and the dynamic in section 7. The simulations in sensorless operation are done using a machine model in MATLAB Simulink and presented in section 8. Also, improvements in the control performance and the flux model are investigated in this section. My supervisor Prof. Roy Nilsen developed the machine model, and it was adjusted by myself. Two drifting correction methods are presented and analyzed. The correction method, based on a filter solution from the square of the stator flux linkage amplitude estimation, presented first by Niemelä[5], is analyzed and simulated. Finally, a model based on a combination of the voltage model and current model with a closed loop feedback correction term in the voltage model, developed by the author, is analyzed and simulated.

2 Modeling of a Six-Phase Induction Machine

The induction motor is an AC machine fed by alternating current to the stator windings producing a rotating magnetic field that forces the rotor to rotate by electromagnetic induction. The rotor can be a wound-rotor type where the rotor is made up of windings or a squirrel cage rotor with short-circuited conducting bars.

The full modeling was presented in the project thesis of the author[15] and done in the master thesis of Nebrom[10], and only the final results are presented here. If the reader is interested, the modeling is added in the Appendix E. To summarize the physical modeling is done in a double synchronous reference frame with the stator consisting of two three-phase pairs separated by 30 electrical degrees and the phases separated by 120 electrical degrees. Figure 2.1 shows this. The transformation to the synchronously rotating d-q-0 reference frame is done by Clarke's and Park's transformation to make the inductance's value independent of rotor position and hence make the control more manageable. The assumptions done in the modeling can be summarized as[15][10][8]:

1. The stator windings produce a sinusoidally distributed magnetic field around the air-gap in the machine. Hence only the fundamental component of the field is modeled.

2. The stator windings are equal but oriented in different directions of winding axes.

3. Resistances and inductances are independent of temperature and frequency and are known.

4. Magnetic saturation, hysteresis and eddy currents are neglected.

5. It is possible to model the rotor as a wound rotor type.

The final model of the six-phase induction motor in d-q-0 synchronously rotating reference frame in per unit is described by these equations:

$$\begin{aligned}
u_{sd1} &= r_s i_{sd1} + \frac{1}{\omega_n}\frac{d\psi_{sd1}}{dt} - f_k\psi_{sq1}, \quad u_{sq1} = r_s i_{sq1} + \frac{1}{\omega_n}\frac{d\psi_{sq1}}{dt} + f_k\psi_{sd1} \\
u_{sd2} &= r_s i_{sd2} + \frac{1}{\omega_n}\frac{d\psi_{sd2}}{dt} - f_k\psi_{sq2}, \quad u_{sq2} = r_s i_{sq2} + \frac{1}{\omega_n}\frac{d\psi_{sq2}}{dt} + f_k\psi_{sd2} \\
0 &= r_r i_{rd} + \frac{1}{\omega_n}\frac{d\psi_{rd}}{dt} - f_r\psi_{rq}, \qquad 0 = r_r i_{rq} + \frac{1}{\omega_n}\frac{d\psi_{rq}}{dt} + f_r\psi_{rd}
\end{aligned} \tag{2.1}$$

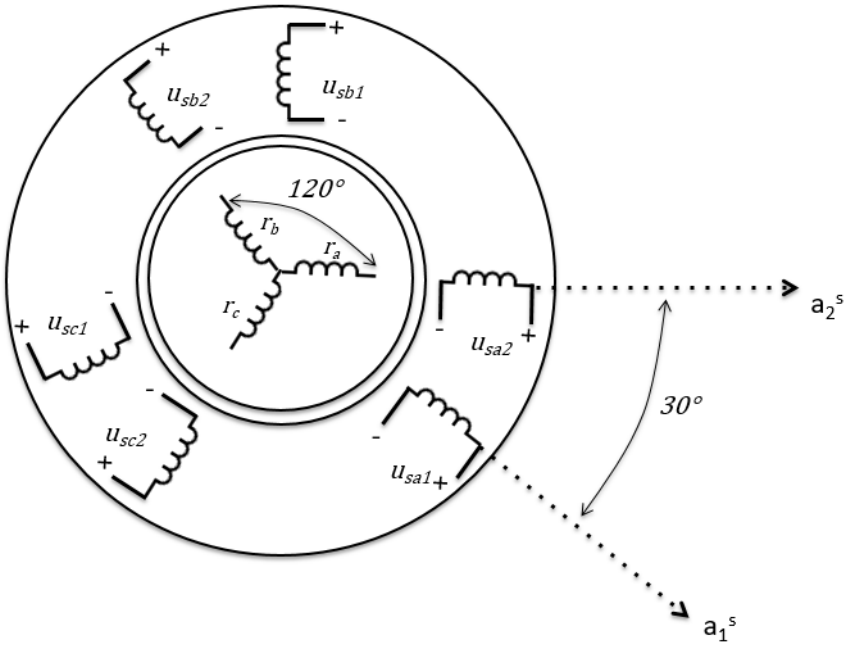

Figure 2.1: Double Synchronous Frame Modeling[15]

$$\begin{aligned}
\psi_{sd1} &= x_s i_{sd1} + x_h i_{sd2} + x_h i_{rd}, & \psi_{sq1} &= x_s i_{sq1} + x_h i_{sq2} + x_h i_{rq} \\
\psi_{sd2} &= x_h i_{sd1} + x_s i_{sd2} + x_h i_{rd}, & \psi_{sq2} &= x_h i_{sq1} + x_s i_{sq2} + x_h i_{rq} \\
\psi_{rd} &= x_h i_{sd1} + x_h i_{sd2} + x_r i_{rd}, & \psi_{rq} &= x_h i_{sq1} + x_h i_{sq2} + x_r i_{rq}
\end{aligned} \tag{2.2}$$

$$\begin{aligned}
m_e &= \frac{\psi_{rq} i_{rd} - \psi_{rd} i_{rq}}{2}, \quad T_m \frac{dn}{dt} = m_e - m_L, \quad T_m = \frac{J\Omega_N^2}{S_N} \\
f_r &= f_k - n, \qquad f_k = \frac{\omega_k}{\omega_n}, \qquad f_r = \frac{\omega_r}{\omega_n}
\end{aligned} \tag{2.3}$$

3 Control Strategy and Simulation Method

3.1 Field-Oriented Control

The idea behind field-oriented control is to control the motor torque and the motor flux separately as for the DC machine. By field-oriented control, the controlling axis system is fixed to some of the machine's flux linkages. When controlling an induction machine, the rotor flux linkage is usually the preferred flux linkage as the rotor flux linkage does not change quickly due to transients[4]. For the six-phase induction motor one ends up with the following basic control equations in the rotor field-oriented control:

$$\psi_{Rd} = \psi_R, \qquad \psi_{Rq} = 0, \qquad \frac{d\psi_{Rq}}{dt} = 0 \tag{3.1}$$

$$\psi_R = x_H \cdot (i_{sd1} + i_{sd2}) \tag{3.2}$$

$$m_e = \psi_R \cdot (i_{sq1} + i_{sq2}) \tag{3.3}$$

The rotor flux linkage is preferred constant just below 1 pu to control the torque by varying the quadrature component of the currents. The direct component of the current controls the rotor flux linkage and hence is held constant(if one neglect the DC magnetization and field-weakening operation). Figure 3.1 shows the principle.

The motor control is speed or torque controlled, but in this thesis, the focus is the torque control. With the torque control, the electrical torque reference gives the quadrature component reference of the current by equation 3.3. The direct component reference of the current is calculated from a flux controller. The reference current is the input in the current controller that is the inner control of the control structure. The current controller controls the real current in the machine to follow the reference current. The output of the current controller gives a voltage reference for the PWM modulator which enables the best duty ratio according to this reference. This signal is sent to the inverters that supply the motor with the stator voltage.

It is expensive and not practical to measure the rotor flux linkage and its position, and hence the performance of the motor control highly depends on the estimation of these variables. For estimating the rotor flux linkage SV one uses different models which are sensitive to various parameters. The models discussed in the sensitivity analysis here are the voltage model and the current model. Section 6 and 7 present the parameter sensitivity analysis both stationary and dynamic for the voltage model. The current model is analyzed only in the steady state case as the dynamics of the voltage model and the phenomenon of drifting is more interesting. The current model is generally

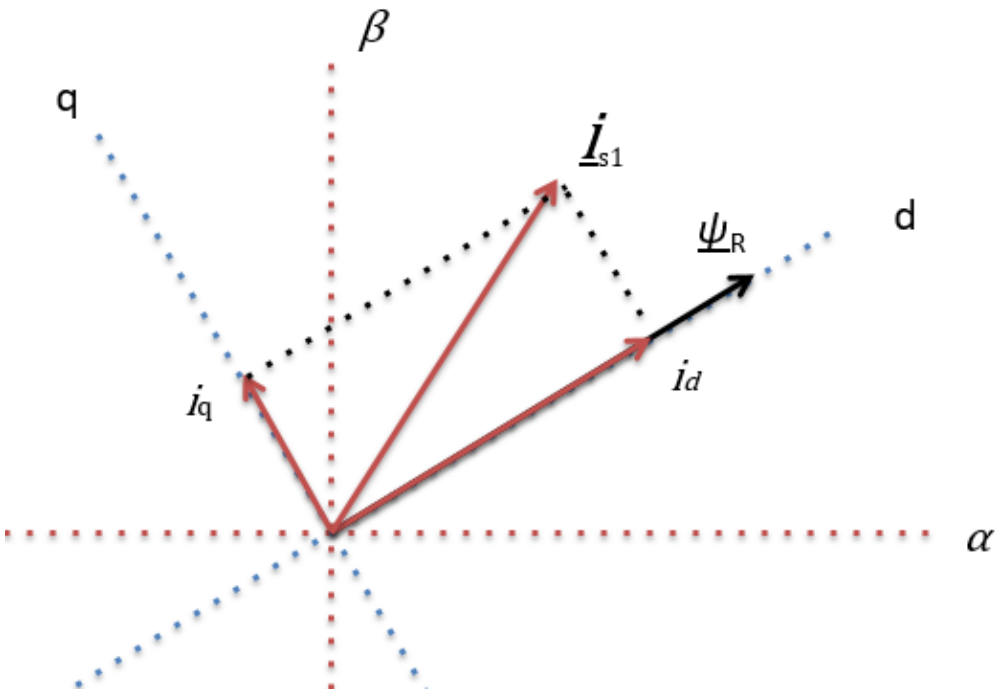

Figure 3.1: The principle of field oriented control

not speed-sensorless, but later when the sensorless operation is discussed, a solution with a combination of the voltage and the current model shows great promise. In this combination the operation is still speed-sensorless since the estimated rotor flux linkage position from the voltage model is the input in the current model.

The choice of d-q-0 reference frame following the rotor flux linkage space vector has an impact on the flux equations in equation 2.2:

$$\begin{aligned} \psi_{sd1} &= x_\sigma i_{sd1} + (x_\sigma - x_{s\sigma}) i_{sd2} + \psi_R, & \psi_{sq1} &= x_\sigma i_{sq1} + (x_\sigma - x_{s\sigma}) i_{sq2} \\ \psi_{sd2} &= x_\sigma i_{sd2} + (x_\sigma - x_{s\sigma}) i_{sd1} + \psi_R, & \psi_{sq2} &= x_\sigma i_{sq2} + (x_\sigma - x_{s\sigma}) i_{sq2} \\ \psi_r &= x_h i_{sd1} + x_h i_{sd2} + x_r i_{rd}, & 0 &= x_h i_{sq1} + x_h i_{sq2} + x_r i_{rq} \end{aligned} \tag{3.4}$$

Where:

$$x_\sigma = x_s - \frac{x_h^2}{x_r}, \qquad x_{s\sigma} = x_h - x_s, \qquad \psi_R = \frac{x_h}{x_r}\psi_r = \frac{\psi_r}{1+\sigma_r} \tag{3.5}$$

3.2 Decouple Equations for a Six-Phase Induction Motor

It can be shown that [10]:

$$\frac{d\psi_R}{dt} = -\frac{\psi_R}{T_r} + \frac{x_H}{T_r}(i_{sd1} + i_{sd2}), \qquad f_r = \frac{x_H(i_{sq1} + i_{sq2})}{T_r \omega_n \psi_R} \tag{3.6}$$

Where

$$x_H = \frac{x_h}{1+\sigma_r}, \qquad T_r = \frac{x_r}{\omega_n r_r}, \qquad \sigma_r = \frac{x_r}{x_h} \tag{3.7}$$

Then modifying the stator voltage equations (equation 2.1) one can divide them in one part used as the control equations for the current controller, and one decouple part (feed-forward) that is used to improve the calculation of the voltage reference.[10][15] The decouple equations for a 6-phase induction motor are written[15]:

$$\begin{aligned}
u_{sd1,ff} &= \frac{u_{sd2}}{1+\sigma'_s} - \frac{r''_s}{1+\sigma'_s} i_{sd2} - \frac{\sigma'_s}{1+\sigma'_s}\frac{\psi_R}{\omega_n T_r} - f_k x'_s i_{sq1} \\
u_{sq1,ff} &= \frac{u_{sq2}}{1+\sigma'_s} - \frac{r''_s}{1+\sigma'_s} i_{sq2} + \frac{\sigma'_s}{1+\sigma'_s} n\psi_R + f_k x'_s i_{sd1} \\
u_{sd2,ff} &= \frac{u_{sd1}}{1+\sigma'_s} - \frac{r''_s}{1+\sigma'_s} i_{sd1} - \frac{\sigma'_s}{1+\sigma'_s}\frac{\psi_R}{\omega_n T_r} - f_k x'_s i_{sq2} \\
u_{sq2,ff} &= \frac{u_{sq1}}{1+\sigma'_s} - \frac{r''_s}{1+\sigma'_s} i_{sq1} + \frac{\sigma'_s}{1+\sigma'_s} n\psi_R + f_k x'_s i_{sd2}
\end{aligned} \tag{3.8}$$

Here subscript ff means feed-forward and in equation 3.8 the parameters are explained as:

$$\begin{aligned}
\sigma'_s &= \frac{x_{s\sigma}}{x_\sigma - x_{s\sigma}} \\
x'_s &= x_\sigma(1 - (\frac{x_\sigma - x_{s\sigma}}{x_\sigma})^2) = x_\sigma(1 - \frac{1}{(1+\sigma'_s)^2}) \\
r'_s &= r_s + \frac{x_{s\sigma}}{x_\sigma} r_R = r_s + \frac{\sigma'_s}{1+\sigma'_s} r_R \\
r''_s &= r_s - \frac{x_{s\sigma}}{x_\sigma - x_{s\sigma}} r_R = r_s - \sigma'_s r_R \\
r_R &= \frac{x_H}{\omega_n T_r} = \frac{r_r}{(1+\sigma_r)^2}
\end{aligned} \tag{3.9}$$

3.3 Simulation Model

The simulations done in this thesis is done in MATLAB Simulink with the ode23tb solver with a maximum step time of 100μs, and the solver reset method set to robust. The power system library is used. My supervisor, Prof. Roy Nilsen, implemented the

machine model, converters, PWM modulator, load model and some controllers before the project thesis started the fall semester of 2017. In the project thesis, modifications were done by the author. Also, in work for this master thesis, some new adjustments were made to improve the motor control performance.

4 Flux Models

4.1 The Voltage Model

In the voltage model, the input variables are an estimation of the stator voltage from the measured dc link voltage in the inverter or a direct measurement of the voltages and the measured current in the inverter. In this thesis, it is assumed that the voltage is directly measured. Using the Faraday's law one can obtain an estimation of the stator flux linkage SV:

$$\underline{\hat{\psi}}_{s1} = \int_{t_0}^{t} (\underline{u}_{s1} - \hat{r}_{s1}\underline{i}_{s1})dt \tag{4.1}$$

As seen from equation 4.1 the stator resistance needs to be estimated, and if this estimation is wrong, one ends up with a wrong stator flux linkage SV. Generally, the voltage SV and the current SV are not in phase in an induction machine because of slip. Hence an error in the stator resistance estimation gives both errors in the estimated amplitude and angle of the stator flux linkage SV

After one has estimated the stator flux linkage SV, one can estimate the position or angle of the rotor flux linkage SV by a trigonometric identity. First one finds the angle between the current SV and the stator flux linkage SV:

$$\hat{\varepsilon}_{s1}^{\psi_{s1}} = \varepsilon_{s1}^{s1} - \hat{\xi}_{s1}^{s1} \tag{4.2}$$

Where ε_{s1}^{s1} is the angle of the current SV projected on the stator a1 axis and this value is measured. $\hat{\xi}_{s1}^{s1}$ is the estimated angle of the stator flux linkage SV projected on the stator a1 axis.

In equation 4.2 one sees that an error in the estimation of the stator flux linkage angle also produces an error in the angle between the current SV and the stator flux linkage SV.

Then one finds the angle between the stator flux linkage SV and the rotor flux linkage SV[11][15]. (Derivation of the equation in Appendix F)

$$\hat{\xi}_{s1}^{R} = \tan^{-1}\left(\frac{\hat{x}_\sigma i_{s1}\sin(\hat{\varepsilon}_{s1}^{\psi_{s1}}) + (\hat{x}_\sigma - \hat{x}_{s\sigma})i_{s2}\sin(\hat{\varepsilon}_{s2}^{\psi_{s1}})}{\hat{\psi}_{s1} - \hat{x}_\sigma i_{s1}\cos(\hat{\varepsilon}_{s1}^{\psi_{s1}}) - (\hat{x}_\sigma - \hat{x}_{s\sigma})i_{s2}\cos(\hat{\varepsilon}_{s2}^{\psi_{s1}})}\right) \tag{4.3}$$

In equation 4.3 the leakage reactance, $\hat{x}_\sigma$, and the stator leakage reactance, $\hat{x}_{s\sigma}$ are all estimated, and if they are estimated wrong, the estimated angle will be wrong. On the other hand, the reactance is usually found by a hysteresis curve, and this estimation is more precise than the estimation of the stator resistance. Since the angle between

the current SV and the stator flux linkage SV is a function of the estimation of the stator resistance, an error in this estimation also produces an estimation error in the rotor flux linkage angle. Now one can find the angle between the rotor flux linkage SV and the stationary a1 axis.

$$\hat{\theta}_R^{s1} = \hat{\xi}_{s1}^{s1} - \hat{\xi}_{s1}^{R} \tag{4.4}$$

As assumed, errors in the recent estimations of $\hat{\xi}_{s1}^{s1}$ and $\hat{\xi}_{s1}^{R}$ will give an erroneous $\hat{\theta}_R^{s1}$.

Now as one has estimated the rotor flux linkage angle projected on the stator a1 axis, one can project the current SV and the stator flux linkage SV on the synchronous rotating d-q-axis following the rotor flux linkage SV. Hence the estimated rotor flux linkage amplitude is given by:

$$\hat{\psi}_R = \hat{\psi}_{sd1} - \hat{x}_\sigma \hat{i}_{sd1} - (\hat{x}_\sigma - \hat{x}_{s\sigma})\hat{i}_{sd2} \tag{4.5}$$

In equation 4.5 the estimation depends on the estimated leakage and stator leakage reactance, and the estimations of the direct components of the currents. Also, the estimated rotor flux linkage amplitude depends on the estimation of the stator flux linkage amplitude.

To summarize the voltage model depends on the estimation of three parameters: the stator resistance, r_s, the leakage reactance, x_σ, and the stator leakage reactance, $x_{s\sigma}$. However, the most critical parameter is the stator resistance since it is a part of the open integration in equation 4.1. As will be shown later, a wrongly estimated stator resistance can produce significant errors both stationary and dynamic in the voltage model.

4.2 The Current Model

In the current model, the input variables are the speed or the position of the rotor and the current measurement. By knowing the angle and frequency of the stator current SV and the speed of the motor, one estimates the rotor frequency and the rotor flux linkage amplitude by the equations:

$$\frac{d\hat{\psi}_R}{dt} = -\frac{\hat{\psi}_R}{\hat{T}_r} + \frac{\hat{x}_H}{\hat{T}_r}(\hat{i}_{sd1} + \hat{i}_{sd2}) \tag{4.6}$$

$$\hat{f}_r = \frac{\hat{r}_R(\hat{i}_{sq1} + \hat{i}_{sq2})}{\hat{\psi}_R} \tag{4.7}$$

$$\hat{\theta}_R^{s1} = 2\pi \int_{t_0}^{t} (\hat{f}_r + n)\ dt + \hat{\theta}_{R0}^{s1} \tag{4.8}$$

$$\hat{T}_r = \frac{\hat{x}_H}{\omega_n \hat{r}_R} \tag{4.9}$$

$$n = f_\psi - f_r \tag{4.10}$$

The precision of the model depends on the estimation of the rotor resistance, r_R and the main(magnetizing) reactance x_H. Again, the resistance is the most critical parameter to estimate correctly since the magnetizing reactance is generally known from a hysteresis curve. Besides, the rotor resistance is integrated, and hence of extra importance to estimate correctly.

In the current model, it is not necessary to estimate the stator flux linkage SV. On the other hand, there is a possibility that one can estimate the stator flux linkage from both the models and then compare these two signals to estimate the resistances for example, and hence improve the models. Another possibility is to compare the signals and use the difference as an error signal to improve one of the models. This possibility is analyzed later. To estimate the stator flux linkage in the current model one estimate first the stator flux linkage equations in direct and quadrature component to estimate the amplitude.

$$\begin{aligned} \hat{\psi}_{sd1} &= \hat{\psi}_R + \hat{x}_\sigma \hat{i}_{sd1} + (\hat{x}_\sigma - \hat{x}_{s\sigma})\hat{i}_{sd2} \\ \hat{\psi}_{sq1} &= \hat{x}_\sigma \hat{i}_{sq1} + (\hat{x}_\sigma - \hat{x}_{s\sigma})\hat{i}_{sq2} \end{aligned} \tag{4.11}$$

$$\hat{\psi}_{s1} = \sqrt{\hat{\psi}_{sd1}^2 + \hat{\psi}_{sq1}^2} \tag{4.12}$$

The angle is estimated by turning equation 4.4:

$$\hat{\xi}_{s1}^{s1} = \arctan \frac{\hat{\psi}_{sq1}}{\hat{\psi}_{sd1}} + \hat{\theta}_R^{s1} \tag{4.13}$$

Using the current model, it is evident that the estimation of the stator flux linkage SV is parameter sensitive to the leakage reactance, the main reactance and the rotor resistance.

5 Deviation in Parameters and Measurement Errors

5.1 Resistance Deviation

There are mainly three reasons for the deviation in the resistance estimation. Firstly the measurement obtains some error. Secondly, under high stator and rotor frequencies, the skin effect takes part. This only occurs under AC operation, and hence the resistance under DC magnetization and rotating operation are not the same. Thirdly and the most important reason is the temperature dependency of the resistance. The windings in the stator are usually made of copper and the conductivity of copper is $\sigma = 57 \cdot 10^6$ S/m at a temperature of 20°C. The resistivity of copper varies with temperature coefficient $\alpha = 3.81 \cdot 10^{-3}1/\text{K}$[4]. The DC resistance and the AC resistance are generally different following the equations[4]:

$$\begin{aligned} R_{DC} &= \frac{l}{\sigma A} \\ R_{AC} &= R_{DC}(T) + R_{skin}(f, T) \end{aligned} \tag{5.1}$$

The temperature is by far the most crucial reason for variations in the resistance, and in a temperature range from 20° to 150° the resistivity of copper increases by 50%[2].

In the induction motor, there are a stator resistance and a rotor resistance. As the resistances are both dependent of temperature, they are usually varying at the same scale.

5.2 Reactance Deviation

The reactance varies mainly due to the saturation phenomena in the magnetic material. Also, the temperature can be a factor, but usually this factor is neglected due to its small value. Most often the reactances are saturated at rated operation and hence increase in the field-weakening operation[2]. Klaes[1] says that the main reactance (magnetizing reactance) can vary by 20% in each direction and the leakage reactance can vary by 10% in each direction.

5.3 Error in Measurements

The voltage is usually not measured directly due to technical and economic reasons but measured indirectly in the DC-link, and then the stator voltage is estimated[2]. Using this technique, one has to estimate the nonlinear voltage drop in the inverters

which is complicated to model. Hence due to its complicated nature one usually experiences an error in the measurement of the voltage. Nestli assumes in his doctoral thesis from 1995 on page 28 a voltage measurement error of ± 0.015 pu[2].

The current can also experience measurement errors. Inaccurate resistance sensing and saturation in the measurement device are some of the reasons that cause measurement errors for the current[2]. The errors may deviate in different machines, but Nestli assumed a measurement error of ± 0.015 pu in his doctoral thesis from 1995.

On the other hand, in this thesis, measurement errors are not analyzed. In this thesis, the focus is on the deviation in the parameters with extra attention to the resistances due to its variation with temperature, which can be difficult to estimate correctly.

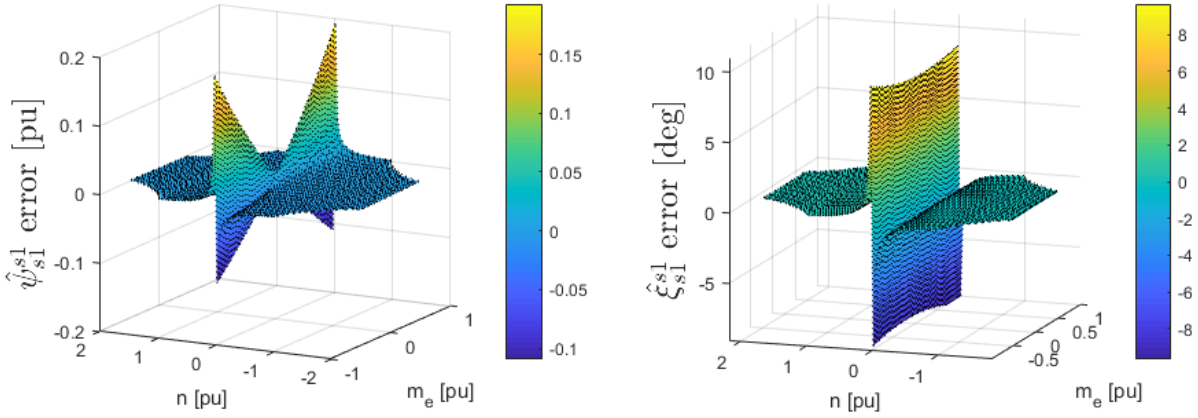

Figure 6.1: Stator Flux linkage estimation with $\hat{r}_s = 1.2r_s$

6 Stationary Parameter Sensitivity Analysis

6.1 Voltage Model

6.1.1 Stator Flux Linkage Estimation

As one can see in figure 6.1 when estimating the stator flux linkage, the voltage model is highly sensitive to errors in the estimation of the stator resistance around zero speed. Hence the estimated value of stator flux linkage amplitude and angle are erroneous.

The reason for the high sensitivity around zero speed is seen by using phasor analysis and investigate equation 4.1 stationary:

$$\bar{\Psi}_{s1}^{s1} = -j\frac{1}{f_\psi}(\bar{U}_{s1}^{s1} - \hat{r}_s\bar{I}_{s1}^{s1}) \tag{6.1}$$

Here f_ψ is the synchronous frequency and is known from the measurement of the voltage.

One sees in the equation 6.1 that when f_ψ is close to zero, and the resistance is estimated wrong, f_ψ amplifies the error. At low speed, the voltage SV amplitude decreases to its minimum and hence the relative error of the voltage minus the stator resistance voltage drop is more prominent. At high speed, the resistive voltage drop term is relatively small compared to the magnitude of the voltage SV, and hence an error in the estimation is not a significant concern. Besides, at high speed, the synchronous frequency, f_ψ, is high and will not amplify the error. From figure 6.2

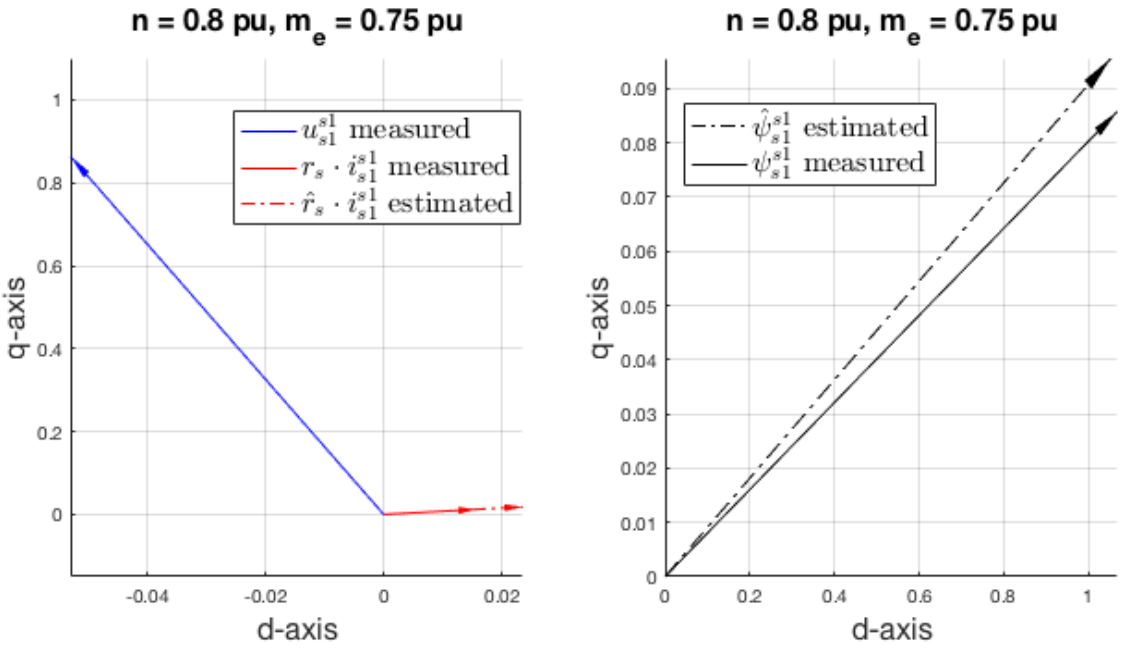

Figure 6.2: $\hat{\psi}_{s1}^{s1}$ and ψ_{s1}^{s1} for high speed with $\hat{r}_s = 1.5 r_s$

and figure 6.3 one can observe why the error increases at low speed by the phasor diagram. As the stator voltage SV, u_{s1}^{s1}, goes down at low speed, the resistive voltage drop estimation, $\hat{r}_s i_{s1}^{s1}$, becomes significant and the estimation of the stator flux linkage, $\hat{\psi}_{s1}^{s1}$, will be more erroneous.

A notable observation from equation 6.1 is if one distinguishes the errors of the stator flux linkage estimation in amplitude and angle error, the angle error is not amplified by a low f_ψ at low speed. The angle error depends only on the measured voltage SV and the estimated resistive voltage drop SV. In figure 6.1 it is observed that the estimation is most erroneous when f_ψ is low but this occurs because the measured voltage SV magnitude decreases at low speed and hence the relative error increases at low speed.

On the other hand, the amplitude error of the stator flux linkage estimation is amplified by a low f_ψ. The most sensitive operational point occurs when $f_\psi = 0$. At this point, the machine works in DC, and hence the measured voltage should be equal to the resistive voltage drop by Ohm's law. If this does not occur because of wrongly estimated stator resistance, the error is amplified to infinity. This fact becomes clearer later when the error functions are investigated.

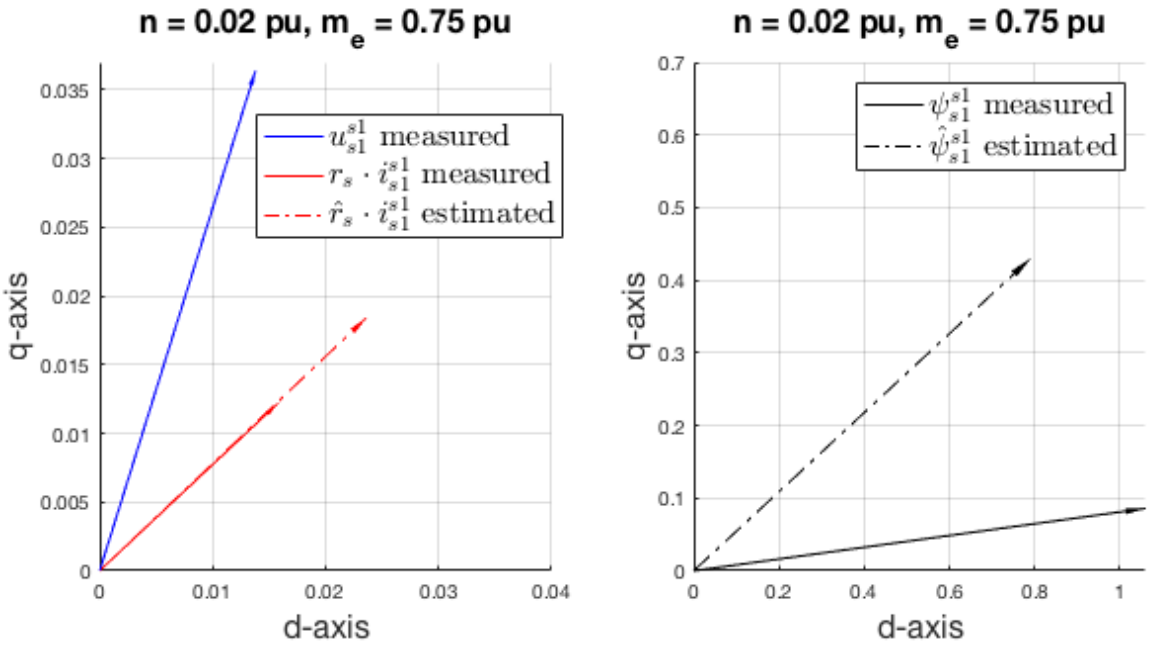

Figure 6.3: $\hat{\psi}_{s1}^{s1}$ and ψ_{s1}^{s1} for low speed with $\hat{r}_s = 1.5 r_s$

As long as the electrical torque is not zero in the motor, the synchronous frequency is not equal to zero when the speed of the motor is zero. This occurs because of the existence of the slip frequency in the rotor. From equation 4.10 it is evident that the synchronous frequency reaches zero whenever $n = -f_r$. Hence, this will be the most sensitive operational point for the estimation of the stator flux amplitude as an error is amplified to infinity. This is observed in figure 6.4 where the estimation of the stator flux linkage, both amplitude and angle, gets more erroneous as n approaches $-f_r$.

An important consideration is that as long as there only exist a slightly error in the resistance estimation the amplitude error is amplified to infinity at the most sensitive operational point; when $n = -f_r$. On the other hand, the rate of the error depends on the size of the estimation error of the resistance. This can be seen in figure 6.5 where $\hat{r}_s$ that is 1.5 times the real r_s has a higher rate than a $\hat{r}_s$ that is 1.2 times the real r_s.

It is shown (Appendix D.1.1) that the error in the stator flux linkage amplitude

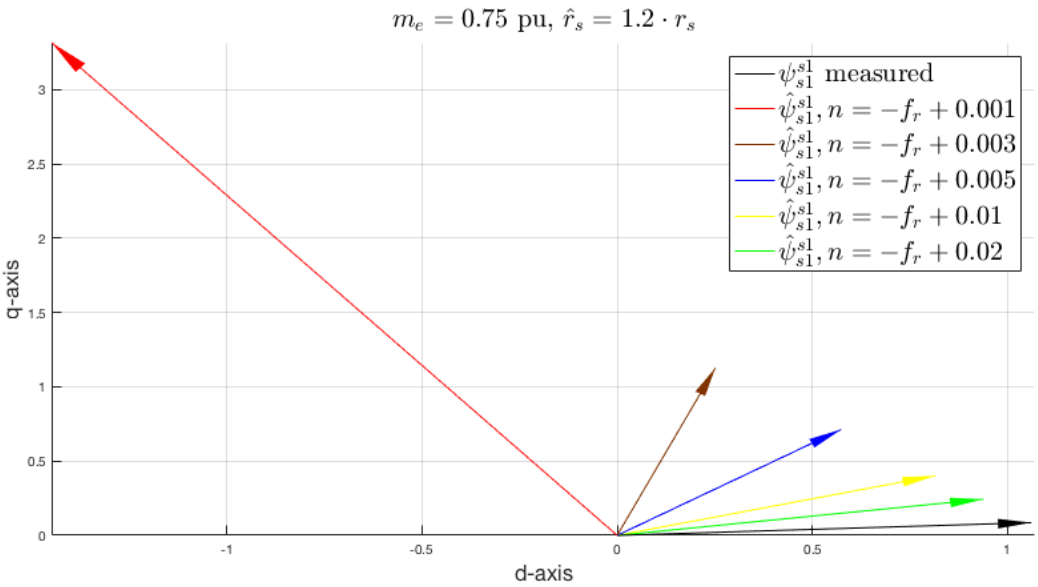

Figure 6.4: How the error evolves as n is approaching $-f_r$

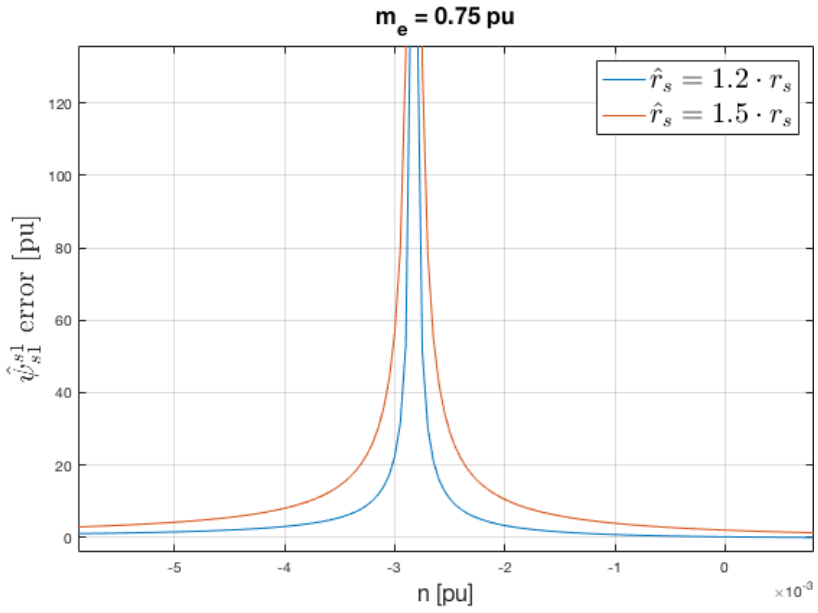

Figure 6.5: The amplitude error increases as $\hat{f}_\psi$ goes towards zero

estimation is given by:

$$\begin{aligned}\hat{\psi}_{s1} - \psi_{s1} = \frac{1}{f_\psi}(&\sqrt{u_{s1}^2 + \hat{r}_s^2 i_{s1}^2 - 2u_{s1}\hat{r}_s i_{s1}\cos(\gamma_{s1}^{s1} - \varepsilon_{s1}^{s1})} \\ &- \sqrt{u_{s1}^2 + r_s^2 i_{s1}^2 - 2u_{s1} r_s i_{s1}\cos(\gamma_{s1}^{s1} - \varepsilon_{s1}^{s1})})\end{aligned} \tag{6.2}$$

In equation 6.2 one sees that when $\hat{r}_s \neq r_s$ there is a nonzero error in the expression and when f_ψ is close to zero this error is amplified. One can also observe that the equation depends on the amplitude of the stator current and at low torque levels the current magnitude will be at its lowest. Hence, the estimated error depends on the electrical torque produced by the motor. Figure 6.6 shows this where the speed of the motor is fixed. It is evident that the error variate as a function of the electrical torque produced in the motor, and the slope is different at each speed level. Besides, it is clear that as n is , the variation increases. An observation is that at low torque levels the estimation error is relatively small compared to at high torque levels. This is because at lower torque levels the stator current amplitude is at its lowest. Another notable observation from figure 6.6 is that the error is zero at different torque levels for different speeds. For example, for $n = -0.03$ pu the error function crosses zero error at a torque level below zero, and at $n = 0.05$ pu the error function crosses zero at a torque level above zero. The reason for this is seen in equation 6.2 where it is evident that the expression is a function of the difference between the angles of the stator voltage and the stator current. These angles deviate at the different speed and torque levels. It is shown in the Appendix D.1.1 that the error is zero when $r_s = \hat{r}_s$ or:

$$\text{if} \quad i_{s1} = \frac{2u_{s1}\cos(\gamma_{s1}^{s1} - \varepsilon_{s1}^{s1})}{\hat{r}_s + r_s} \quad \Rightarrow \hat{\psi}_{s1} - \psi_{s1} = 0 \tag{6.3}$$

In equation 6.3 i_{s1} and its angle, ε_{s1}^{s1}, vary with torque and u_{s1} and its angle, γ_{s1}^{s1}, vary with both torque and speed.

As the phase of the current and the voltage generally are not the same in an induction machine, the angle is also misestimated, in contrast to a synchronous machine, where the voltage and current are in phase, and only the amplitude is estimated wrongly. (If one distinguish the dynamical drifting phenomenon which causes the angle to be misestimated in both synchronous and induction motors.)

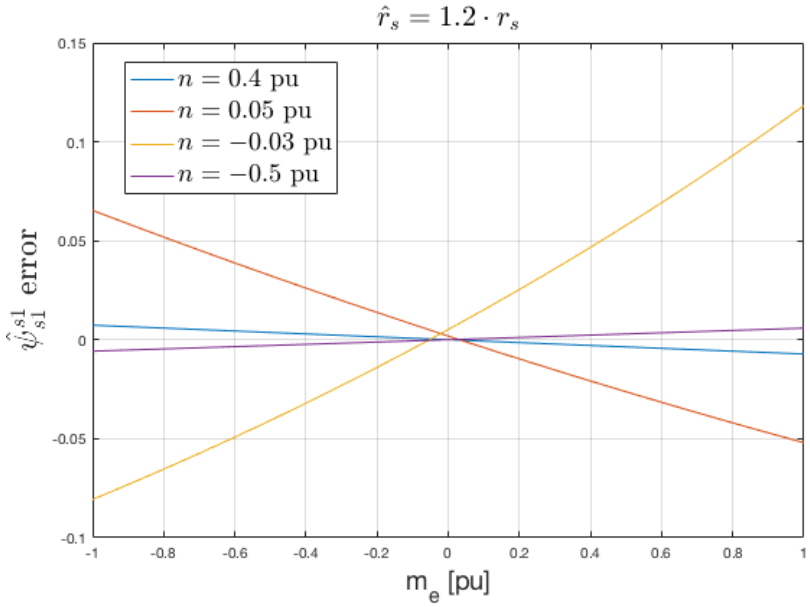

Figure 6.6: How the $\hat{\psi}_{s1}^{s1}$ error variate with electrical torque for different speeds

The estimated stator flux linkage's angle error can be written like(Appendix D.1.2):

$$\hat{\xi}_{s1,error}^{s1} = \begin{cases} \arctan\frac{y}{x} - \arctan\frac{\psi_{sq1}}{\psi_{sd1}}, & \text{if } x > 0 \\ \arctan\frac{y}{x} + \pi - \arctan\frac{\psi_{sq1}}{\psi_{sd1}}, & \text{if } x < 0 \text{ and } y \geq 0 \\ \arctan\frac{y}{x} - \pi - \arctan\frac{\psi_{sq1}}{\psi_{sd1}}, & \text{if } x < 0 \text{ and } y < 0 \\ \frac{\pi}{2} - \arctan\frac{\psi_{sq1}}{\psi_{sd1}}, & \text{if } x = 0 \text{ and } y > 0 \\ -\frac{\pi}{2} - \arctan\frac{\psi_{sq1}}{\psi_{sd1}}, & \text{if } x = 0 \text{ and } y < 0 \\ \text{undefined}, & \text{if } x = 0 \text{ and } y = 0 \end{cases} \tag{6.4}$$

where

$$\begin{aligned} y &= \hat{r}_s i_{s1} \cos\left(\varepsilon_{s1}^{s1}\right) - u_{s1} \cos\left(\gamma_{s1}^{s1}\right) \\ x &= u_{s1} \sin\left(\gamma_{s1}^{s1}\right) - \hat{r}_s i_{s1} \sin\left(\varepsilon_{s1}^{s1}\right) \end{aligned} \tag{6.5}$$

As long as the stator resistance estimation is wrong, there will be an error in the estimated stator flux linkage's angle. If $\hat{r}_s = r_s$, equation 6.4 is zero since $\arctan\frac{y}{x} = \arctan\frac{\psi_{sq1}}{\psi_{sd1}}$. In figure 6.7 it is evident that a more wrongly estimated stator resistance produces more error. In the figure, the result is shown for four different estimated stator resistances, and the error rises steeper to the maximum point the more wrongly the estimated stator resistance is. The most sensitive operational point is the same for all the scenarios. It occurs when $f_\psi = 0$ and $n = -f_r$. At this point, one must remember that $u_{s1} = r_s i_{s1}$, and hence the voltage and the current will be in phase

and the machine operates in DC. If the voltage and the current are in phase it implies that $\varepsilon_{s1}^{s1} = \gamma_{s1}^{s1}$, and if the resistance is estimated wrong then $u_{s1} \neq \hat{r}_s i_{s1}$. The estimated stator flux linkage lags 90 degrees from the result of $\underline{u}_{s1} - \hat{r}_s \underline{i}_{s1}$, and when they are in phase the estimated angle of the stator flux linkage depends on if the estimated stator resistance is too big or too small. At the operational point $f_\psi = 0$, both the estimated and the real stator flux linkage SV is not observable since the principle of lagging/leading needs a positive or negative frequency. However, if the synchronous frequency is slightly positive or slightly negative and the estimated stator resistance is estimated too big or too small, one can analyze and observe the limit of the error function. This is seen in figure 6.8, and the resulting estimated stator flux linkage's angle lags 90 degrees on the result of $\underline{u}_{s1} - \hat{r}_s \underline{i}_{s1}$. Hence, for an estimated stator resistance too low, an estimated stator flux linkage SV leads 90 degrees on the current vector for a slightly negative frequency and lags 90 degrees for a somewhat positive frequency. For an estimated stator resistance too high the opposite is the result. This is the reason why the graphs are mirrored depending on the size of the estimated stator resistance relative to the real stator resistance in figure 6.7. Since the estimated stator flux linkage SV leads or lags 90 degrees on the current vector, the error at the most sensitive operational point depends on the angle of the current vector. The angle of the current vector depends on the torque level of the machine and hence varies as a function of torque. Besides, the operational point $f_\psi = 0$ occurs when $n = -f_r$, and f_r is a function of the torque level in the machine. Then the speed of the rotor at the most sensitive operational point changes depending on the torque level in the machine, but will always be close to zero since f_r has a low value. On the other hand, the torque dependency is just where the most sensitive operational point is located at the speed axis and the value at this point, but the wrongly estimated stator resistance is the factor that creates the error of the estimated angle at every operational point.

6.1.2 Rotor Flux Linkage Estimation

By applying equations 4.3, 4.4 and 4.5, one estimates the rotor flux linkage, both amplitude, and angle. By examining the equation 4.3, one sees that the expression is a function of the estimation of the leakage reactances, $\hat{x}_\sigma$ and $\hat{x}_{s\sigma}$, and the estimated stator flux linkage's amplitude, $\hat{\psi}_{s1}$. Since a wrongly estimated stator resistance, $\hat{r}_s$, gives an erroneously estimated magnitude of the stator flux linkage, equation 4.3 is also sensitive to the stator resistance estimation. The final estimation of the rotor flux linkage angle is given by equation 4.4, and one observes that the estimation of the stator flux linkage angle is a term in the equation. As investigated in section 6.1.1

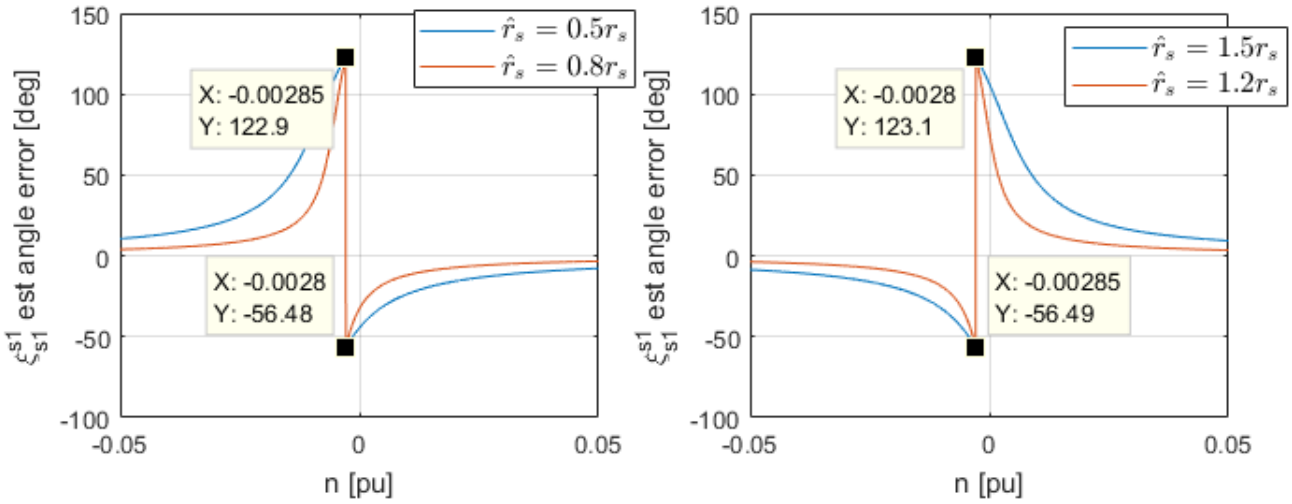

Figure 6.7: Error in the angle stator flux linkage estimation for different values of $\hat{r}_s$ at $m_e = 0.75$ pu

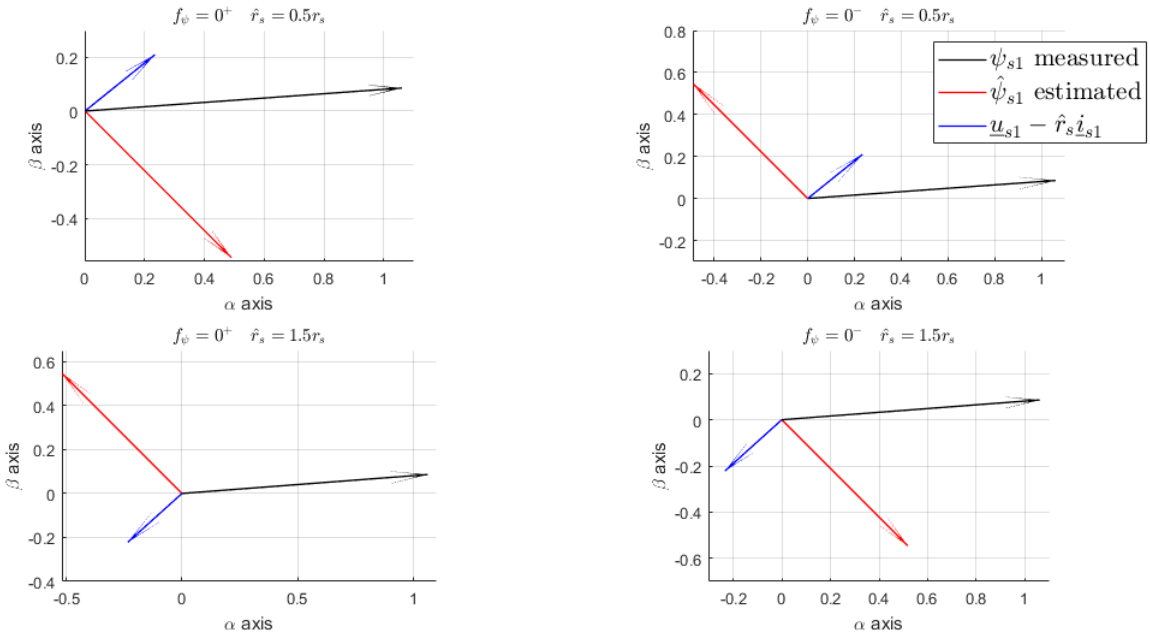

Figure 6.8: The estimated stator flux linkage around $f_\psi = 0$

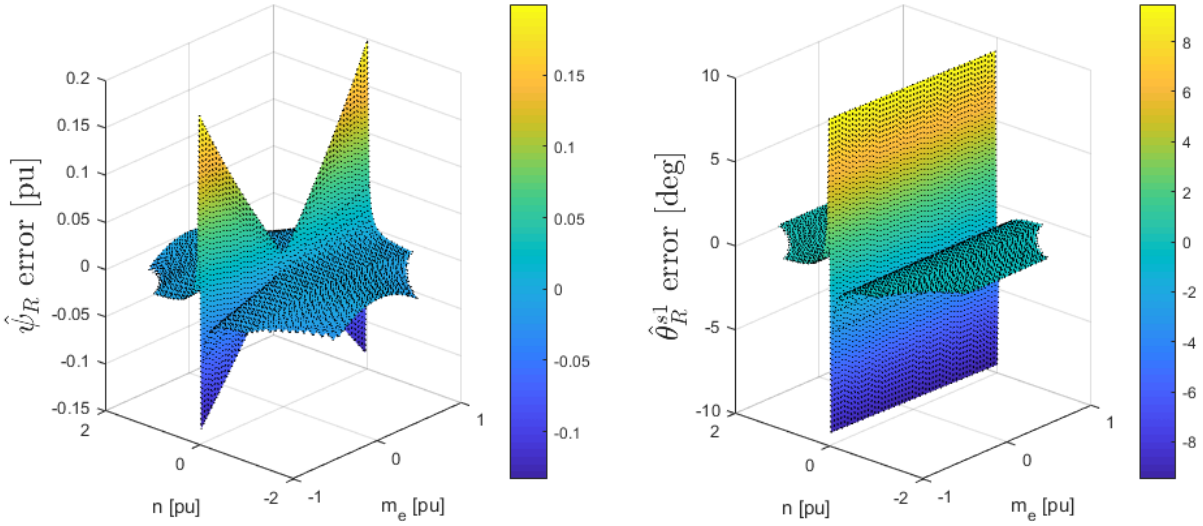

Figure 6.9: Rotor Flux linkage estimation with $\hat{r}_s = 1.2r_s$

the angle is highly sensitive to errors in the estimation of the stator resistance. Hence the conclusion is that the rotor flux linkage's estimated angle is parameter sensitive to both the estimation of the leakage reactances and the stator resistance. By the same logic, examining equation 4.5, it is evident that the rotor flux linkage's estimated amplitude is also parameter sensitive of the estimation of the leakage reactances and the stator resistance.

In the figures 6.9, 6.10, 6.11 and 6.12, one observes the parameter sensitivity to the stator resistance and the leakage reactances. It is clear that the maximum error produced by a wrongly estimated stator resistance is higher than the maximum error created by the improperly estimated leakage reactances. And again, the error is at most during low-speed operation. On the other hand, the error produced by a wrongly estimated stator resistance is low when the speed is high, but for the improperly estimated leakage reactances, the dependency of speed is not that clear. Examining figures 6.10, 6.11 and 6.12, even though the error for the amplitude is relatively small, the error is stable in the normal operating area and decreases in the field-weakening area. The angle error seems to be a function of the electrical torque generated in the motor in the normal operating area. In the field-weakening area, where the error increases, the estimated angle error seems to be a function of both the speed and the electrical torque. Besides, the error produced by a wrongly estimated stator leakage reactance, $\hat{x}_{s\sigma}$, is less critical than an improperly estimated leakage

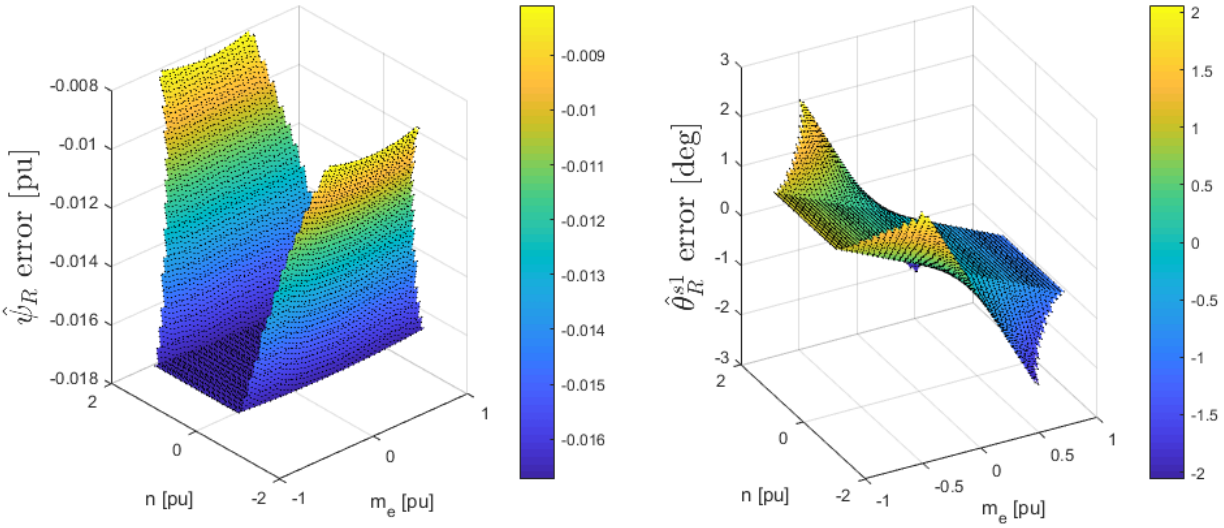

Figure 6.10: Rotor Flux linkage estimation with $\hat{x}_\sigma = 1.1 x_\sigma$

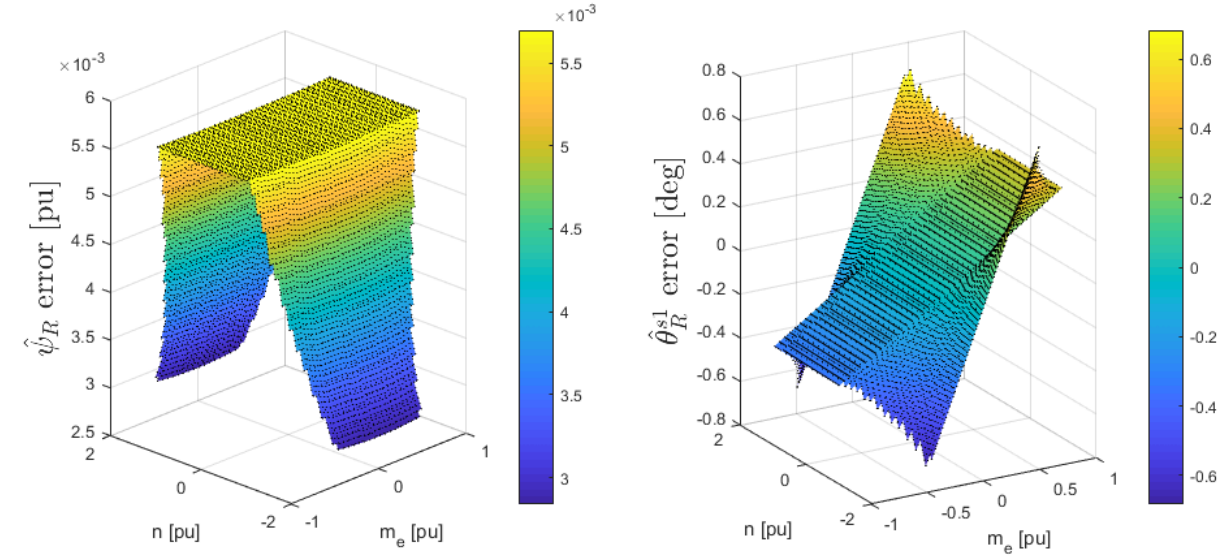

Figure 6.11: Rotor Flux linkage estimation with $\hat{x}_{s\sigma} = 1.1 x_{s\sigma}$

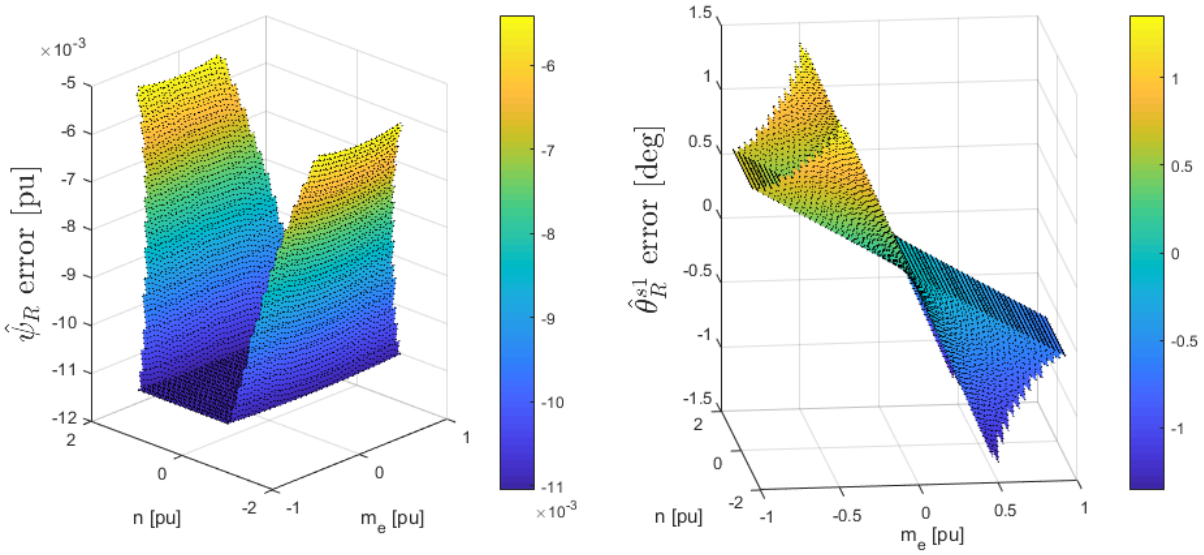

Figure 6.12: Rotor Flux linkage estimation with $\hat{x}_\sigma = 1.1x_\sigma$ and $\hat{x}_{s\sigma} = 1.1x_{s\sigma}$

reactance, $\hat{x}_\sigma$. This is evident by comparing figure 6.10 and 6.11. Another important observation is that an error in the estimation of the leakage reactance, $\hat{x}_\sigma$, produces an error oppositely as an error from a wrongly estimated stator leakage reactance, $\hat{x}_{s\sigma}$. Hence, as observed in figure 6.12, it is better to estimate wrongly in both leakage reactance, $\hat{x}_\sigma$, and stator leakage reactance, $\hat{x}_{s\sigma}$, than only in the leakage reactance, $\hat{x}_\sigma$. The error of the rotor flux linkage's angle estimation is given by:

$$\begin{aligned}\hat{\theta}_{R,err}^{s1} &= \hat{\theta}_R^{s1} - \theta_R^{s1} = (\hat{\xi}_{s1}^{s1} - \hat{\xi}_{s1}^{R}) - (\xi_{s1}^{s1} - \xi_{s1}^{R}) = \hat{\xi}_{s1,err}^{s1} - \hat{\xi}_{s1,err}^{R} \\ &= \hat{\xi}_{s1,err}^{s1} - (\arctan\frac{a}{b} - \xi_{s1}^{R})\end{aligned} \tag{6.6}$$

where $\hat{\xi}_{s1,err}^{s1}$ is given by equation 6.4 and 6.5 and

$$a = i_{s1}\sin(\hat{\varepsilon}_{s1}^{\psi_{s1}})(2\hat{x}_\sigma - \hat{x}_{s\sigma}), \qquad b = \hat{\psi}_{s1} - i_{s1}\cos(\hat{\varepsilon}_{s1}^{\psi_{s1}})(2\hat{x}_\sigma - \hat{x}_{s\sigma})$$

Where

$$i_{s1} = i_{s2}, \qquad \hat{\varepsilon}_{s1}^{\psi_{s1}} = \hat{\varepsilon}_{s2}^{\psi_{s1}} = \varepsilon_{s1}^{s1} - \hat{\xi}_{s1}^{s1} \tag{6.7}$$

By examining equation 6.6, one observes that one term in the equation is the stator flux linkage's angle estimation. As discussed in section 6.1.1, this expression is highly sensitive for a wrongly estimated stator resistance at low-speed operation. Hence an error in the estimation of the stator flux linkage angle creates an error in the

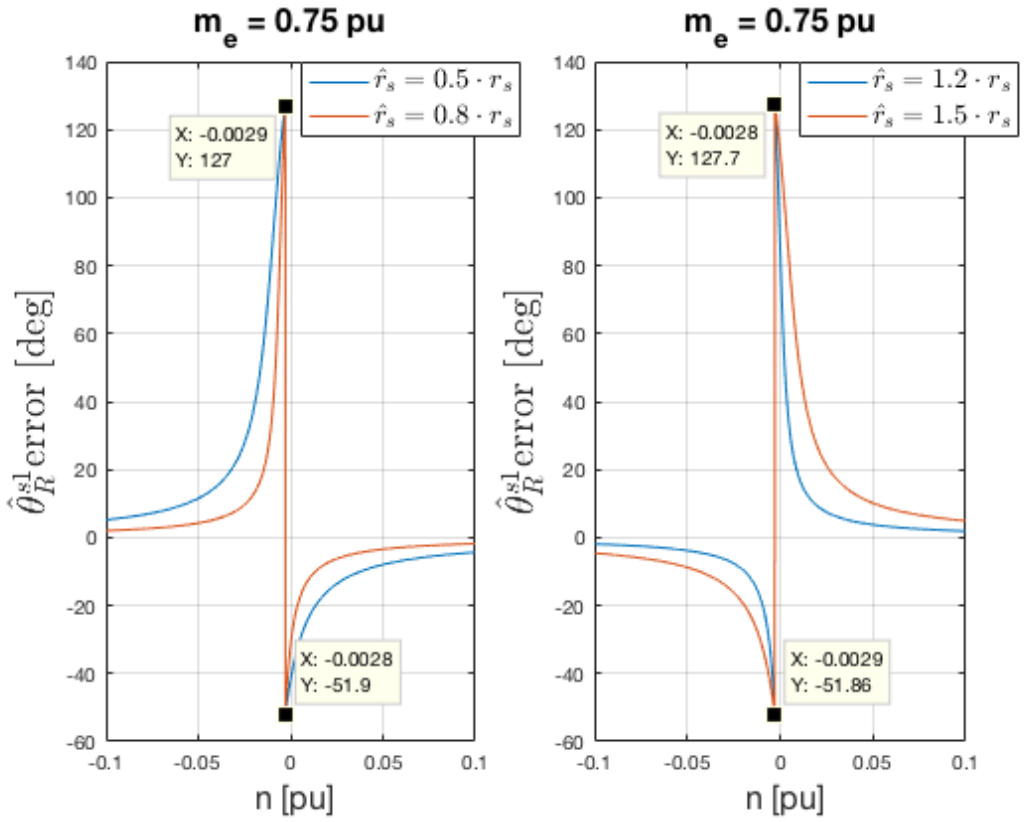

Figure 6.13: Sensitivity to the stator resistance, r_s, for the rotor flux linkage angle estimate, $\hat{\theta}_R^{s1}$, at low speed

rotor flux linkage's angle estimation, and as seen in figure 6.13 the error increases at low-speed operation. Besides, by looking at equation 6.7, it is evident that the estimation of the stator flux linkage angle is a term to estimate the angle between the current SV and the stator flux linkage SV. Also, the estimate of the stator flux linkage amplitude is a part of the arctan term in equation 6.6. As discussed in section 6.1.1, this estimated amplitude is also very sensitive for the stator resistance estimate.

In section 6.1.1 it is shown that a wrongly estimated stator resistance produces significant errors in low-speed operation for the stator flux linkage angle. Hence, it is interesting to see how decisive the stator flux linkage's angle estimation is for the rotor flux linkage's angle estimation. In figure 6.14 it is shown how the rotor flux linkage's angle estimation error becomes assuming that the stator flux linkage's angle estimation is correct. An interesting observation is that the maximum error for the estimated angle is way less than for the stator flux linkage's angle estimation. Hence

one can conclude that an improvement in the estimation of the stator flux linkage's angle estimation also improves the rotor flux linkage's angle estimation.

If one assumes that the estimation of the stator resistance is correct, the stator flux linkage estimation of both angle and amplitude is right, and the only erroneous source in the estimation of the rotor flux linkage angle is the angle between the stator and the rotor flux linkage SVs. The stator flux linkage equations in the d-q rotating reference frame were presented in section 2 and the equation 2.2. From this equation, it is clear that the q-component of the stator flux linkage varies with the q-component of the current linearly. This q-component of the current is proportional to the electrical torque generated in the motor, and hence an error in the stator flux linkage q-component varies linearly with the electrical torque level in the machine. This is observed in figure 6.15, where one sees clearly that the error in the rotor flux linkage's angle estimation varies linearly with the torque level with an error in the estimated leakage reactance, $\hat{x}_\sigma$. On the other hand, the error in the estimated rotor flux linkage angle caused by a wrongly estimated leakage reactance is very low, and hence not significant relative to the error caused by the improperly estimated stator resistance.

As mentioned earlier, the d-component of the current will decrease in the field-weakening area, and hence the error depends both on speed and torque. Also, it is clear from equation 6.7, that the expression is more sensitive to the leakage reactance, x_σ, than the stator leakage reactance, $x_{s\sigma}$ because of factor 2 in the leakage reactance term.

It is shown(Appendix D.1.3)that the error in the rotor flux linkage's amplitude estimation is given by:

$$\hat{\psi}_{R,err} = (\psi_{s1}\cos\xi_{s1}^R - \hat{\psi}_{s1}\cos\hat{\xi}_{s1}^R) - i_{s1}(\cos\varepsilon_{s1}^R(2x_\sigma - x_{s\sigma}) - \cos\hat{\varepsilon}_{s1}^R(2\hat{x}_\sigma - \hat{x}_{s\sigma})) \quad (6.8)$$

Where:

$$\varepsilon_{s1}^R = \varepsilon_{s1}^{s1} - \theta_R^{s1}, \qquad \hat{\varepsilon}_{s1}^R = \varepsilon_{s1}^{s1} - \hat{\theta}_R^{s1} \quad (6.9)$$

In equation 6.8 and 6.9 one sees that the error in the estimation of the rotor flux linkage amplitude depends on the estimate of the stator flux linkage amplitude and angle, the rotor flux linkage angle and the leakage reactances, $\hat{x}_\sigma$ and $\hat{x}_{s\sigma}$. Since the stator flux linkage's amplitude estimation goes theoretically towards infinity at zero frequency when the stator resistance is estimated wrong, the rotor flux linkage's amplitude estimation does the same. This can be seen in figure 6.16 where the sensitivity on the parameters is shown at low-speed operation. In the figure, it is evident that the rotor flux linkage's amplitude estimation is more sensitive for an error in the estimated stator resistance than the leakage reactances, and especially at low speed. On

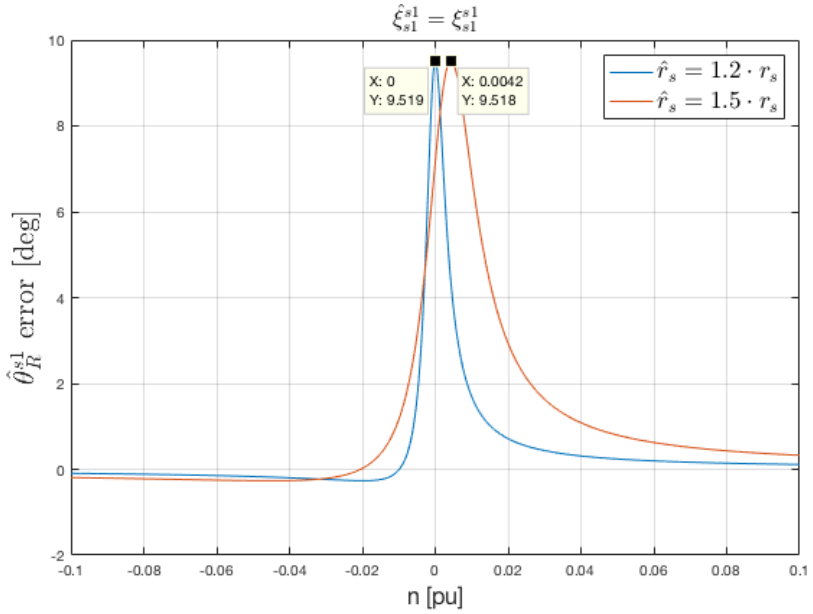

Figure 6.14: Sensitivity to the stator resistance, r_s, for the rotor flux linkage angle estimate, $\hat{\theta}_R^{s1}$, at low speed when $\hat{\xi}_{s1}^{s1} = \xi_{s1}^{s1}$ and $m_e = 0.75$ pu

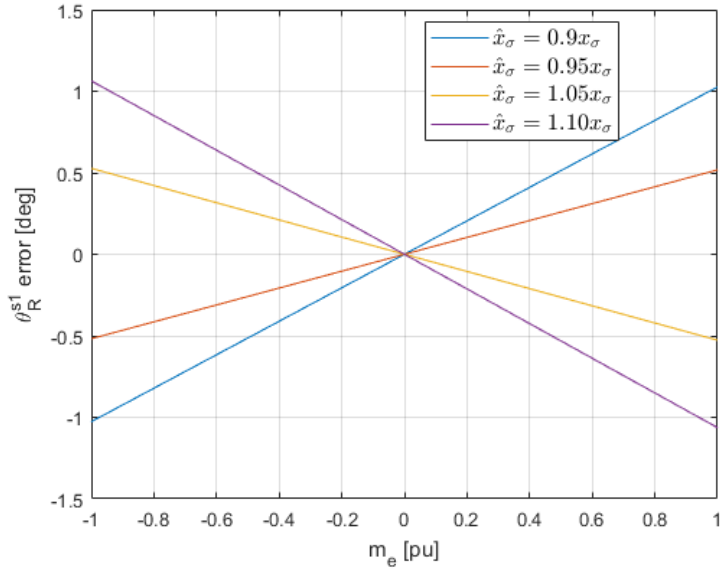

Figure 6.15: Sensitivity to the leakage reactance, x_σ, for the rotor flux linkage angle estimate, $\hat{\theta}_R^{s1}$, and dependency of electrical torque.

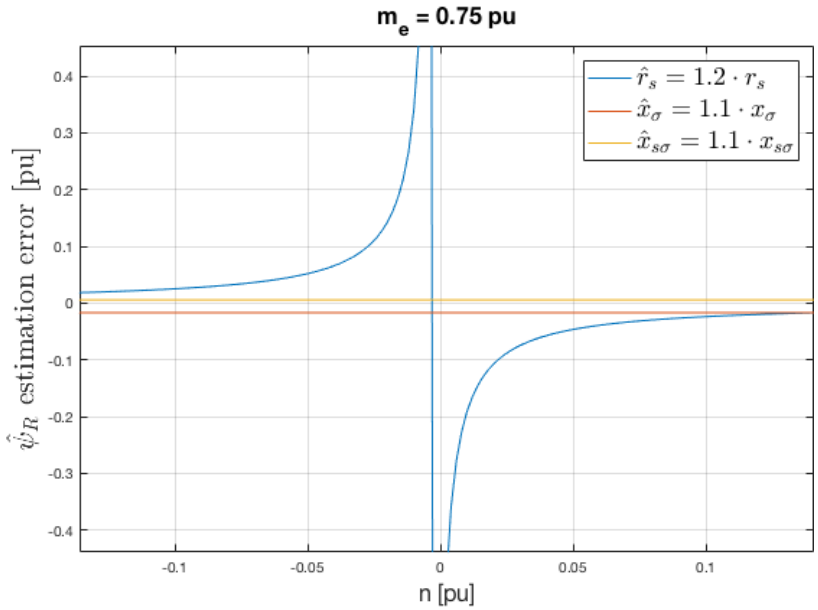

Figure 6.16: Sensitivity of $\hat{\psi}_R$ for the parameters at low speed

the other hand, since the term of the error from the leakage reactances are invariant of the speed, these errors will not decrease in a high-speed operation. By examining equation 6.8, it is evident that the error in the estimated amplitude is more sensitive to the leakage reactance, x_σ, than for the stator leakage reactance, $x_{s\sigma}$, since the term gets multiplied by 2. Besides, the value of the leakage reactance is generally higher than for the stator leakage reactance. Hence a 10% increase/decrease in the leakage reactance, x_σ, will produce a more inaccurate estimation for the rotor flux linkage amplitude than a 10% increase/decrease in the stator leakage reactance, $x_{s\sigma}$.

In the field-weakening area, as the speed increases above 1 pu, the rotor flux linkage amplitude will decrease. By equation 3.2 it is evident that the d-component current will then lower and then also the current magnitude, i_{s1}. By observing again equation 6.8, one sees that if the magnitude of the current decreases the error of the estimation will also decrease. This is observed in figure 6.17 where it is clear that in the field-weakening area the error lowers.

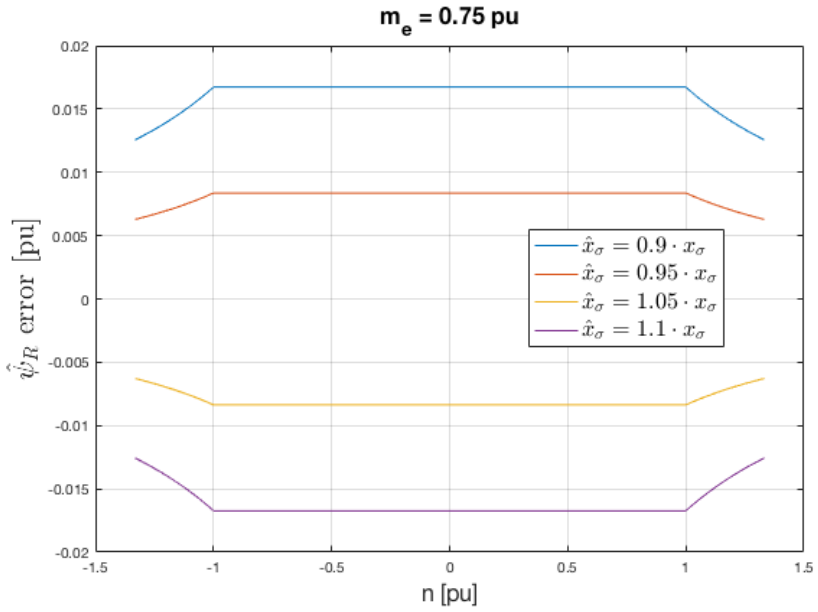

Figure 6.17: Sensitivity of $\hat{\psi}_R$ by wrong estimation of x_σ. Here is $\hat{r}_s = r_s$

6.1.3 Torque Estimation

By looking at equation 3.3 and realizing that the two q-component currents contribute the same for the generated torque($i_{sq1} = i_{sq2}$), one can write the error in the estimation of the torque as:

$$\hat{m}_e - m_e = \hat{\psi}_R(\hat{i}_{sq1} + \hat{i}_{sq2}) - \psi_R(i_{sq1} + i_{sq2}) = 2i_{s1}(\hat{\psi}_R \sin(\hat{\varepsilon}_{s1}^R) - \psi_r \sin(\varepsilon_{s1}^R)) \quad (6.10)$$

As known from the previous analysis, the rotor flux linkage estimate of both amplitude and angle are most sensitive for a wrongly estimated stator resistance. The error caused by improperly estimated leakage reactances is relatively insignificant. The estimation of the generated electrical torque with a wrongly estimated stator resistance can be seen in figure 6.18. Here, it is clear that the estimation has errors at the low-speed operation which is a consequence of the estimation of both the rotor flux linkage amplitude and angle.

In figure 6.19 it is shown the estimation error of the torque for different estimations of the stator resistance. As assumed the more wrongly the stator resistance is estimated, the more wrong does the estimation of the torque gets.

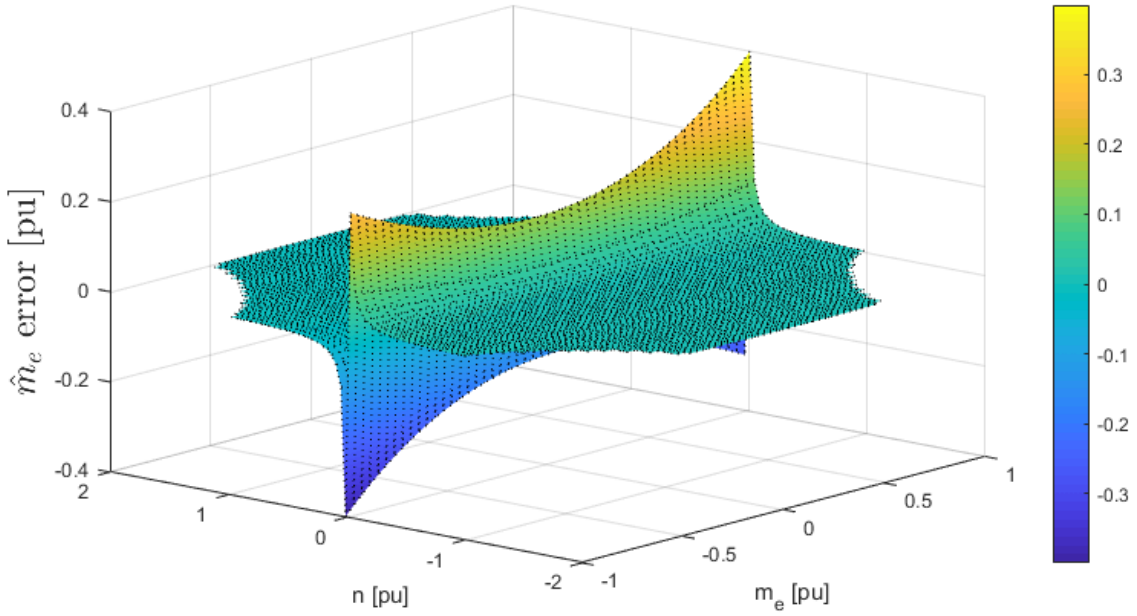

Figure 6.18: Estimation of torque with $\hat{r}_s = 1.2r_s$

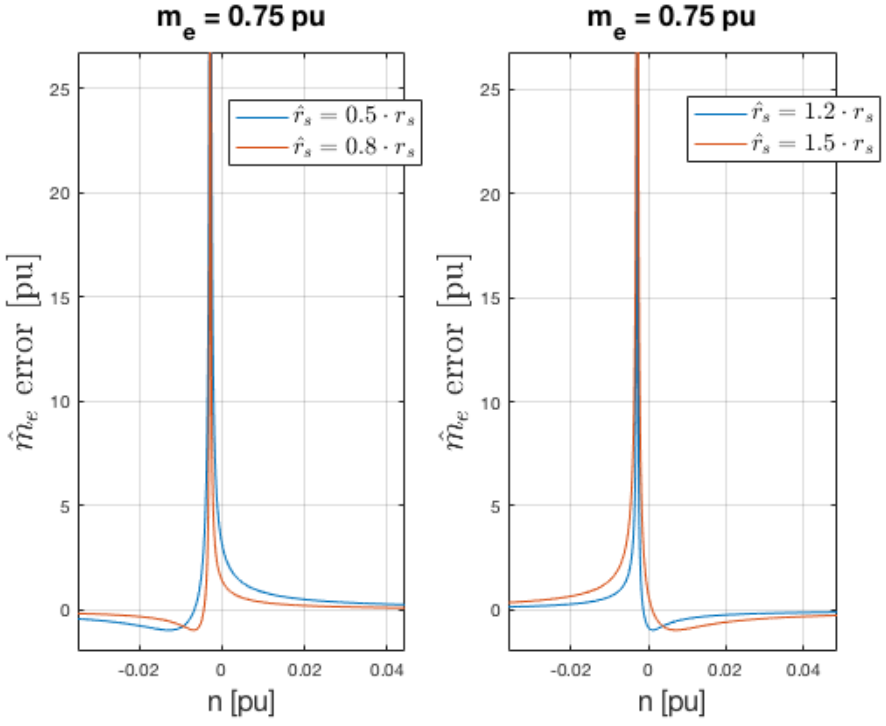

Figure 6.19: Estimation of torque with different stator resistance estimation at low speed using the voltage model

It is also worth noting that at higher torque levels the error increases. This can also be seen in figure 6.18 where at low speed it is clear that at higher torque the estimated torque is more erroneous than at low torque levels. This is because at high torque levels the amplitude of the current is higher.

6.2 The Current Model

6.2.1 Rotor Flux Linkage Estimation

Rotor flux linkage estimation in the current model is ,unlike the voltage model, parameter sensitive to the rotor resistance, r_R, and the main reactance, x_H. This is seen in figure 6.20 and 6.21. Unlike the voltage model, the error of the rotor flux linkage estimation of amplitude and angle is not speed dependent in the normal operation area but torque dependent. In the flux-weakening area, it is observed in the figures that the errors are both speed and torque dependent.

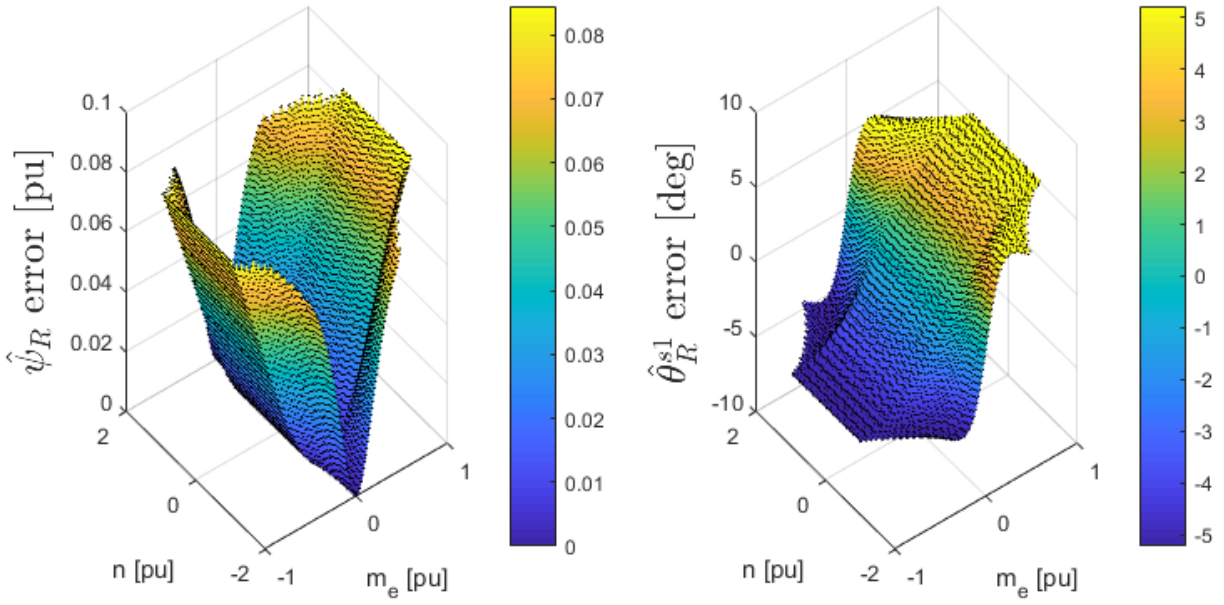

Figure 6.20: Estimation of rotor flux linkage amplitude and angle with $\hat{r}_R = 1.2r_R$ using the current model

It is shown (Appendix D.2.1) that the estimated error for the rotor flux linkage angle is:

$$\hat{\theta}_{R,err}^{s1} = \arctan(\frac{i_{sq1}}{i_{sd1}}) - \arctan(\frac{\hat{x}_H r_R i_{sq1}}{\hat{r}_R x_H i_{sd1}}) \tag{6.11}$$

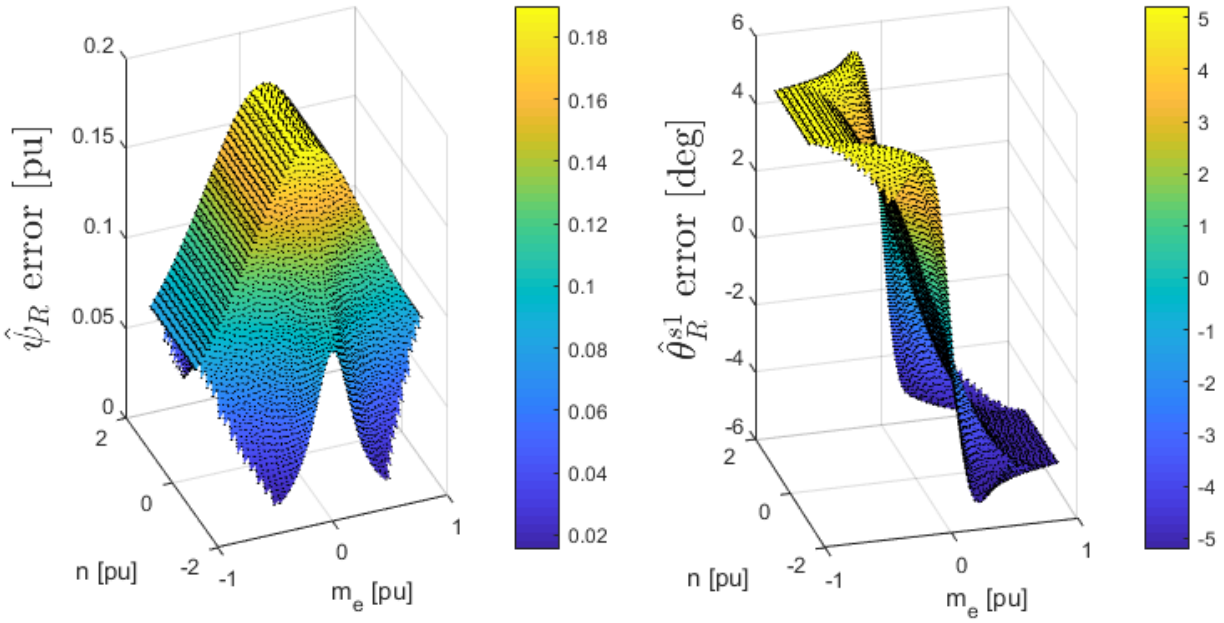

Figure 6.21: Estimation of rotor flux linkage amplitude and angle with $\hat{x}_H = 1.2x_H$ using the current model

From equation 6.11, it is evident the dependency of both the estimation of the rotor resistance and the main reactance. If $\hat{x}_H = x_H$ and $\hat{r}_R = r_R$ there is no error as assumed, but if $\frac{\hat{x}_H r_R}{\hat{r}_R x_H}$ there is also no error. This is not suspected, but just a random and lucky estimation gives this scenario, and as long as this does not occur there is an error in the estimate. Besides, one observes from the equation the dependency of the q-component of the current. Since this component of the current is proportional to the electrical torque produced by the motor, one understands that the error varies with the torque level and one observes from figure 6.22 that at zero torque level there is no error. Hence at low torque levels, the error estimated is relatively small. Another observation from figure 6.22, which is not that clear from equation 6.11, is that the most sensitive operational point does not imply maximum torque produced in the motor. This is observed by noting that the maximum of the angle estimation error with $\hat{r}_R = 0.5r_R$ occurs at a torque level of $m_e \approx \pm 0.67$. It can be shown by finding the derivative of equation 6.11 (Appendix D.2.1) with respect to electrical torque,

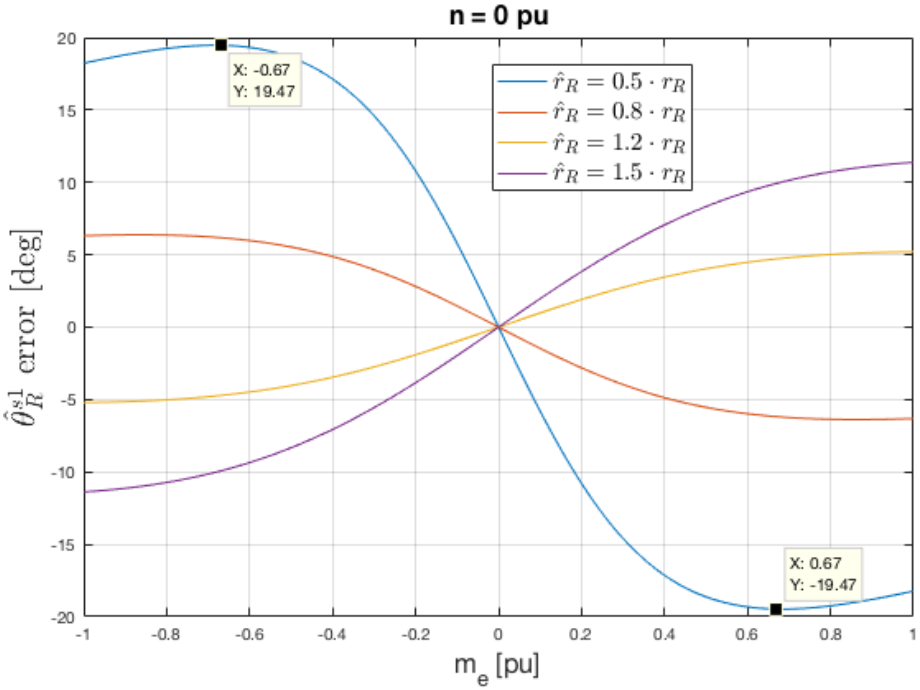

Figure 6.22: $\hat{\theta}_R^{s1}$ error with different values of $\hat{r}_R$ vs electrical torque in motor

that the most sensitive operational point in the normal operation area is when:

$$m_e = \pm 4 x_H i_{sd1}^2 \sqrt{\frac{\hat{r}_R x_H}{r_R \hat{x}_H}} \tag{6.12}$$

Another interesting observation from figure 6.22 is that the error is worse for a rotor resistance estimation below the real one than an estimation higher than the real rotor resistance. This will become clear by observing the equation 6.11, where one sees that it is the relationship between the parameter estimations that produce the error. Hence a division of for example $\hat{r}_R = 0.5 r_R$ gives a higher increase in $\frac{\hat{x}_H r_R}{x_H \hat{r}_R}$ than the decrease if $\hat{r}_R = 1.5 r_R$. Then by our assumed deviation levels of the rotor resistance and the main reactance from section 5, the worst scenario happens when $\hat{x}_H = 1.2 x_H$ and $\hat{r}_R = 0.5 r_R$.

On the other hand in the flux-weakening area the d-component of the current decreases and hence the error is also speed dependent in this area.

To estimate the rotor flux linkage amplitude stationary the derivative term in equation 4.6 gets zero and the result is:

$$\hat{\psi}_R = \hat{x}_H \cdot (\hat{i}_{sd1} + \hat{i}_{sd2}) = 2 \cdot \hat{x}_H \cdot \hat{i}_{sd1} \tag{6.13}$$

The error of the amplitude estimation will hence be:

$$\hat{\psi}_R - \psi_R = \hat{\psi}_{R,err} = 2i_{s1}\left(\frac{\hat{x}_H}{\sqrt{(\frac{\hat{x}_H r_R i_{sq1}}{\hat{r}_R x_H i_{sd1}})^2 + 1}} - \frac{x_H}{\sqrt{(\frac{i_{sq1}}{i_{sd1}})^2 + 1}}\right) \tag{6.14}$$

From equation 6.15, it is evident that the rotor flux linkage's amplitude estimation is parameter sensitive to both the rotor resistance and the main reactance. As long as $\hat{x}_H = x_H$ and $\hat{r}_R = r_R$ there is an error in the estimate. One interesting observation is when the torque is zero, and hence $i_{sq1} = 0$, the only parameter that matters for the error function is the estimation of the main reactance. The explanation to this is that the error in the estimation of the rotor flux linkage angle is zero at these operational points.

In the flux-weakening area, the d-component of the current varies also. Higher speed in the flux-weakening area gives a decrease in the d-component of the current. This is because i_{sd1} is proportional to the rotor flux linkage in the machine and hence a drop in rotor flux linkage gives a reduction in the d-current.

6.2.2 Torque Estimation

The equation for the error in the torque estimation is the same as equation 6.10 from the voltage model. On the other hand, the torque estimation in the current model is not parameter sensitive to the same parameters as in the voltage model. In the current model, the estimated torque is parameter sensitive to the rotor resistance and the main reactance. In figure 6.23 one sees the torque estimation with deviations in both the rotor resistance and the main reactance. If one compares these two figures with figure 6.18, it is evident that the current model has not the same problems as the voltage model around zero speed. The torque estimation of the current model is not dependent on speed in normal operation, but only dependent on the torque level in the machine. In the field-weakening operation, the torque estimation is dependent on both speed and torque in the machine.

6.2.3 Stator Flux Linkage Estimation

The stator flux linkage estimation is not necessary for the current model, but it is interesting to compare the estimation precision of the models. As discussed in section 6.1.1, the stator flux linkage estimation is highly dependent on the estimate of the stator resistance at low-speed operation in the voltage model. In the current model, the estimation is not dependent on the stator resistance but the rotor resistance. Besides, the sensitivity dependency of speed in the current model does not exist in the

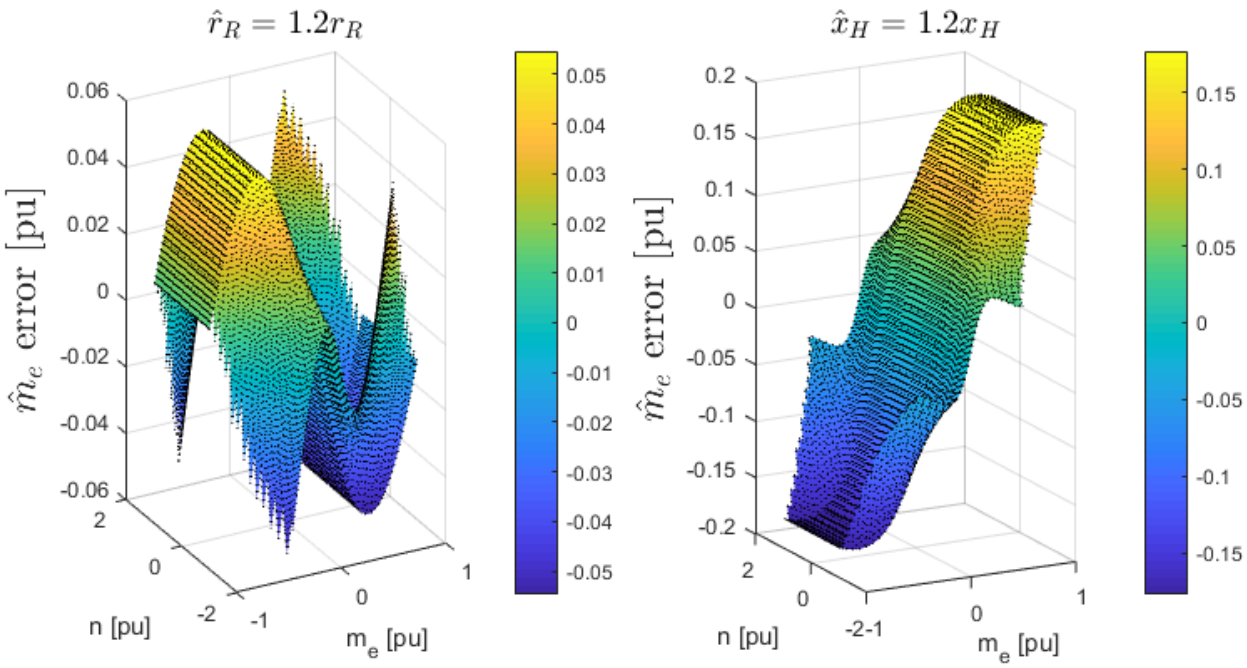

Figure 6.23: Error in estimation of torque using the current model with deviation in rotor resistance and main reactance

normal operation area. Also, the estimation of the stator flux linkage SV is parameter sensitive to the main reactance and also the leakage reactances, but a correct estimate of the main reactance is more vital than the leakage reactances.

The error in the estimation of the stator flux linkage amplitude is written as:

$$\hat{\psi}_{s1,err} = \sqrt{\hat{\psi}_{sd1}^2 + \hat{\psi}_{sq1}^2} - \psi_{s1} \tag{6.15}$$

Where

$$\begin{aligned} \hat{\psi}_{sd1} &= \hat{\psi}_R + \hat{x}_\sigma \hat{i}_{sd1} + (\hat{x}_\sigma - \hat{x}_{s\sigma})\hat{i}_{sd2} \\ \hat{\psi}_{sq1} &= \hat{x}_\sigma \hat{i}_{sq1} + (\hat{x}_\sigma - \hat{x}_{s\sigma})\hat{i}_{sq2} \end{aligned} \tag{6.16}$$

As seen in equation 6.15 and 6.16 the error of the stator flux linkage's amplitude estimation depends on the rotor flux linkage's amplitude estimation, the direct and quadrature components of the current (which implies the rotor flux linkage's angle estimation) and the leakage reactances. By comparing figure 6.20 and 6.24, it is observed that the shape of the figures looks alike. This indicates that the estimation of the rotor flux linkage amplitude is significant for estimating the stator flux linkage amplitude. In addition, the figures 6.21 and 6.25 are very similar and it confirms the

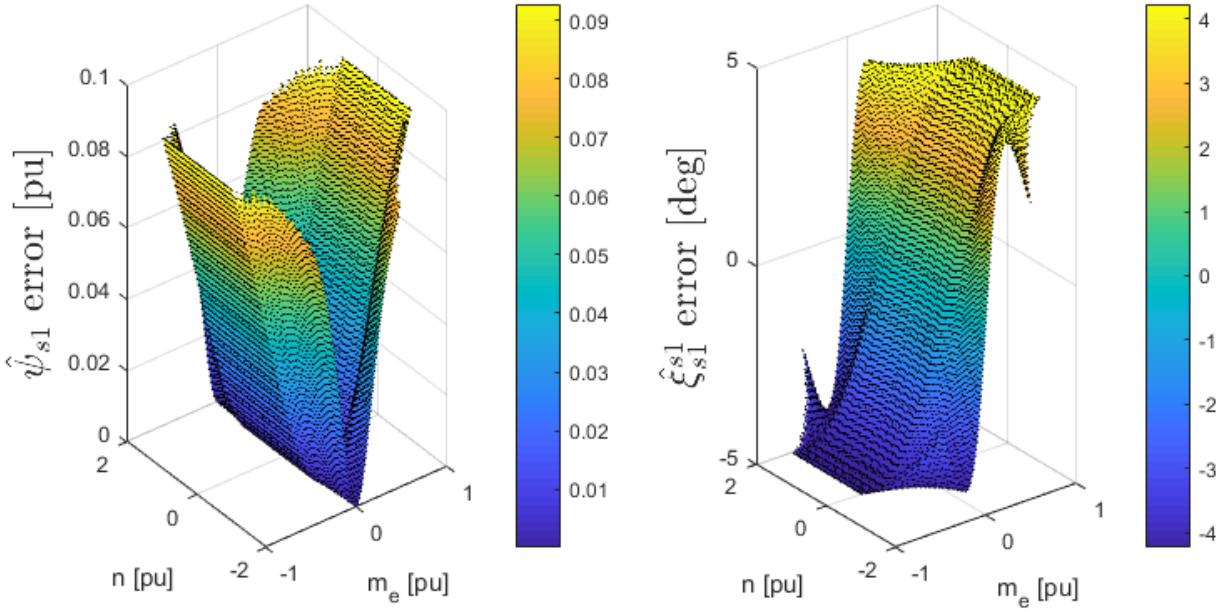

Figure 6.24: Error in estimation of stator flux linkage using the current model with $\hat{r}_R = 1.2r_R$

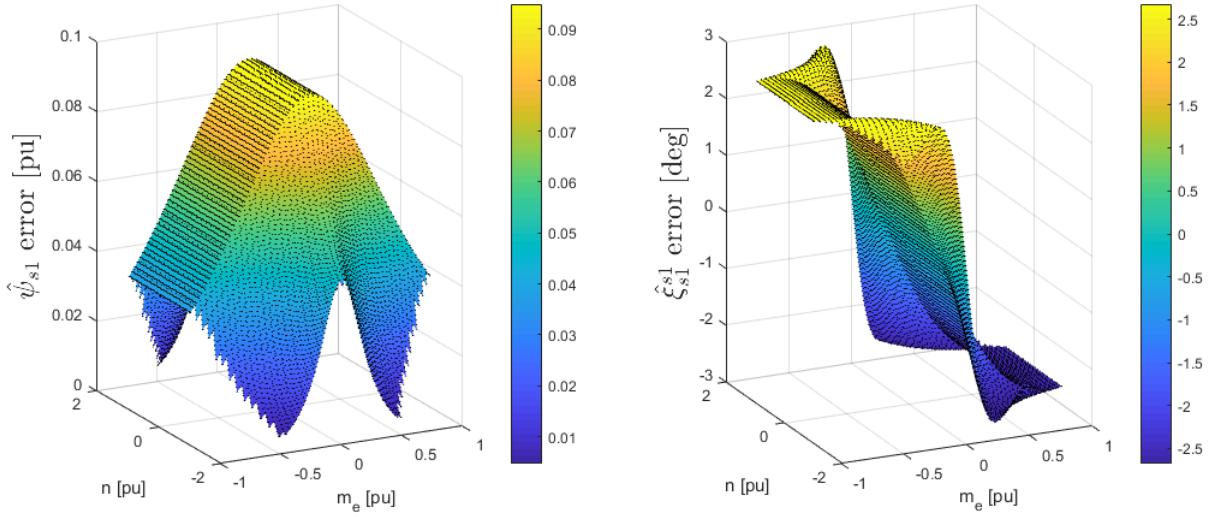

Figure 6.25: Error in estimation of stator flux linkage using the current model with $\hat{x}_H = 1.1x_H$

same.

The error in the estimation of the stator flux linkage angle is written as:

$$\hat{\xi}^{s1}_{s1,err} = \arctan \frac{\hat{\psi_{sq1}}}{\hat{\psi}_{sd1}} + \hat{\theta}^{s1}_{R} - \xi^{s1}_{s1} \tag{6.17}$$

Hence, the estimation error is given by equation 6.11 and 6.16 and is parameter sensitive to the rotor resistance, main inductance and the leakage reactances. The error from a wrongly estimated rotor resistance and main reactance is seen in figure 6.24 and 6.25.

7 Dynamic Parameter Sensitivity Analysis and Drifting

In the voltage model, the method to obtain the estimation of the stator flux linkage is done by an open integration. In this open integration, non-linear voltage losses, time delays, and a wrongly estimated stator resistance cause a phenomenon called drifting[11]. The name drifting motivates from the fact that the origo of the stator flux linkage estimated SV seems to drift away from the real origo. Vector addition explains the phenomenon and the most obvious way to understand it is by imagining a DC offset in the measurement of the voltage or the current. This DC offset causes the estimated SV to move away from the correct position at every instant. Then the origo drifts away more and more for every time instant the DC offset is present. The drifting phenomenon is drawn in figure 7.1 where the origo of the estimated stator flux linkage SV is drifted to the right, which can be a result of a DC offset under magnetization.

$$\begin{aligned}\hat{\psi}_{s1,\alpha}[k] &= \hat{\psi}_{s1,\alpha}[k-1] + \omega_n T_{samp}(u_{s1,\alpha} - \hat{r}_s i_{s1,\alpha}[k-1]) \\ \hat{\psi}_{s1,\beta}[k] &= \hat{\psi}_{s1,\beta}[k-1] + \omega_n T_{samp}(u_{s1,\beta} - \hat{r}_s i_{s1,\beta}[k-1])\end{aligned} \tag{7.1}$$

By examining the discrete equation of the stator flux linkage estimation (equation 7.1) one clearly understands that the error in an earlier time instant does not disappear and is a part of the estimation for all future. This means that if drifting has already happened, the origo is misplaced for all future if not some correction is done. In some cases the cause of drifting is symmetrical in steady state(for example a wrongly estimated stator resistance) that creates an error function with a sum of zero over one period. Hence, a filter can be a solution against the drifting phenomenon. In the literature, there exist different solutions against drifting. Hu and Wu investigated different methods for modifying the pure integrator and make it behave like a low pass filter[3]. Later in this section, a correction method presented by Niemelä in his doctoral thesis from 1999[5] is analyzed.

Figure 7.2 shows the principle of drifting. It is imagined that the estimated stator resistance is wrong and the reference of the electrical torque changes its value, and hence the current changes its q component value. Then rotation of the stator flux linkage SV, voltage SV, and current SV start rotating, all with the same rotational speed. However, as the integral of the estimated stator flux equation is wrong since the stator resistance is estimated wrong, the estimated stator flux linkage SV follows a different path than the original stator flux linkage SV. This is seen by following the dashed blue vectors in the figure. As the voltage generally is proportional to the speed of the motor, the voltage SV is not stationary until the speed is constant. Then when

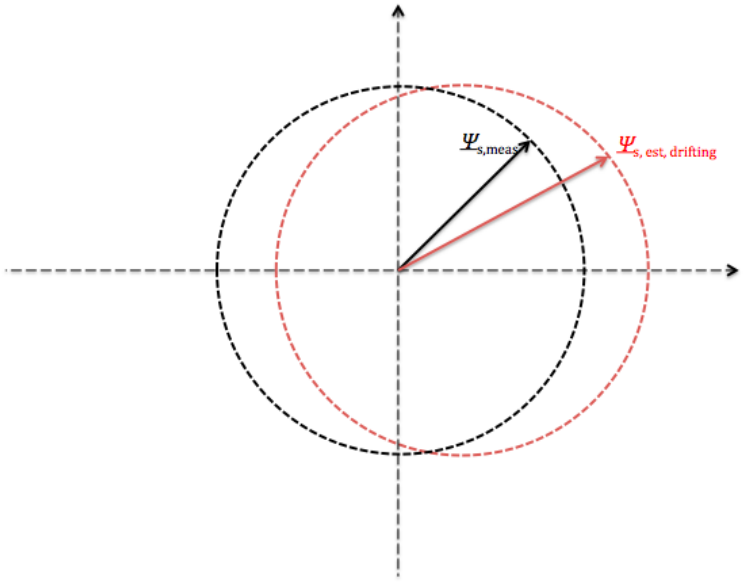

Figure 7.1: Stator flux linkage vector measured vs estimated and drifted[15]

the voltage SV is stationary, the stator flux linkage integral is also stationary. Then at each new time step, the magnitude of the vectors in the integral (second term of equation 7.1) is the same as before. Hence, the estimated stator flux linkage rotates along a circular path again which in the figure corresponds to the red dashed circle. On the other hand, the time between the electrical torque reference changed until the speed was stationary (during the dynamics), the origo of the estimated stator flux linkage drifted away from its original origo, and like that drifting occurs. The estimated rotor flux linkage SV experiences also drifting since it is a function of the estimated stator flux linkage SV.

In this thesis, the measurement errors in the voltage and current measurements are not analyzed. Hence, the error analyzed is how a wrong estimation of the stator resistance produces drifting. The error is explained mathematically by the following equations:

$$\begin{aligned}\hat{\boldsymbol{\psi}}_{s1,err} = \boldsymbol{\psi}_{s1} - \hat{\boldsymbol{\psi}}_{s1} &= \int \mathbf{u}_{s1}dt - r_s \int \mathbf{i}_{s1}dt - \int \mathbf{u}_{s1} + \hat{r}_s \int \mathbf{i}_{s1}dt \\ &= \Delta r_s \int \mathbf{i}_{s1}dt \\ &= \Delta r_s \int i_{s1,peak}(t)e^{j\omega(t)t}dt\end{aligned} \tag{7.2}$$

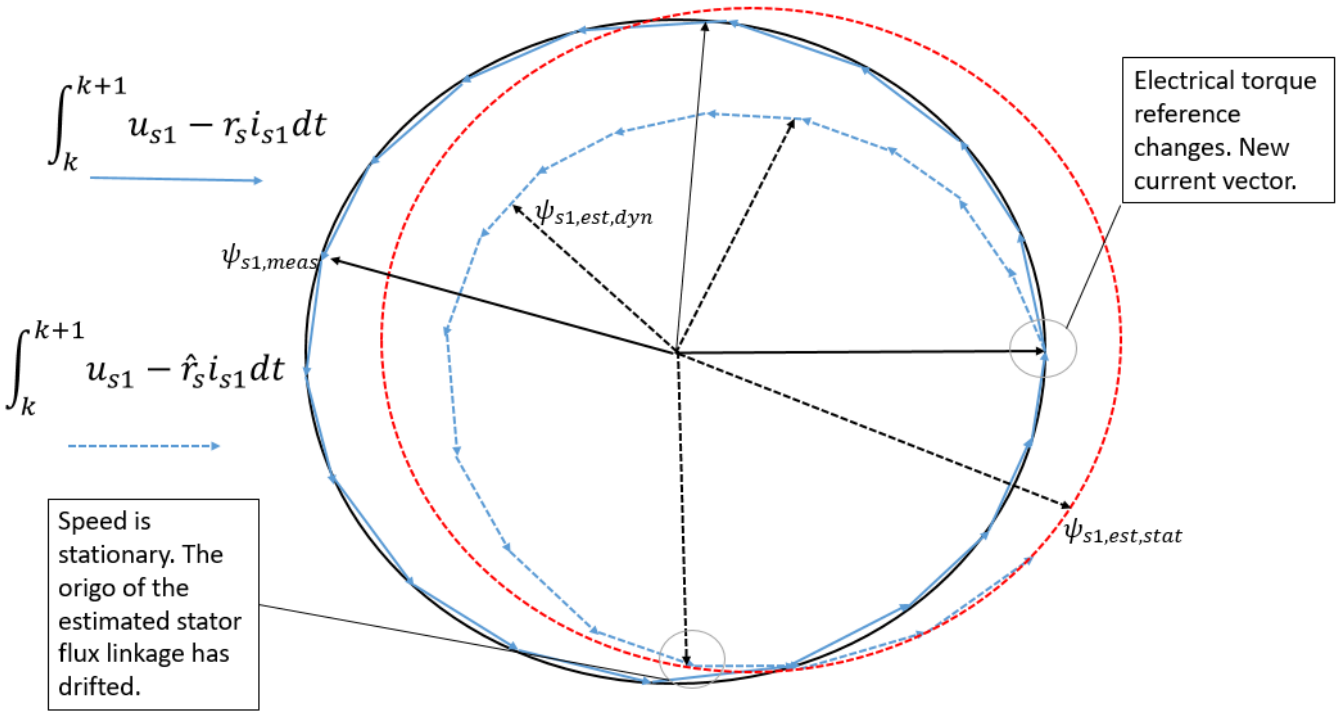

Figure 7.2: The principle of drifting as consequence of a wrongly estimated stator resistance

$$i_{s1,peak}(t) = \sqrt{i_{sd1}(t)^2 + i_{sq1}(t)^2} \tag{7.3}$$

$$\omega(t) = 2\pi f_s = 2\pi \frac{1}{J} \int m_e(t) - m_L(t) dt - f_r(t) \tag{7.4}$$

As observed, this set of equations sum up to a nonlinear system that is complicated to analyze. However, some observations are possible. For example, if the electrical reference torque changes, the q component of the current alters its value to change the electrical torque level to the reference. This dynamic happens almost instantly compared to the change in speed. The difference between the electrical torque generated in the motor and the load torque produces the change in speed. Hence, the characteristics of the load torque are significant for the dynamics. In the simulations done in this thesis, the load torque had pump characteristics. The rate of the speed change is a function of the moment of inertia in the machine. Since drifting occurs during dynamics in the machine, and the speed changes slower than the generated electrical torque, the time the speed changes is vital for the magnitude of drifting.

This is understood intuitively by the more time in dynamics before steady-state operation with a wrongly estimated stator resistance, the more drifting magnitude. Also, in equation 7.4 the rotor frequency as it is a function of the q component of the current and the rotor flux in the machine have an impact dynamically. Especially around zero speed, the rotor frequency has an impact as its magnitude is relatively significant for the equation. At the high-speed level, it can be neglected. On the other hand, the rotor frequency changes relatively instant compared to the change in speed, and it can be assumed constant at each electrical torque level. In equation 7.3 the d component, which controls the rotor flux of the machine, is present. The rotor flux of the machine is generally constant during operation (if flux-weakening operation and DC magnetization are neglected) and hence the d component of the current is assumed constant.

7.1 DC Magnetization

To start the machine DC magnetization is done before the machine starts rotating, giving the rotor flux linkage vector an appropriate value (1 pu), and hence the electrical torque can be controlled up to 1 pu. At DC magnetization one cannot use the voltage model since the frequency is zero, and hence the stator flux linkage is not observable in the stator flux equation. The stator flux equation is simply Ohm's law:

$$u_{s1} = r_s i_{s1} \tag{7.5}$$

To magnetize the machine one uses the current model at zero speed and project the current in the α axis. Hence the direct axis is equal to the α axis, and the machine is magnetized following the expression:

$$\frac{d\hat{\psi}_R}{dt} = -\frac{1}{\hat{T}_r}\hat{\psi}_R + \frac{\hat{x}_H}{\hat{T}_r}(i_{s\alpha 1} + i_{s\alpha 2}) \tag{7.6}$$

In a discrete representation:

$$\hat{\psi}_R[k] = \frac{\hat{x}_H T_{samp}}{\hat{T}_r + T_{samp}}(i_{s\alpha 1} + i_{s\alpha 2})[k-1] + \frac{\hat{T}_r}{\hat{T}_r + T_{samp}}\hat{\psi}_R[k-1] \tag{7.7}$$

The direction of the rotor flux linkage SV is the same as the current SV, hence the direct component of the rotating axis corresponds the α axis under magnetization.

One can see from equation 7.7 that if the main inductance is estimated wrong, the rotor flux linkage is also estimated wrong. This gives further a wrongly estimated stator flux linkage.

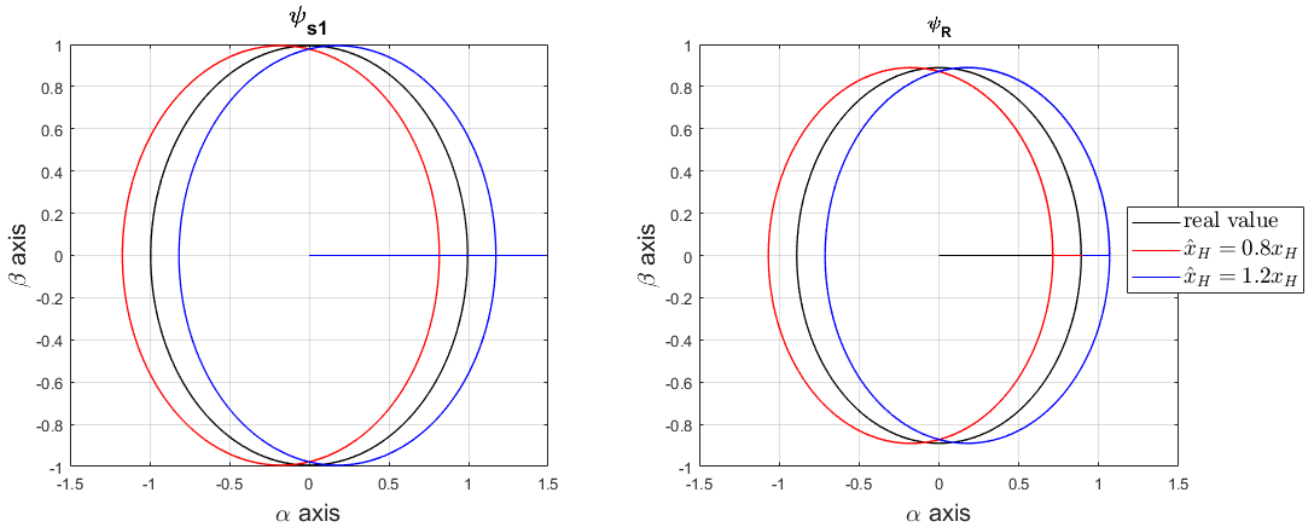

Figure 7.3: DC magnetization with a wrongly estimated main reactance.

To estimate the stator flux linkage under magnetization one uses the expression:

$$\hat{\psi}_{s1} = \hat{\psi}_{sd1} = \hat{\psi}_{s\alpha 1} = \hat{x}_\sigma i_{s\alpha 1} + (\hat{x}_\sigma - \hat{x}_{s\sigma}) i_{s\alpha 2} + \hat{\psi}_R \tag{7.8}$$

Which in a discrete representation is written:

$$\hat{\psi}_{s1}[k] = \hat{x}_\sigma i_{s\alpha 1}[k] + (\hat{x}_\sigma - \hat{x}_{s\sigma}) i_{s\alpha 2}[k] + \hat{\psi}_R[k-1] \tag{7.9}$$

In equation 7.9 one sees that the stator flux linkage estimate is a function of both the estimated leakage reactance and the estimated stator leakage reactance, as well as the estimated rotor flux linkage magnitude. Hence when the machine starts rotating and the voltage model is used for estimating the stator flux linkage, both the stator flux linkage estimate and the rotor flux estimate would have experienced a drifting in the direction of the current vector, if some of the reactances are estimated wrong. In figure 7.3, it is shown two examples of DC offsets under magnetization caused by a wrongly estimated main reactance. If the estimated main reactance has a lower value than the real one, the estimated flux origo drifts to the left and oppositely if the estimated main reactance has a higher value than the real main reactance.

7.2 Torque/Speed Reference Change

As the machine is torque or speed regulated, a change in the reference of these values creates a dynamic situation where the current and voltage change. If the stator

resistance is estimated wrong in a dynamic situation, the open integration integrates an error, and the integrated error varies until the torque and speed are fixed, and the machine operates in steady-state. When the machine operates stationary (fixed speed and torque) the error still gets integrated, but since the current and voltage SV rotate and have a constant amplitude, the error function is integrated to zero in one period, and there is no more drifting.

In figure 7.4, it is simulated torque steps which generate speed change and change in the error of the estimated stator flux linkage amplitude. It is shown that even though the speed is not low a dynamic situation, which occurd as a consequence of the steps in the electrical torque reference, creates a change in drifting. As assumed the change in drifting (change in error of the stator flux linkage amplitude) is at most when the speed is at lowest (around 0.5 pu). The change in drifting is also a function of the direction of the current vector, and hence for some steps, the error of the estimated stator flux linkage amplitude decreases. This occurs because the direction of the drifting is in the opposite direction of the drifting that already had happened.

7.3 Frequency Dependency

In figure 7.5 it is observed the frequency dependency of the drifting. In time t=1.8s there is a sudden change in the estimated resistance and the estimated stator flux linkage SV starts drifting. This is simulated for different frequencies and observed that the error oscillates with a different amplitude for both amplitude and angle error for the stator flux linkage estimate. From the figure 7.5's cursor points it is observed that the amplitude error is approximately inversely proportional to the frequency at the time the drifting starts. The blue frequency is 2.14078 times the frequency of the green line. The peak-to-peak error in amplitude estimation of the blue line is 1.98855 times the green line, and the peak-to-peak error in angle estimation is 2.0528 times the green line.

Investigating equation 7.2 again and assuming constant peak current and speed:

$$\begin{aligned} \hat{\psi}_{s1,err} &= \Delta r_s \int i_{s1,peak} e^{j\omega t} dt \\ &= \frac{\Delta r_s i_{s1,peak}}{\omega} [-j e^{j\omega t}] \\ &= \frac{\Delta r_s i_{s1,peak}}{2\pi f_s} [-j e^{j\omega t}] \end{aligned} \tag{7.10}$$

As seen in equation 7.10 the error is inversely proportional to frequency if one assumes a constant speed and peak current. In figure 7.5 the speed is close to constant, and

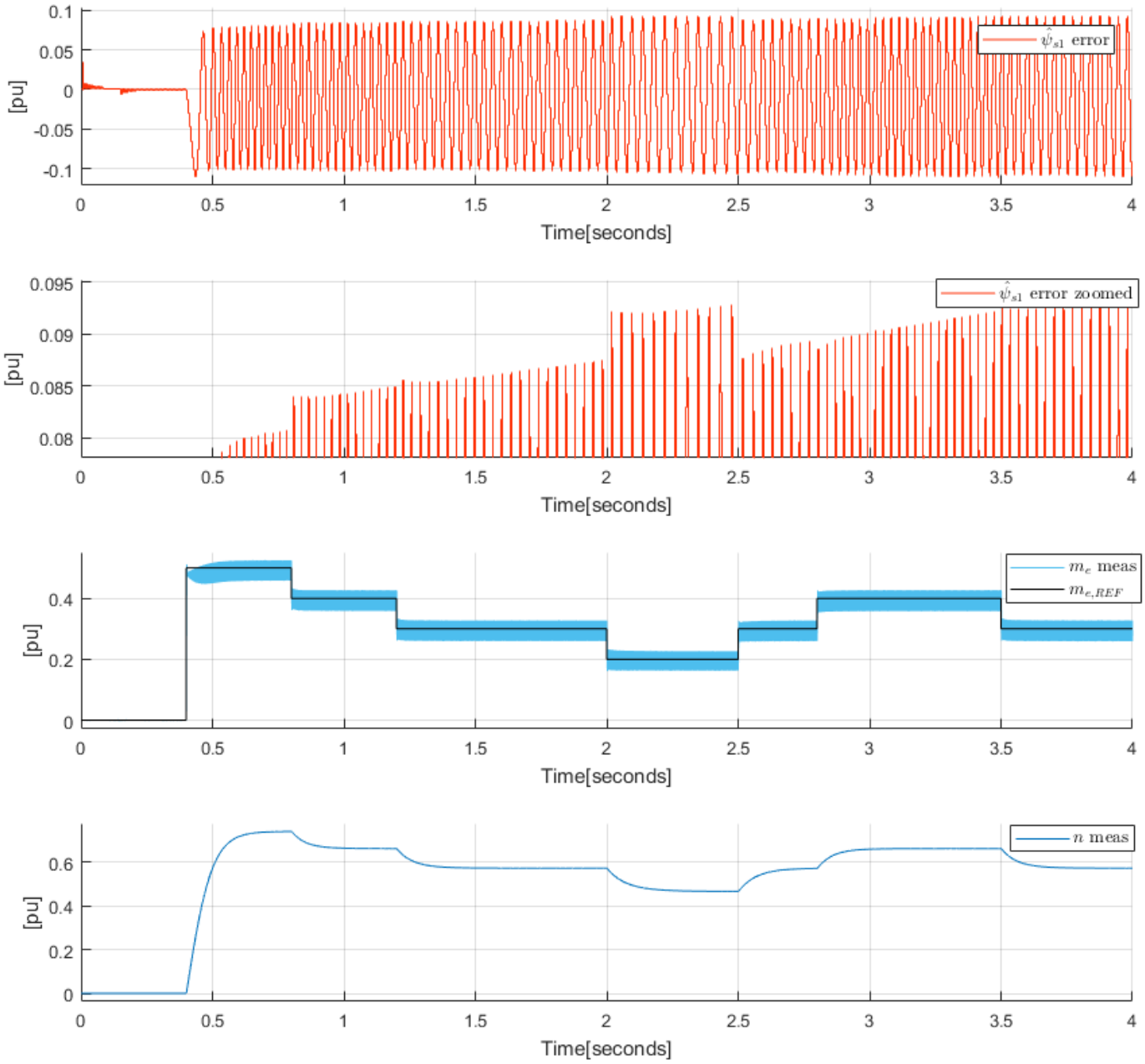

Figure 7.4: Step change in electrical torque reference which produces changes in the drifting of the stator flux linkage estimation

the peak current is assumed constant. Hence, the equation 7.10 can serve as an approximation of a mathematical expression for drifting.

7.4 Crossing Zero Speed and Low-Speed Operation

As discussed in the stationary parameter sensitivity analysis, when the speed decreases the voltage also drops which implies a more critical resistance estimation. Stationary the integral of the error caused by the wrongly estimated resistance(equation 7.5), is a sinusoidal function with an amplitude inversely proportional to the frequency of the stator flux linkage. Hence at low frequencies this amplitude is high.

In figure 7.6 and 7.7, it is clear that the error of the estimated stator flux linkage amplitude and angle changes because of drifting when the motor crosses zero speed. This is natural because at a motor speed close to or at zero the voltage SV decreases to a minimum value and the current SV multiplied with the estimated resistance has a significant impact. Hence, if the estimated resistance is wrong (as it is in figure 7.6 and 7.7) it is natural that drifting occurs. It is also clear after comparing the dashed black circle (measured values) to the blue (estimated circle after magnetization) in figure 7.6, that there is a drift problem starting after the magnetization period of the machine because of a wrongly estimated stator resistance. This fact is also clear in figure 7.7, where one sees that after the motor starts rotating the error of both the amplitude and angle is nonzero. The drifting from the blue circle to the red, which is seen in the first figure in figure 7.6, occurs the first time the motor speed crosses zero. This is seen in figure 7.7 and occurs around Time= 1.4[sec], and the error increases for both amplitude and angle because of the estimated circle drifts away from the real measured circle of the stator flux linkage SV. In the second figure in figure 7.6, the next crossing through zero speed occurs, and as seen in figure 7.7, this occurs approximately when Time= 2.3[sec] and again the error increases due to the direction of the drifting is away from the original and real circle. Then in the third and last figure of figure 7.6, another crossing through zero speed takes place and now the error decreases since the drifting direction is towards the original and real stator flux linkage SV circle. From figure 7.7 it is observed that this occurs at Time= 2.7[sec] and indeed the error of both amplitude and angle drops.

Like discussed earlier in this section, drifting is a dynamical phenomenon, and during the dynamics, the error gets integrated, and the origo of the estimated flux linkage is misplaced. This is seen in figure 7.8 and 7.9 where the speed decreases for a longer period. Here the estimated stator resistance is simulated with a 50% value of the real stator resistance. It is observed that from the start after the DC magnetization, the estimated fluxes drift away from the real origo. This is because, in the same way as in

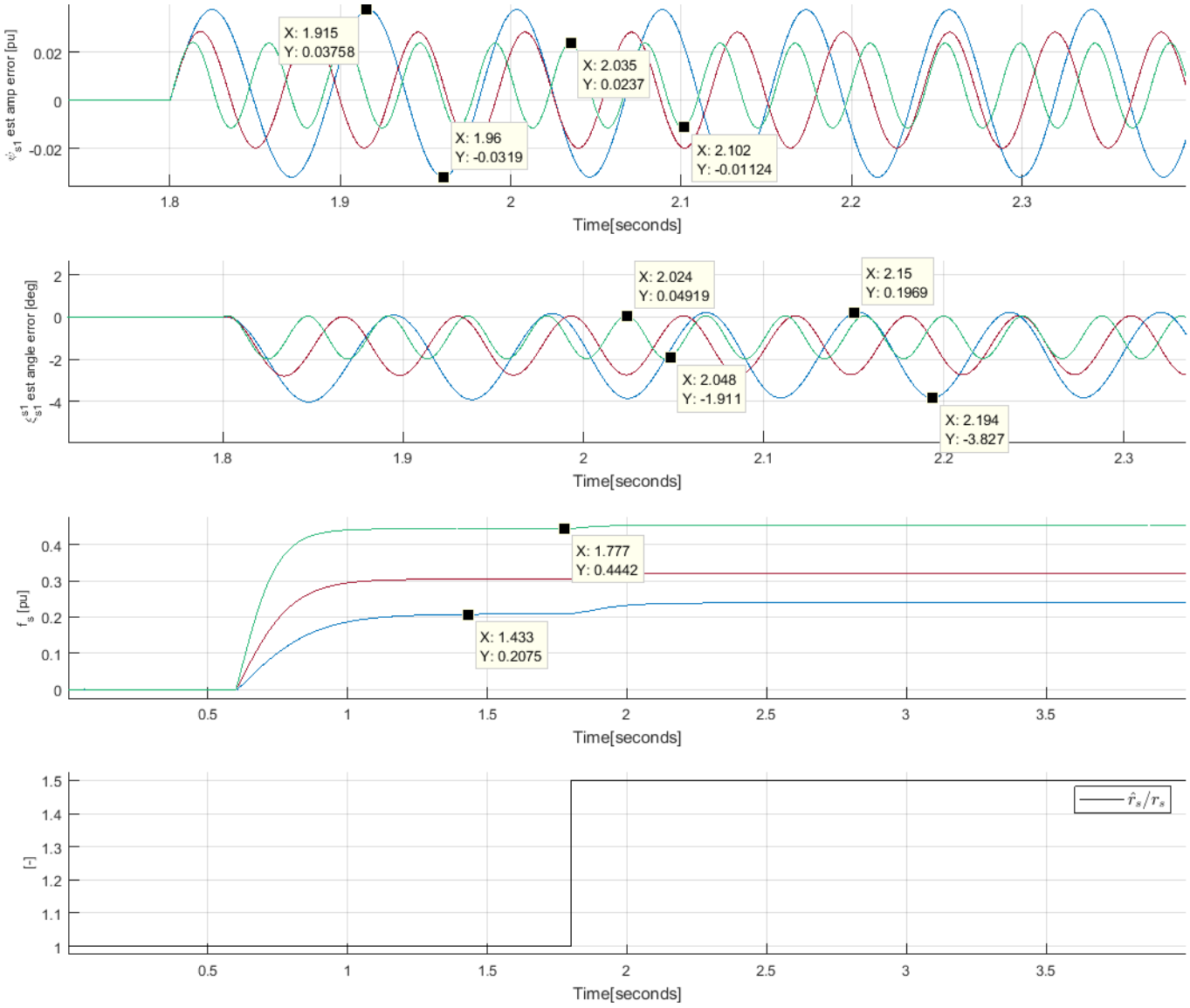

Figure 7.5: Frequency dependency at the dynamic start

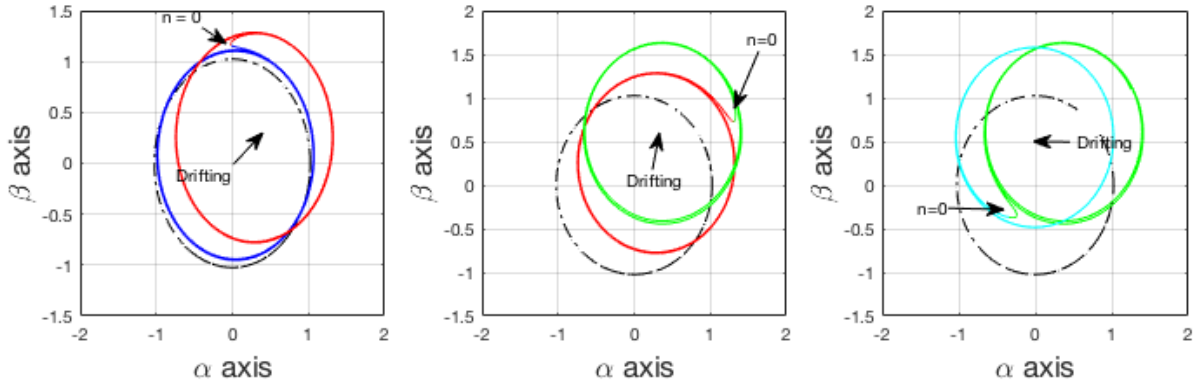

Figure 7.6: Drifting of the $\hat{\psi}_{s1}$ space vector at zeros speed crossing with $\hat{r}_s = 0.5r_s$. The black circle is from the measured stator flux linkage space vector

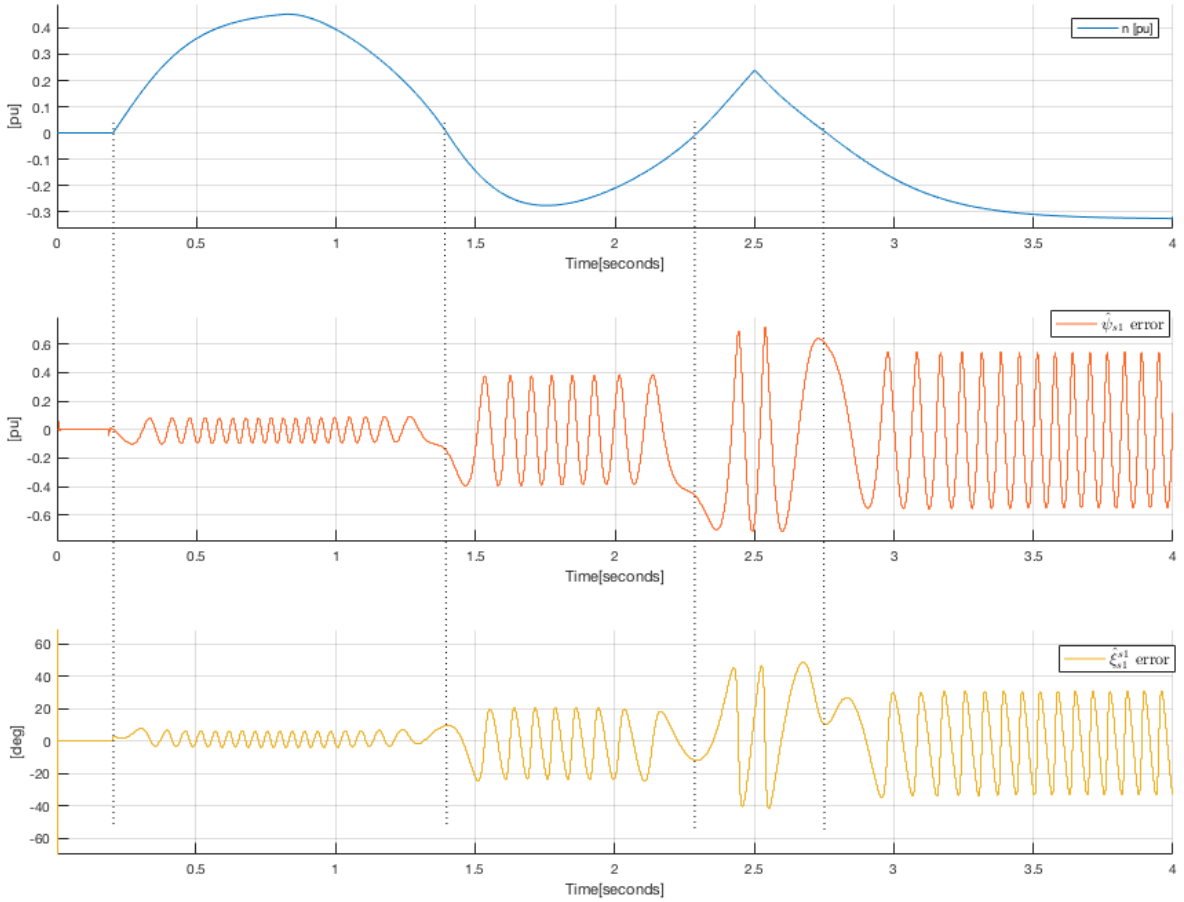

Figure 7.7: Estimated stator flux linkage amplitude and angle error changes for every crossing over zero speed

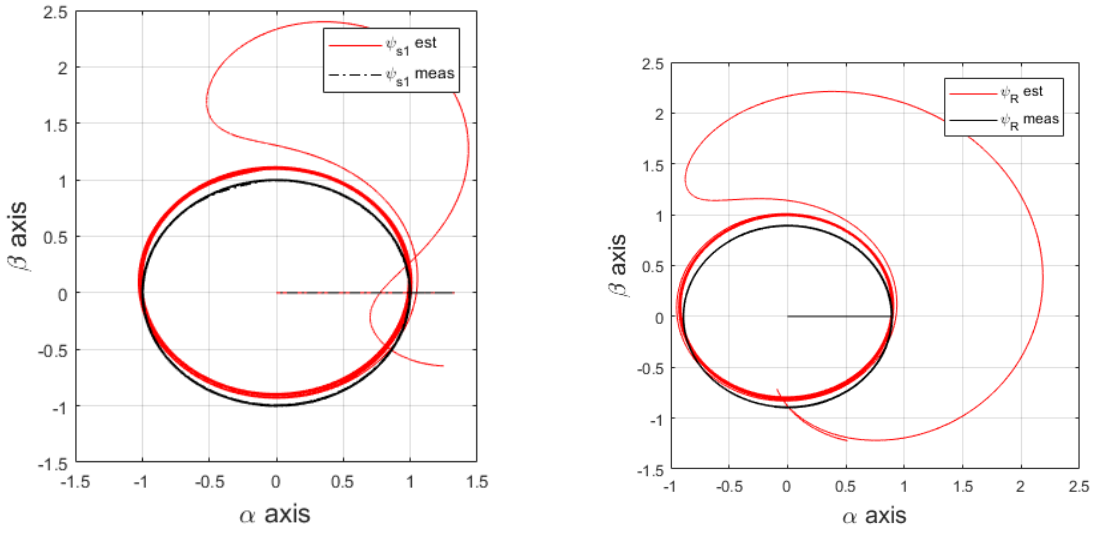

(a) ψ_{s1} est and measured

(b) ψ_R est and measured

Figure 7.8: Drifting of $\hat{\psi}_{s1}$ and $\hat{\psi}_R$ as a consequence of a wrongly estimated stator resistance. At around zero speed the error gets integrated for a long time in the same direction and the estimated stator flux linkage becomes unstable

figure 7.6 and 7.7, that after DC magnetization is done, the machine starts rotating which implies a dynamical situation. Since the wrongly estimated stator resistance is multiplied by the current in the voltage model, the error is integrated and drifting of the origo has started. The origo drifts away until the speed is constant and hence the voltage in the stator flux linkage integral is fixed. Then the estimated stator flux linkage's origo is fixed until a new dynamic situation takes place(change in the current or voltage). A new dynamic situation starts when the speed drops just before 1 second has passed, which can be seen in figure 7.9. Then the speed decreases and passes zero for two times, and as expected the estimation for both the stator and the rotor flux cannot be trusted in this region. It is seen in figure 7.8 that the error gets integrated over some time, and hence increases. In figure 7.9 it is seen that the amplitude error of both stator and rotor fluxes is estimated wrong by nearly 1.5 pu at maximum and the angles are estimated wrong by around 100 degrees at maximum. This confirms the stationary parameter sensitivity analysis which stated that the voltage model is highly sensitive to stator resistance estimation errors around zero speed.

In figure 7.10 and 7.11, it is evident that different speeds give different drifting magnitudes. It is seen that if the speed is low for a more extended period (turquoise line), the drifting magnitude becomes larger. Like discussed before, this is a consequence

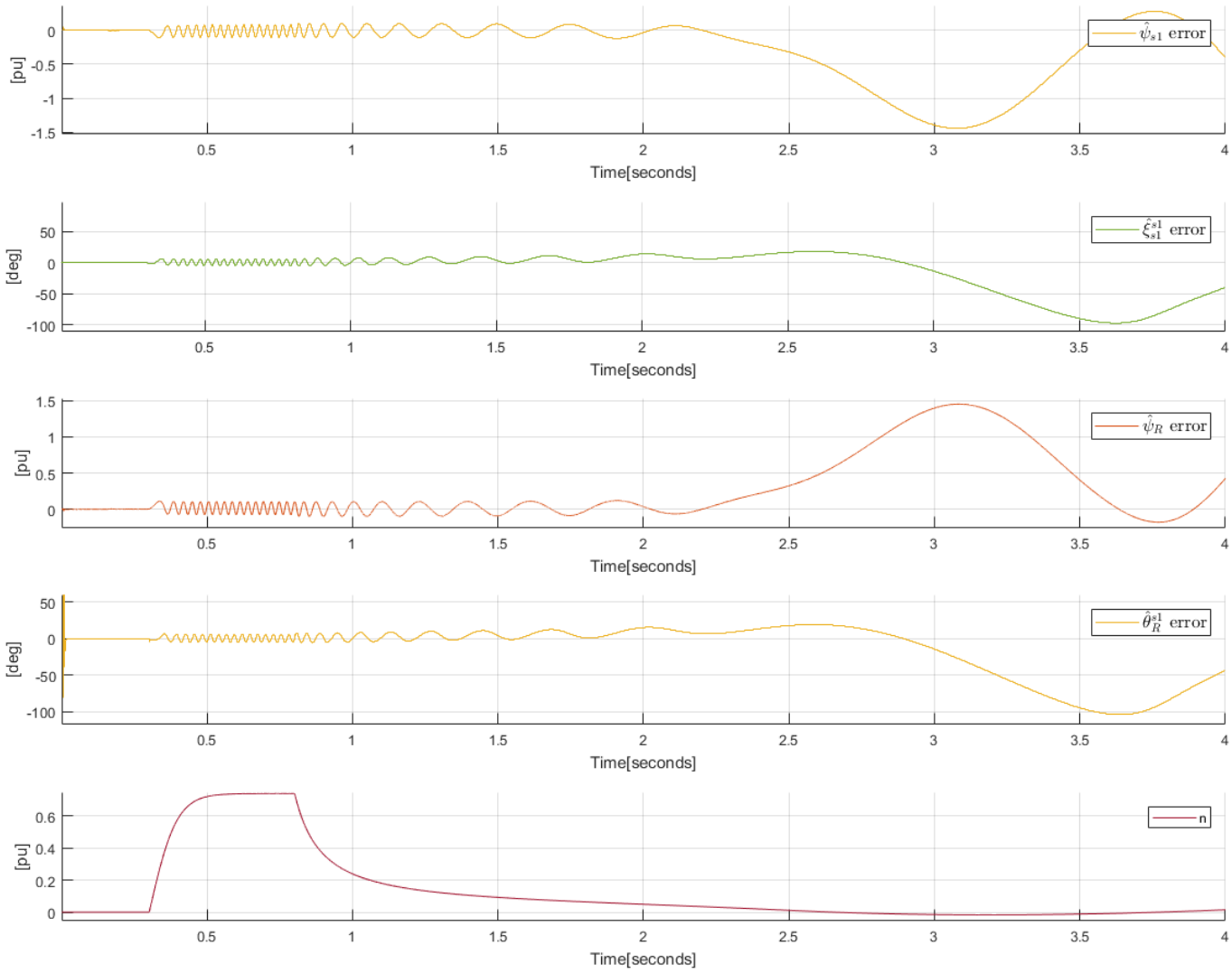

Figure 7.9: Figure 7.8 shown with referenced time and speed

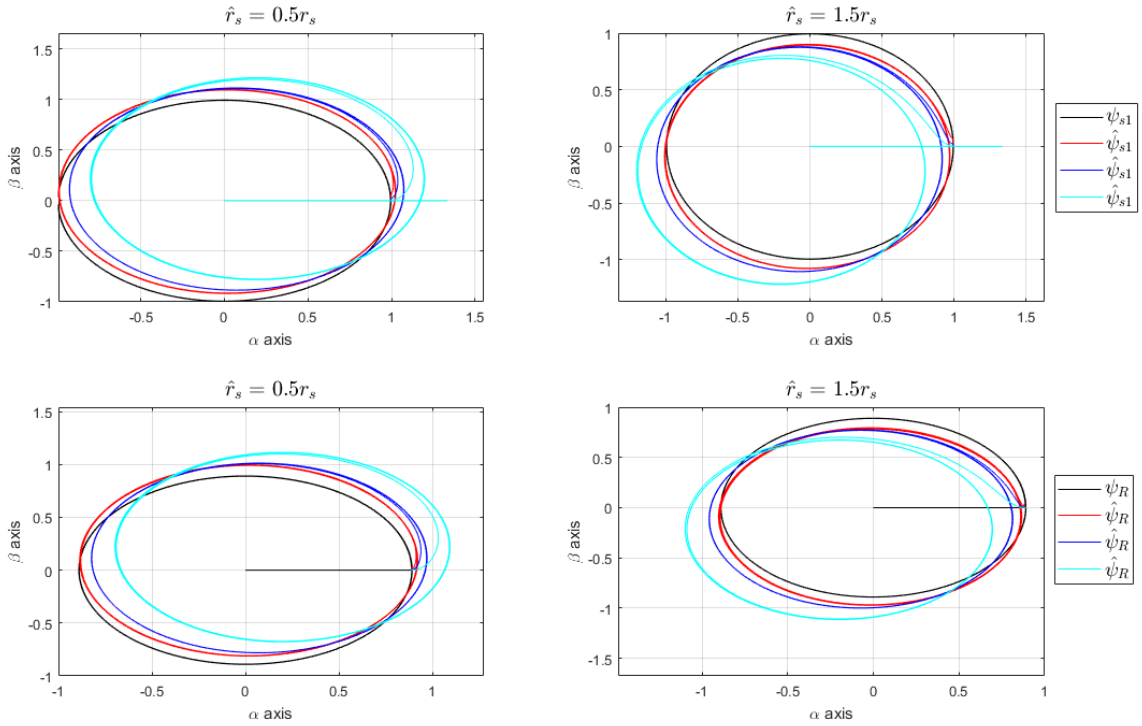

Figure 7.10: Drifting of estimated stator and rotor flux linkage space vectors as a consequence of wrongly estimated stator resistance and a change in speed

of that the estimated resistance multiplied with the current space vector is more significant in equation 7.1 at lower speeds. If one increases the speed (red and blue line) drifting lowers in magnitude.

7.5 Moment of Inertia

As seen in equation 7.2 and 7.4, the moment of inertia has an impact on drifting. Intuitively this is understood by a higher moment of inertia implies a slower speed change, and hence the dynamics occur for a more extended period. Since drifting is a dynamical phenomenon, it is clear that if the dynamics occur for a longer period of time, the drifting will also occur for a more extended period. Especially, as discussed earlier, when the speed is low, and the estimate of the stator resistance is wrong, then drifting is problematic. Hence if the speed is low for a long time because the speed changes very slowly due to a high moment of inertia, the estimated stator flux linkage drifts from its origo. It can be seen in figure 7.12 that drifting is more problematic

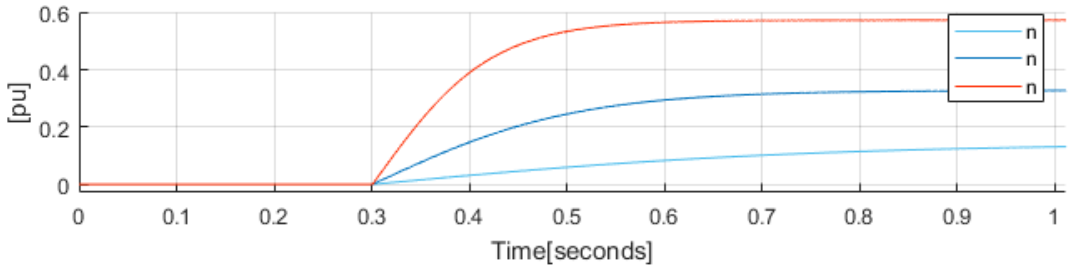

Figure 7.11: Speed change and causes drifting. The colors match with figure 7.10 and it is observed that a slower rise in speed causes more drifting.

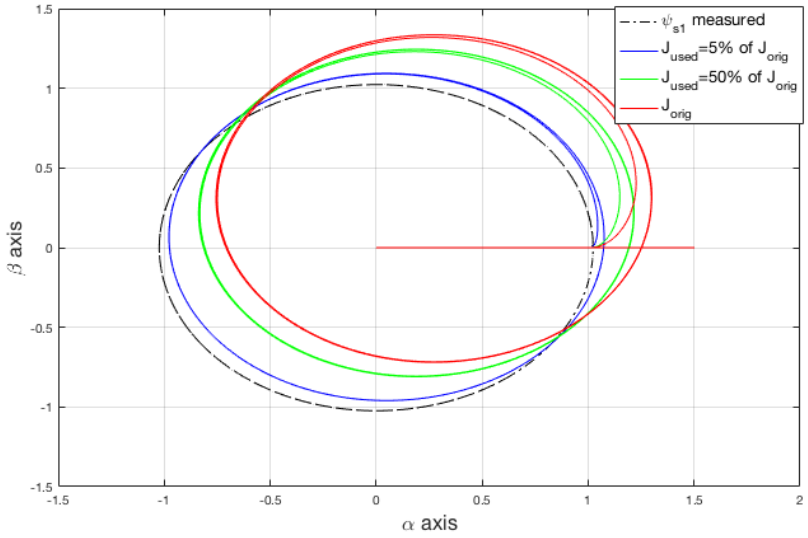

Figure 7.12: Drifting with different values of moment of inertia. Here $\hat{r}_s = 0.5r_s$.

for a machine with a high moment of inertia. As seen in the figure as the value of the moment of inertia goes down, drifting is less critical.

7.6 Correction Method Against Drifting

The correction method against the drifting phenomenon used in this thesis was presented by Niemelä in his doctoral thesis in 1999[5]. This method was presented as an alternative for the more traditional filter solutions and was tested with direct flux linkage control and direct torque control then. Later, this correction method was investigated for a six-phase symmetrical synchronous PM machine by Fossen with field- oriented control (Indirect flux linkage control) in his project thesis in 2016[11]. Now it is investigated with simulations for a six-phase induction motor in this thesis

using field-oriented control.

The principle of the correction method is based on that the square of the estimated stator flux linkage subtracted by the square of a low pass filtered value of the estimated stator flux linkage has a maximum in approximately the same direction as the eccentricity(direction) of the drifting flux component. Hence, this is used as a scalar factor in a correction function. Besides, the estimated stator flux linkage minus a low pass filtered value gives a good indication of how much the estimated stator flux linkage has drifted. For example, if the estimation has drifted relatively much, the estimated stator flux linkage minus the low pass filtered value gives a high value and contribute a lot to the correction function. On the other hand, if the estimated stator flux linkage has not drifted much the low pass filtered value is approximately the same, and the subtraction is nearly zero. The correction factor is calculated by the following function[5]:

$$\begin{aligned} \psi_{s\alpha 1,corr} &= k_{corr}(\hat{\psi}^2_{s1,filt} - \hat{\psi}^2_{s1})\hat{\psi}_{s\alpha 1} \\ \psi_{s\beta 1,corr} &= k_{corr}(\hat{\psi}^2_{s1,filt} - \hat{\psi}^2_{s1})\hat{\psi}_{s\beta 1} \end{aligned} \tag{7.11}$$

The time constant in the low pass filter is suggested by Fossen[11]:

$$T_{filter} = min\{1.75, \frac{2}{f_s f_N}\} \tag{7.12}$$

Hence, the filter is frequency dependent which gives better performance at low frequencies. A notable improvement made by Fossen of the filter is to introduce a zero point to prevent that a change in the current is corrected as drifting in the low pass filter. The ratio of the time constant of the zero point and the filter time constant is called k_t, and this ratio is tuned as a gain to prevent drifting correction during torque steps in the machine.

$$k_t = \frac{T_{zero}}{T_{filter}} \tag{7.13}$$

k_{corr} in equation 7.11 is a correction coefficient that shall depend on the stator flux linkage frequency. After the correction factor is calculated, the new and corrected estimation of the stator flux linkage is hence:

$$\begin{aligned} \hat{\psi}_{s\alpha 1}[k] &= \hat{\psi}_{s\alpha 1}[k-1] + \psi_{s\alpha 1,corr} \\ \hat{\psi}_{s\beta 1}[k] &= \hat{\psi}_{s\beta 1}[k-1] + \psi_{s\beta 1,corr} \end{aligned} \tag{7.14}$$

The block diagram of the process is seen in figure 7.13. The expression for the correction coefficient, k_{corr}, is suggested adaptive in an IEEE paper from Luukko,

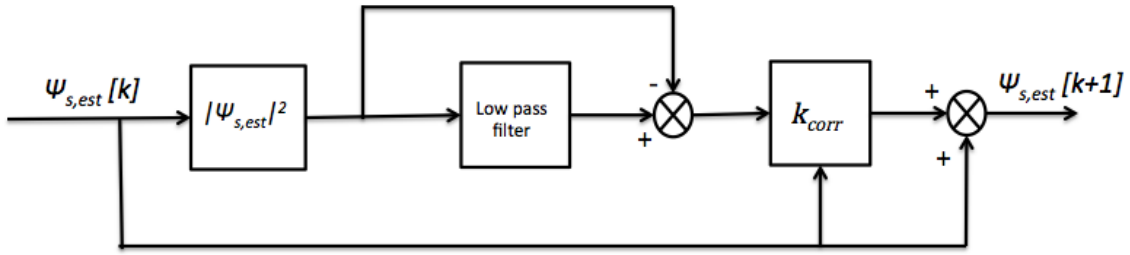

Figure 7.13: Block diagram correction method against drifting[15]

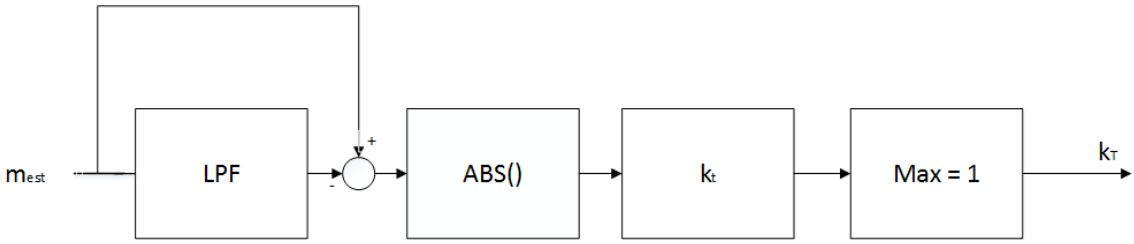

Figure 7.14: Adaptive calculation of k_T

Niemelä and Pyrhönen[7] and also worked on by Fossen in his project thesis[11]:

$$k_{corr} = (1 - k_T)k_{corr,0} \tag{7.15}$$

Here k_{corr} has an adaptive value that is dependent on torque steps in the machine. If a torque step occurs the estimated stator flux linkage should not be corrected. The estimated torque gets filtered through a low pass filter which is not fast enough to filter a step. Hence after a step in torque one exploits the difference between the estimated torque and the filtered as a signal to indicate torque steps. This is multiplied with k_t which can be tuned and in the end, limited to be maximum 1. k_t is suggested chosen of how big response k_T should have for a given torque step[7]. For example if one wants $k_T = 1$ for a torque step of 0.5 one chooses $k_t = 2$. The whole process of calculating k_T is seen in figure 7.14. If $k_T = 1$ one sees in equation 7.15 that the correction coefficient, k_{corr} is then zero and no correction on the estimated stator flux linkage is done. $k_{corr,0}$ is used as a base value in equation 7.15 and can be tuned. In the end the discrete filtered value can be calculated by the function:

$$\hat{\psi}^2_{s1,filt}[k] = \hat{\psi}^2_{s1,filt}[k-1](1 - \frac{T_{samp}}{T_{filt}}) + \hat{\psi}^2_{s1}[k]\frac{T_{samp}}{T_{filt}} + (\hat{\psi}^2_{s1}[k] - \hat{\psi}^2_{s1}[k-1])k_T \tag{7.16}$$

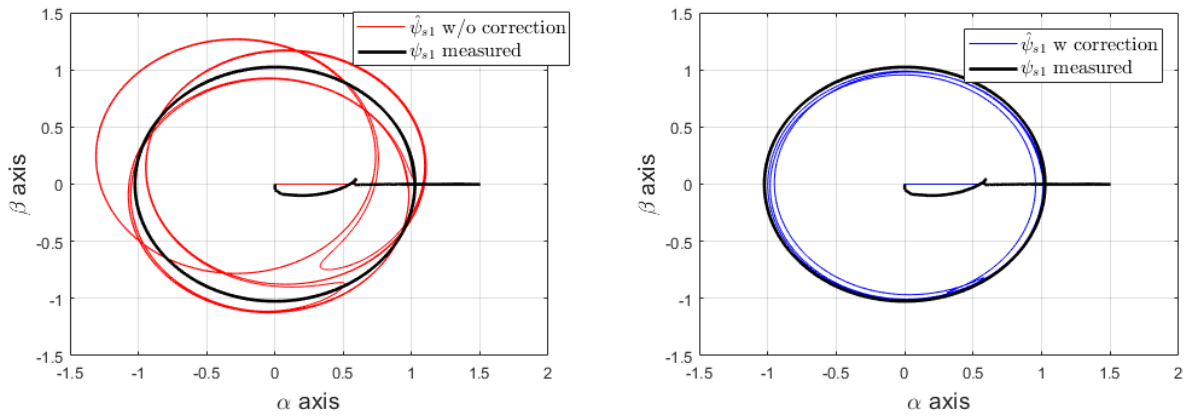

Figure 8.1: XY plot of the drifting of estimated stator flux linkage and correction. $\hat{r}_s = 1.5 r_s$.

8 Speed-Sensorless Operation Performance

8.1 Corrector block

From figure 8.1 and 8.2, it is evident that the corrector block improves the estimation of the stator flux linkage SV. In this simulation, the estimated stator resistance is 150% of the real value, and hence this can be considered as an extreme scenario. To the left of the figures, it is evident that the drifting is a critical problem for the estimation and the error varies in a sinusoidal way and increases for each dynamical situation that occurs in the motor. The error is increasing for both amplitude and angle because the drifting is in a direction away from the real origo. On the right side of the figure, there is a blue circle (estimated stator flux linkage) that nearly corresponds to the real and measured stator flux linkage SV. It is observed in figure 8.2 that at each dynamical situation (change in torque reference) the corrector block removes the drifting adequately.

8.1.1 Disturbance When Estimated Stator Resistance Is Correct

In figure 8.3, it is demonstrated a drawback with the correction method. In this simulation, the estimated stator resistance is the same as the real resistance. Hence, no estimation errors. On the other hand, it can be seen that when there is a step in torque the correction method corrects this for a short period, acting as a disturbance on the flux model. Without the correction method, the estimation is without error for both the angle and amplitude estimation of the stator flux linkage. Usually there are some errors in either the measurements of the voltage and current or the resistance

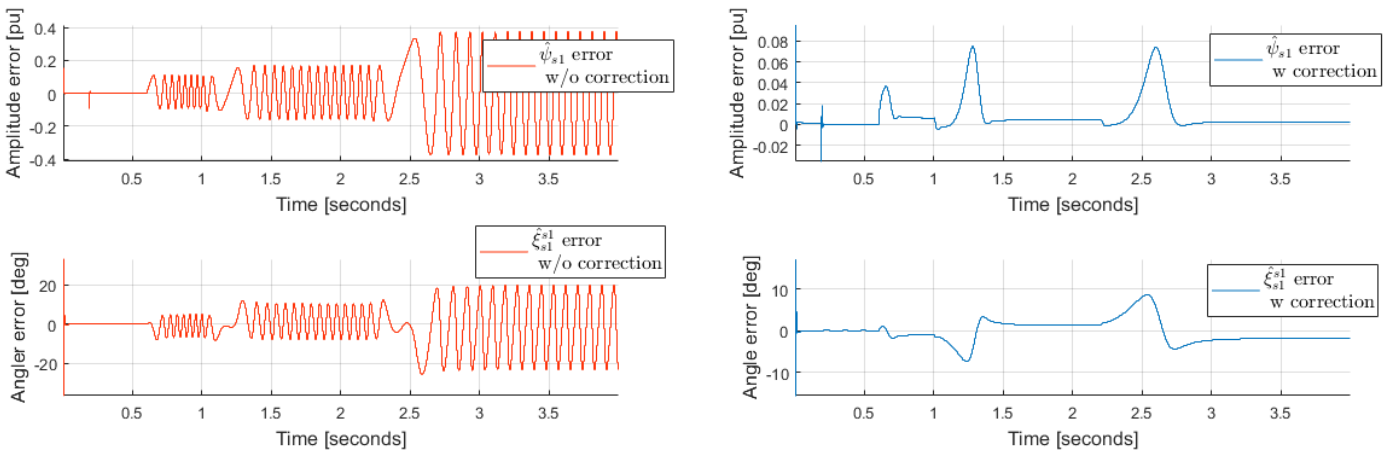

Figure 8.2: Amplitude and angle error vs time with and without correction. $\hat{r}_s = 1.5r_s$.

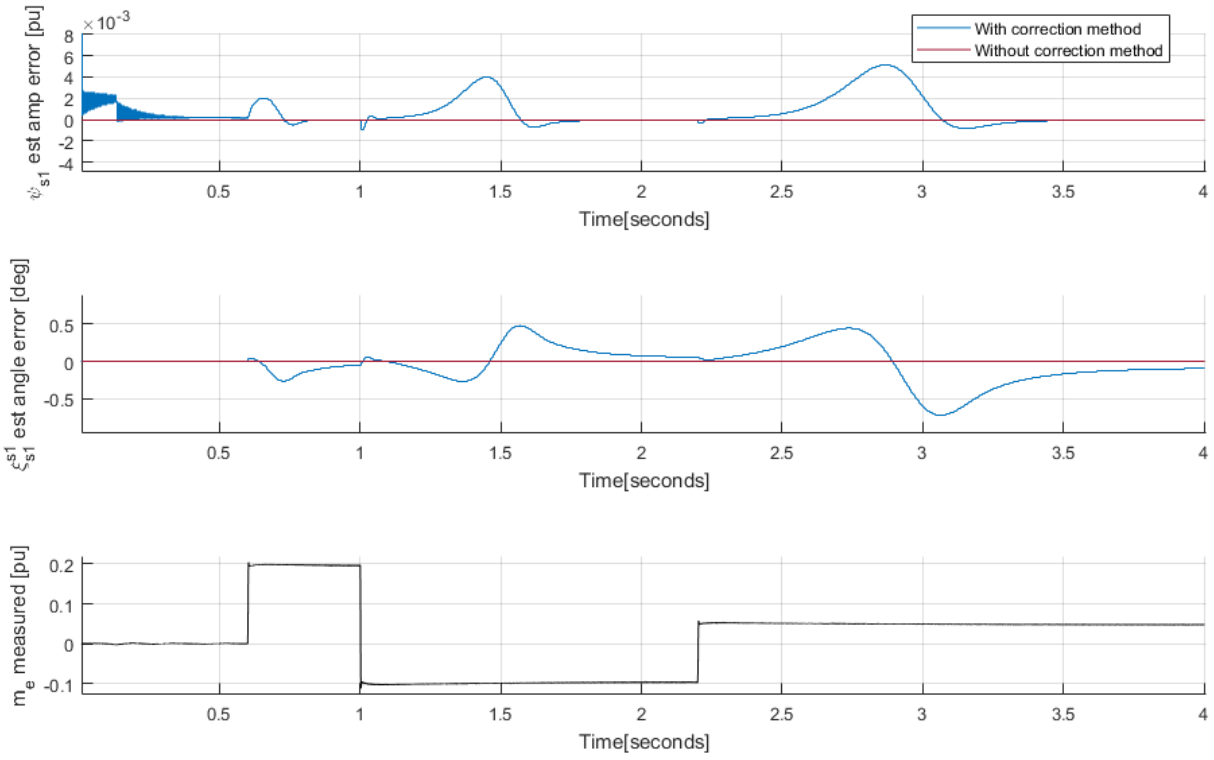

Figure 8.3: With and without correction block for $\hat{r}_s = r_s$

estimation, and hence the correction method is better when this occurs, and the drawback with the disturbance in change of a torque reference is acceptable.

8.1.2 Stationary Error When The Stator Resistance Estimation Is Not Correct

If one investigates the right side of figure 8.2 more closely, it is observed a stationary error in both amplitude and angle of a small value. Hence, the corrector block does not perform flawlessly. As a consequence of this, the rotor flux linkage SV also experiences a stationary error in its estimate. Then the estimated d-q rotating axis is not entirely correct. For most scenarios, the small error in the estimated d-q rotating axis is of small consequences but if the motor operates at a low torque reference, this may cause trouble. In figure 8.4, it is observed that the stationary error seems to be a function of the estimated stator resistance. It is observed that the only scenario without stationary errors is when the estimated stator resistance is equal to the real. However, as seen in the last subsubsection, the transient error is still there. When the estimated stator resistance is estimated at a higher value than the real resistance the error of the amplitude is positive which is indicating a too low estimated stator flux linkage amplitude. The opposite is a fact for an estimated stator resistance too low. For the angle error, the estimated angle is estimated too big when the estimated stator resistance is estimated too big, and the speed of the motor is positive. When the speed is negative, the estimated angle is estimated too low. For a stator resistance estimated too low the opposite is a fact. The reason for this performance error is clear by remembering the stationary parameter sensitivity analysis for the stator flux linkage in the voltage model in section 6.1.1. It was shown that both the stator flux linkage amplitude and angle had estimation errors if the estimated stator resistance was wrong. Hence when the correction method uses the square of the estimated stator flux amplitude as input to correct the drifting, only the amplitude is corrected. The fixed angle error because of a wrongly estimated stator resistance is still present. In Niemelä's work [5] the machined used was the synchronous motor and a standard control strategy for this machine is keeping the voltage and current in phase, producing a stator flux linkage lagging 90 degrees. Hence an error in the estimation of the stator resistance does not create errors to the angle estimation. The same was experienced by my colleague Magnus Bolstad in his thesis, where he analyzed the correction method for a synchronous machine[16].

8.1.3 Tuning of The Corrector Block

The corrector block for the stator flux linkage estimate is tuned to give improved characteristics. The results of the tuning of both k_t and $k_{corr,0}$ is seen in figure

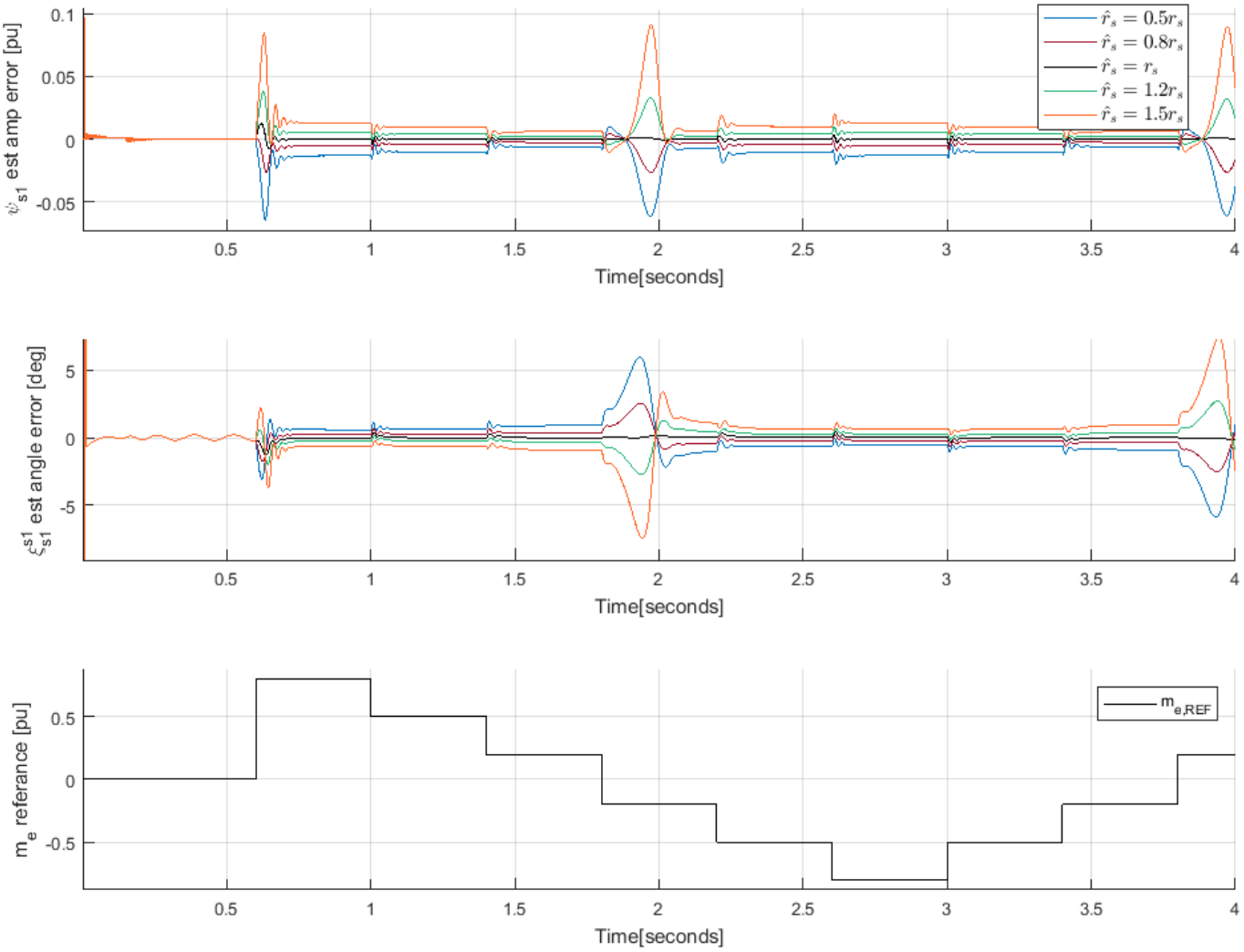

Figure 8.4: Stationary error from the corrector block as a function of the estimated stator resistance

8.5 and a more thoroughly tuning of $k_{corr,0}$ is seen in figure 8.6. In figure 8.5 it is observed that the changing k_t produces few changes but if $k_{corr,0}$ is changed the oscillation of the error function of both amplitude and angle is changing. Especially the oscillation of the error function of the angle is essential since this angle is a term for calculating the rotor flux linkage position and hence the estimated d-q-axis. A wrongly estimated direct and quadrature axis gives a wrongly estimated d and q components of the current. This again gives wrongly estimated electric torque since the q component of the current generates torque. Besides, a wrongly estimated d component of the current produces errors in the estimated rotor flux amplitude which again is proportional to the electrical torque in the machine. As one sees from the figures, the stationary error is not removed by tuning and is the same as in figure 8.5. In figure 8.6 the estimated error in the rotor flux linkage amplitude and position, torque and the measured electrical torque in the motor and speed. It is observed that a lower $k_{corr,0}$ produces more oscillation in the electrical torque of the motor and that a higher $k_{corr,0}$ makes the correction of the rotor flux linkage amplitude and position slower. Here the preferred result is $k_{corr,0} = 0.0020$. On the other hand, the tuning is here done in MATLAB Simulink but is done easier and faster in a laboratory.

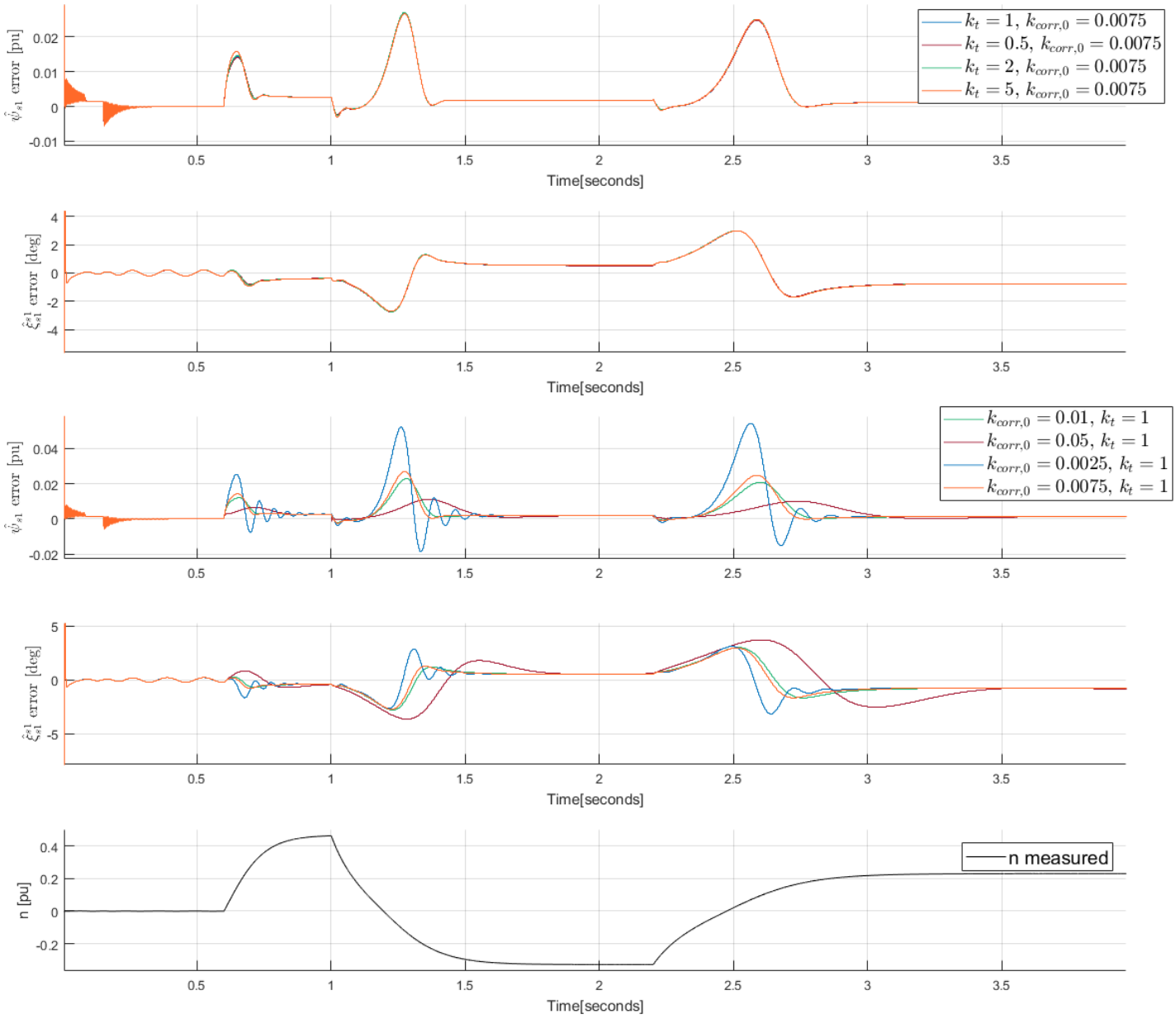

Figure 8.5: Tuning of corrector block

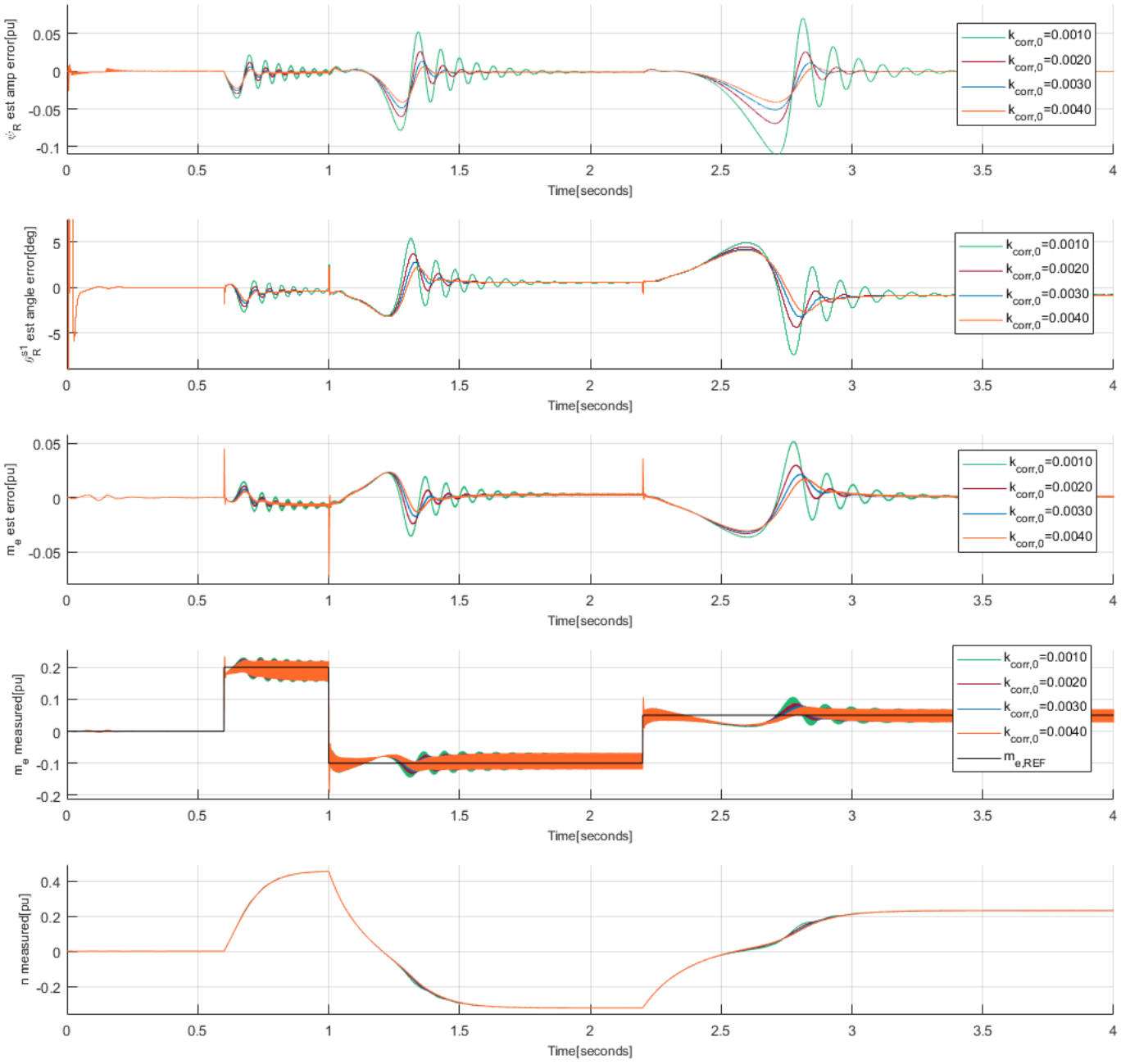

Figure 8.6: Tuning of $k_{corr,0}$ in corrector block

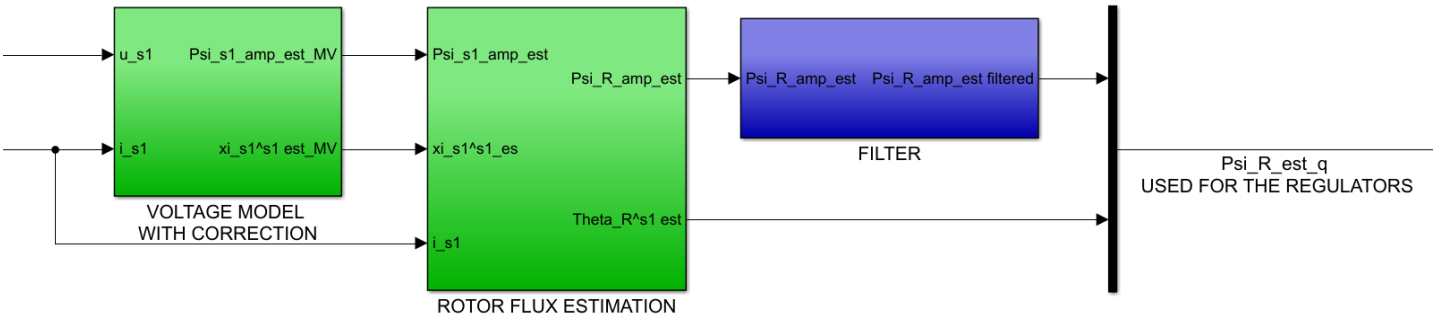

Figure 8.7: Using a filter solution to improve estimate of rotor flux linkage amplitude, here referred to as the filter method

8.2 Improving Rotor Flux Linkage Amplitude Estimation

The estimation of the rotor flux linkage amplitude will be used to calculate the direct component reference of the current in the flux controller by a PI regulator. Unfortunately, the amplitude estimation contains some ripple which acts as disturbances to the flux controller. On the other hand, the ripple observed in the estimation is not a physical phenomenon, since the rotor flux linkage amplitude has inertia and does not change value instantly like the ripple. Hence a proposed solution is to filter the rotor flux linkage's amplitude estimation to improve the performance of the flux controller. This is evaluated and performed. The block diagram of the process is seen in figure 8.7. In addition to a more stable flux regulator, the filtered estimated amplitude produces a better flux linkage amplitude value. This improved method will here in this thesis be called the filter method. The expression for a discrete low pass filter can be written like:

$$G(z) = K\frac{(T_s/T)z^{-1}}{1 + (T_s/T - 1)z^{-1}} \tag{8.1}$$

Where K is the filter gain and is here 1, T is the filter time constant and is here chosen to be T_r from equation 4.9 and T_s is the sample time.

Another suggestion to improve the estimate of the rotor flux linkage amplitude is to use a combination of the voltage model and the current model to remove the ripple caused by the estimation of the rotor flux linkage amplitude in the voltage model. The reason to the reduction in ripple is that the equation 4.6 is a dynamic equation where the rotor flux linkage amplitude has inertia and cannot change instantly. When using the current model to estimate the rotor flux linkage the equation used is equation 4.6, but now the d component of the current is estimated from the voltage

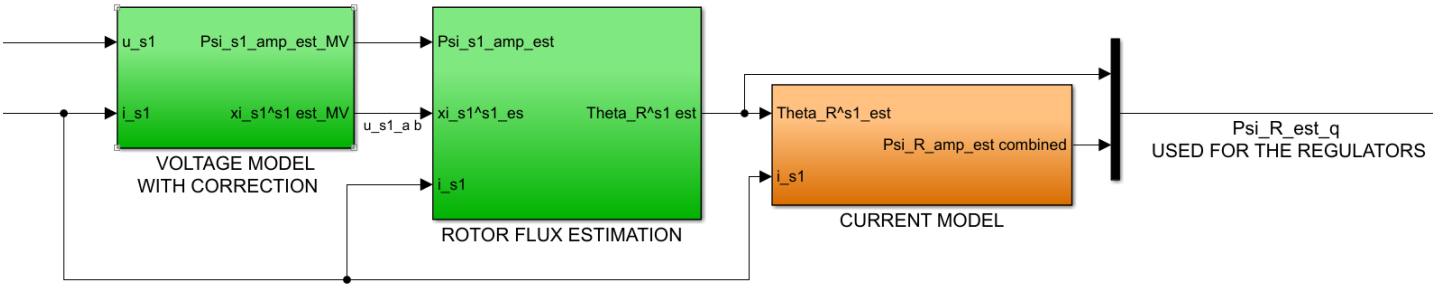

Figure 8.8: Combination of the voltage model and current model for improving rotor flux linkage estimate, here referred to as the combination method

model. The principle is shown in figure 8.8. The equation 4.6 is here repeated for clearness:

$$\frac{d\hat{\psi}_R}{dt} = -\frac{\hat{\psi}_R}{\hat{T}_r} + \frac{\hat{x}_H}{\hat{T}_r}(\hat{i}_{sd1} + \hat{i}_{sd2}) \tag{8.2}$$

In equation 8.2 the estimation of the direct components of the current is different than for the current model discussed in section 4. This is because in the standard current model one measure the rotor position or speed and then estimates the rotor flux linkage SV position. In the combination method, one uses the estimation of the rotor flux linkage angle from the voltage model as input in the current model. This input comes from the voltage model and hence is sensitive for errors in the estimation of the stator resistance, especially at low-speed operation. The standard current model using the measurement of the rotor position is not sensitive for the stator resistance.

Here using equation 8.2(or the current model) the parameter sensitivity which was discussed in section 6 is still valid. Hence, the model will now also be parameter sensitive to the estimated rotor resistance and main inductance as well as the stator resistance.

In figure 8.9 it is observed that the combined model is the best model to estimate the rotor flux linkage amplitude. Both the filtered model and the combined model improves the estimation and the ripple from the voltage model estimation. On the other hand, there is a stationary error in all the models which is probably a consequence of the stationary error in the stator flux linkage estimation from the drifting corrector block, but the improvement from the normal voltage model is clear.

A simulation with correctly estimated parameters is done in figure 8.10. In this

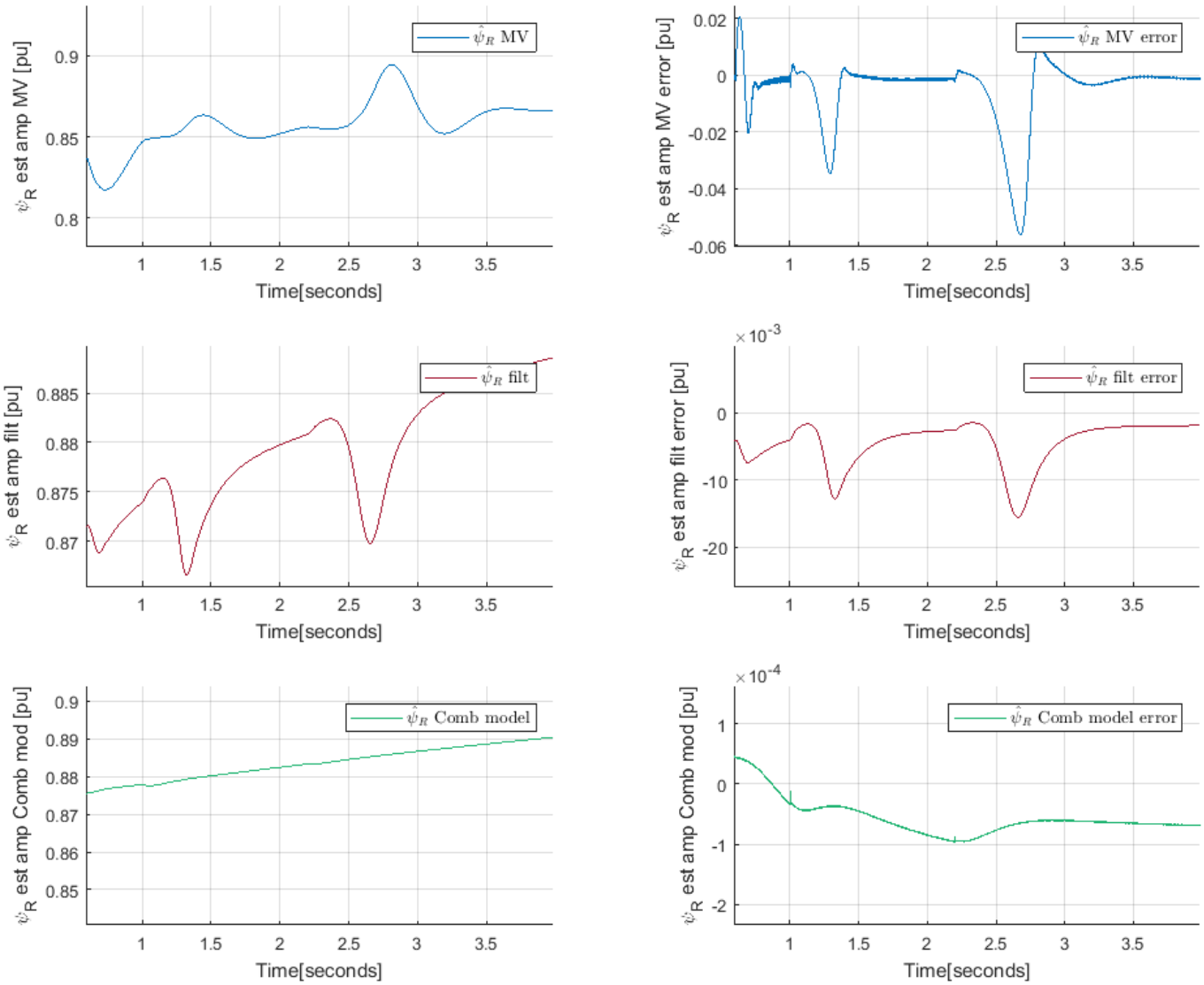

Figure 8.9: Three different estimation models for the rotor flux linkage amplitude: normal voltage model, filtered voltage model and a combined model

simulation, it is clear that the combination method is better than the filter method. Both the rotor flux linkage amplitude and angle is estimated better in the combination method than the filter method. On the other hand, all the estimated parameters are correct. Hence one should assume zero error for both methods. As shown in section 8.1, the corrector block can act as a disturbance when the estimated stator resistance is correct and worsen the flux model. As both the filter method and the combination method use the corrector block to decrease drifting, this disturbance also the rotor flux linkage estimation.

In figure 8.11 it is shown a simulation with wrongly estimated resistances. In this simulation both the stator resistance and the rotor resistance estimation is 1.2 times the correct values. As both the resistances are temperature dependent it is assumed that both the stator and rotor resistance variate with the same relative amount. At first when the DC magnetization occurs from 0-0.6 seconds it is clear that there is a problem with the estimation of the rotor flux linkage amplitude in both methods. This is because that one uses the current model at DC magnetization and the current model is parameter sensitive for the rotor resistance. On the other hand after the machine starts rotating at 0.6 seconds the error in the rotor flux linkage amplitude estimation decreases in both models, but a more smoothly decrease in the combination method. The rotor flux angle estimation will be correct during the DC magnetization period and then when the machine start rotating the corrector block will be enabled and try to filter away the drifting that occurred during magnetization. Hence it is observed a maximum in the error estimation of the rotor flux linkage angle, where the maximum for the filter method is higher than the maximum of the combination method. The next maximum occurs when the motor drives through zero speed at approximately 1.35 seconds in the filter method and 1.4 seconds in the combination method. Again the maximum is higher for the filter method. Then the motor gets a new torque reference at 2.2 seconds but is not able to follow this reference. For the combination method one seems to experience a stationary error of approximately 7 degrees in the rotor flux linkage angle estimation which makes it impossible to follow the torque reference producing a stationary error of approximately 0.05 pu. For the filter method it is difficult to conclude if there will be stationary error or not since it has a more oscillating nature than the combination method. On the other hand it is clear that it is also experiences difficulties following the given torque reference.The reason for these difficulties is the that the machine is running at low speed and in addition but not shown in this figure at a low torque level. Hence small errors in the rotor flux linkage angle estimation and the direct and quadrature current components can produce torque generating currents which opposes the torque reference.

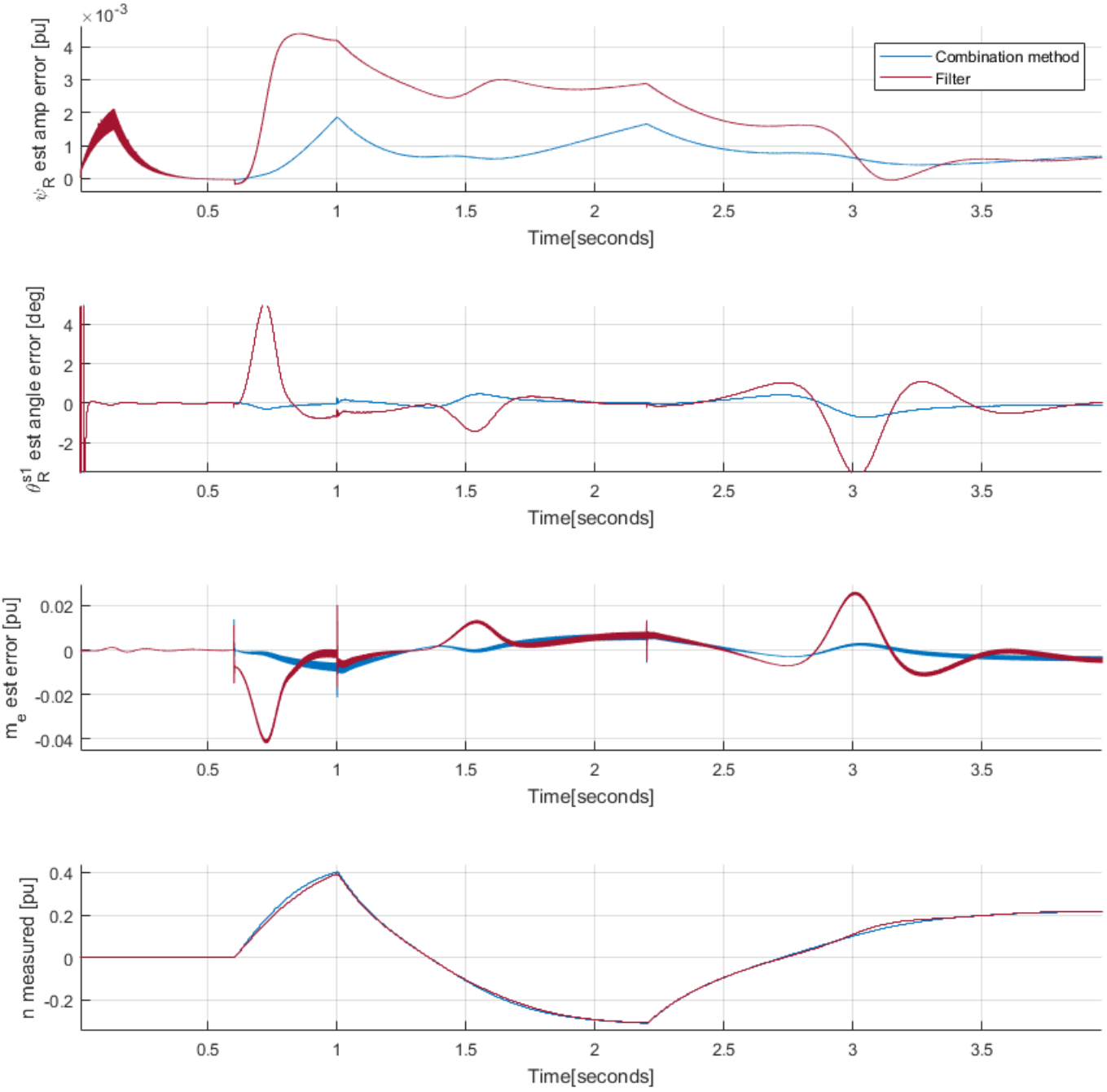

Figure 8.10: Combination model vs filter solution with $\hat{r}_s = r_s$ and $\hat{r}_R = r_R$

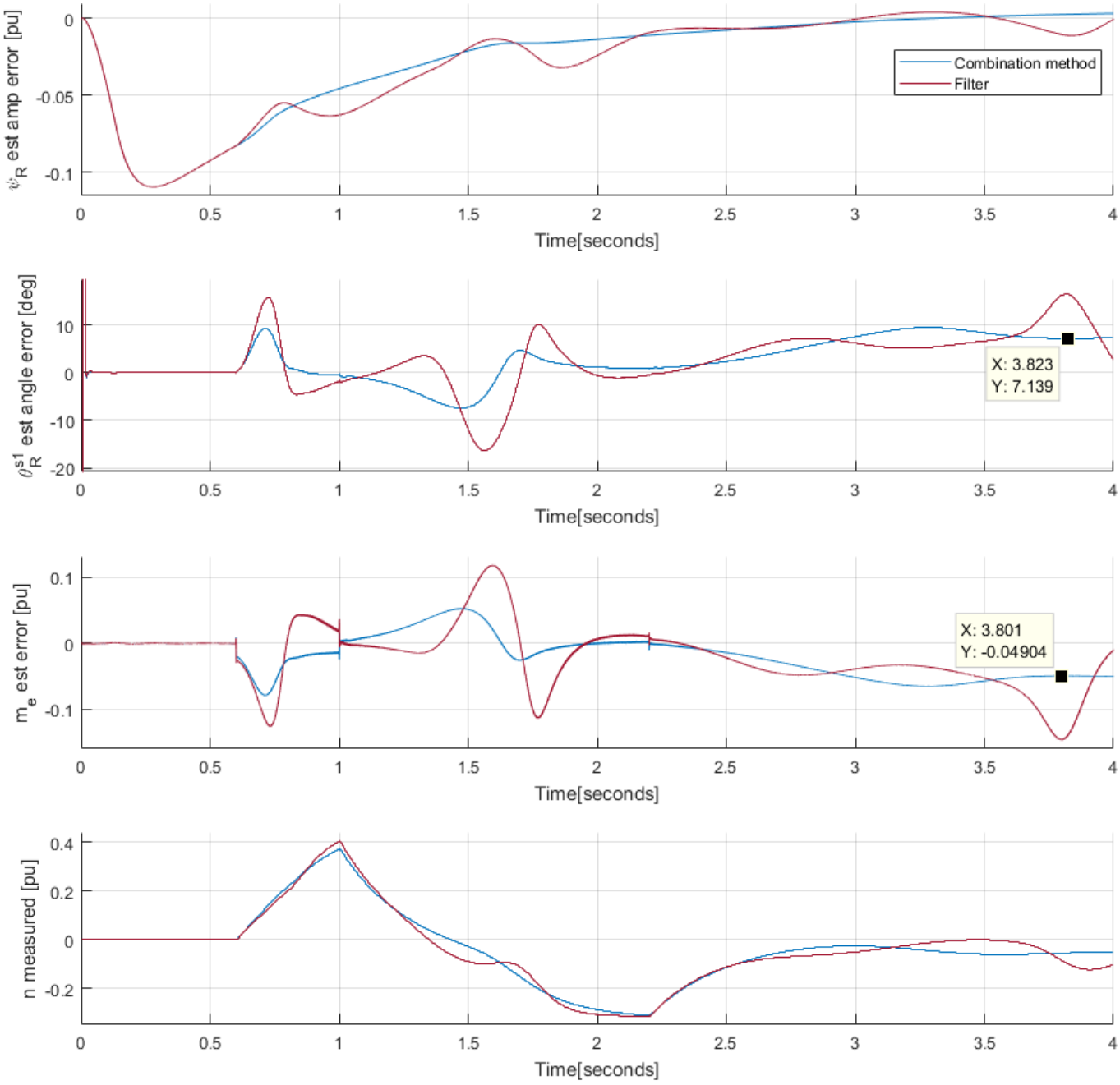

Figure 8.11: Combination model vs filter solution with $\hat{r}_s = 1.2r_s$ and $\hat{r}_R = 1.2r_R$

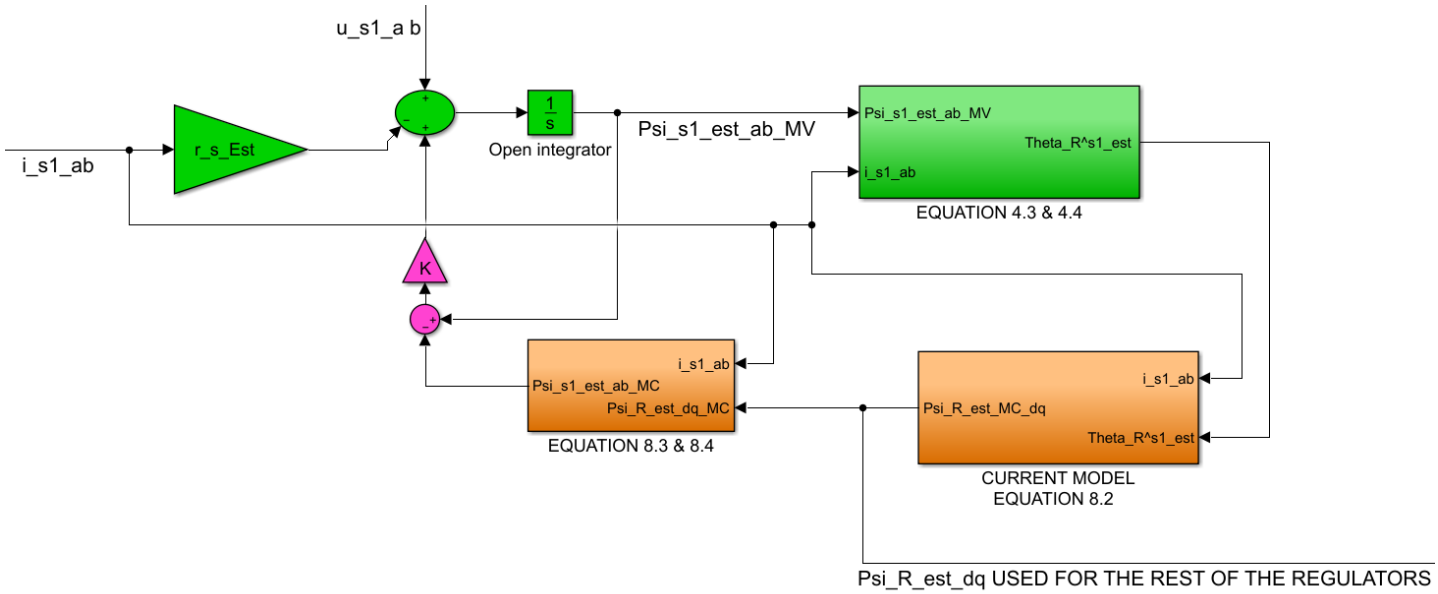

Figure 8.12: Alternative method for correcting drifting using a closed loop observer feedback method

8.3 Closed Loop Observer

The correction block does not work flawlessly and as seen earlier stationary errors in both stator flux linkage amplitude and angle estimation occur when the estimated stator resistance is not correct. This brings motivation to find a new alternative solution for removing the drifting in the voltage model. Inspired by the less oscillating rotor flux linkage estimation using the current model one can exploit this value to estimate a new stator flux linkage (with less oscillation than the original) that can be used to correct the error caused by a wrongly estimated stator resistance. Actually the time constant, T_r, used for estimating the rotor flux linkage amplitude in the current model will act like a low pass filter, and can filter away some of the oscillation caused by drifting. Hence it can be assumed that the new stator flux linkage estimate is more correct than the estimate from the voltage model. Then using the new estimate as a closed loop observer one corrects the voltage model and the drifting will be decreased. The alternative method is shown in a block diagram in figure 8.12. The correction block explained in section 7.6 is not used while using this method. The closed loop observer feedback method (as it will be referred to here) will work as an alternative method for the correction block explained in section 7.6. The equations used for estimating the stator flux linkage from the current model were explained in section 4.2 and by the equations 4.11-4.13. Here repeated with the correct subscripts(MC

indicates current model and MV indicated voltage model):

$$\begin{aligned}\hat{\psi}_{sd1,MC} &= \hat{\psi}_{R,MC} + \hat{x}_\sigma \hat{i}_{sd1,MV} + (\hat{x}_\sigma - \hat{x}_{s\sigma})\hat{i}_{sd2,MV} \\ \hat{\psi}_{sq1,MC} &= \hat{x}_\sigma \hat{i}_{sq1,MV} + (\hat{x}_\sigma - \hat{x}_{s\sigma})\hat{i}_{sq2,MV}\end{aligned} \tag{8.3}$$

$$\hat{\xi}^{s1}_{s1,MC} = \arctan \frac{\hat{\psi}_{sq1,MC}}{\hat{\psi}_{sd1,MC}} + \hat{\theta}^{s1}_{R,MV} \tag{8.4}$$

Where $\hat{\theta}^{s1}_{R,MV}$ is given by equation 4.4.

The difference between the stator flux linkage estimation from the current model and the voltage model will be amplified by a gain K and then used as feedback for the voltage model. The new expression for estimating the stator flux linkage in the voltage model is given by:

$$\underline{\hat{\psi}}_{s1,MV} = \int_{t_0}^{t} (\underline{u}_{s1} - \hat{r}_{s1}\underline{i}_{s1} + K(\underline{\hat{\psi}}_{s1,MV} - \underline{\hat{\psi}}_{s1,MC})dt \tag{8.5}$$

The best value of K was found to be 0.1 by tuning in the model in MATLAB Simulink with correct estimation of the parameters.

8.3.1 Comparing The Combination Method With Correction and The Closed Loop Observer Method

In figure 8.13 the different methods are compared with correct estimation of the parameters. From the figure it is observed that the combination method is better at estimating both the rotor flux linkage amplitude and the angle stationary. For the combination method the error in angle seems to be approximately zero at stationary operation, which is assumed if the estimated parameters are correct. Since both the rotor flux linkage amplitude and the angle is estimated better using the combination method the torque is also estimated better. On the other hand, when the machine drives through zero speed the closed loop observer feedback method experiences a smaller amplitude in the oscillation of the rotor flux linkage angle estimate. This implies that using the closed loop observer feedback method the control model is more reliable crossing zero speed.

The performance of the closed loop observer feedback method compared to the combination method at wrongly estimated resistances is shown in figure 8.14. Investigating the figure it is clear that the closed loop observer feedback method performs better than the combination method. Because the rotor resistance is estimated wrongly the DC magnetization of the machine will be estimated wrongly. This is evident from

investigating the rotor flux linkage amplitude estimation error in the starting time. After the machine starts rotating at 0.6 seconds the estimation of rotor flux linkage angle experience a transient but stabilizes at approximately zero error for both the closed loop observer feedback method and the combination method before next transient starts at time = 1 second. The same occurs again under this transient but it is clear from the figure that using the closed loop observer feedback method driving through zero speed is more reliable. This is evident from observing that the maximum error of the torque and angle estimation is lower for the closed loop observer feedback method compared to the combination method. The last change of torque reference occur at time = 2.6 seconds. Another time the model is challenged to drive through zero speed. It is observed that only the closed loop observer method is able to succeed following the reference. The combination method experience stationary angle error of approximately 8 degrees which is a significant amount and following the torque reference seems impossible.

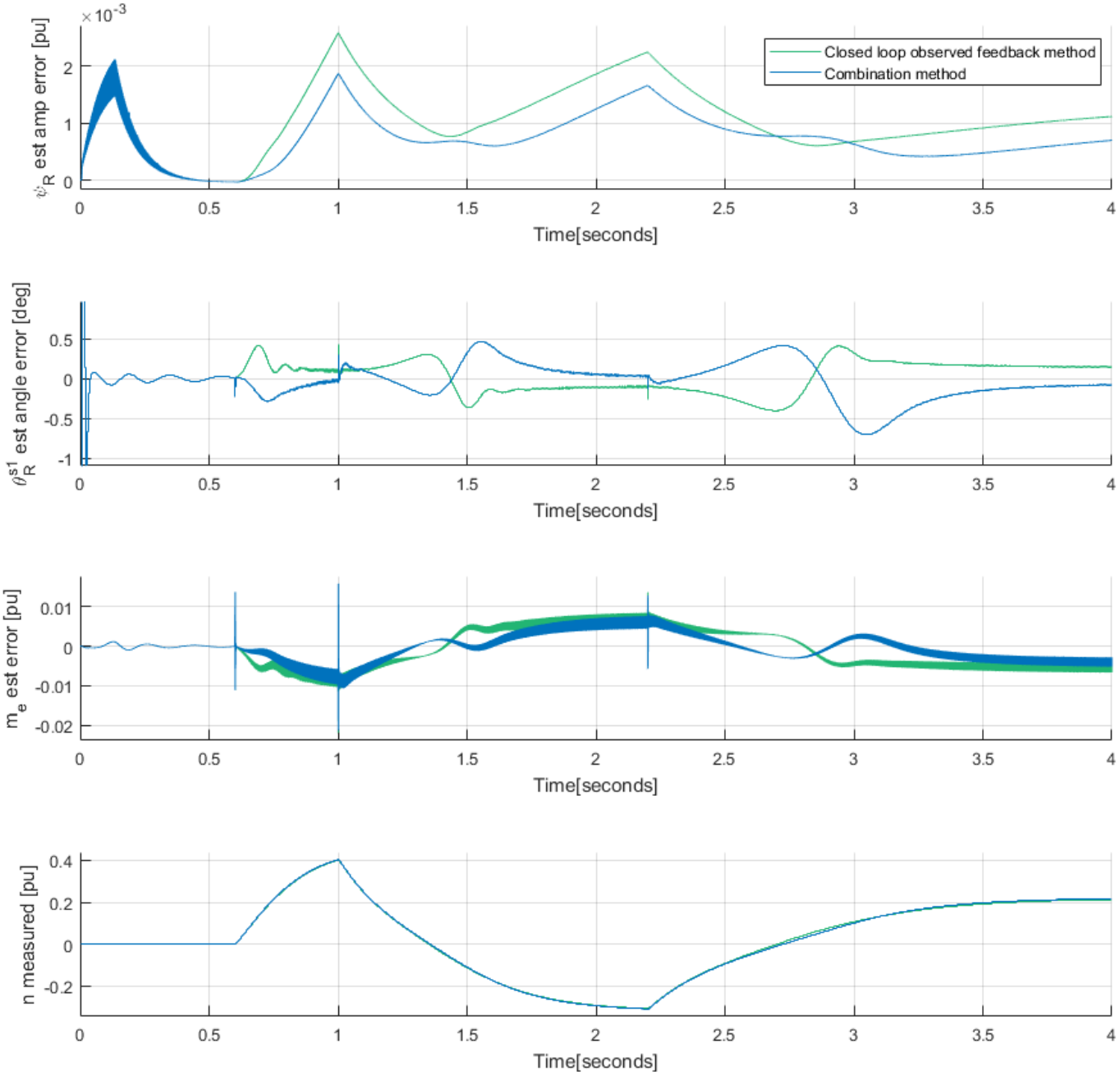

Figure 8.13: Closed loop feedback observer method vs Combination method with correct parameter estimation

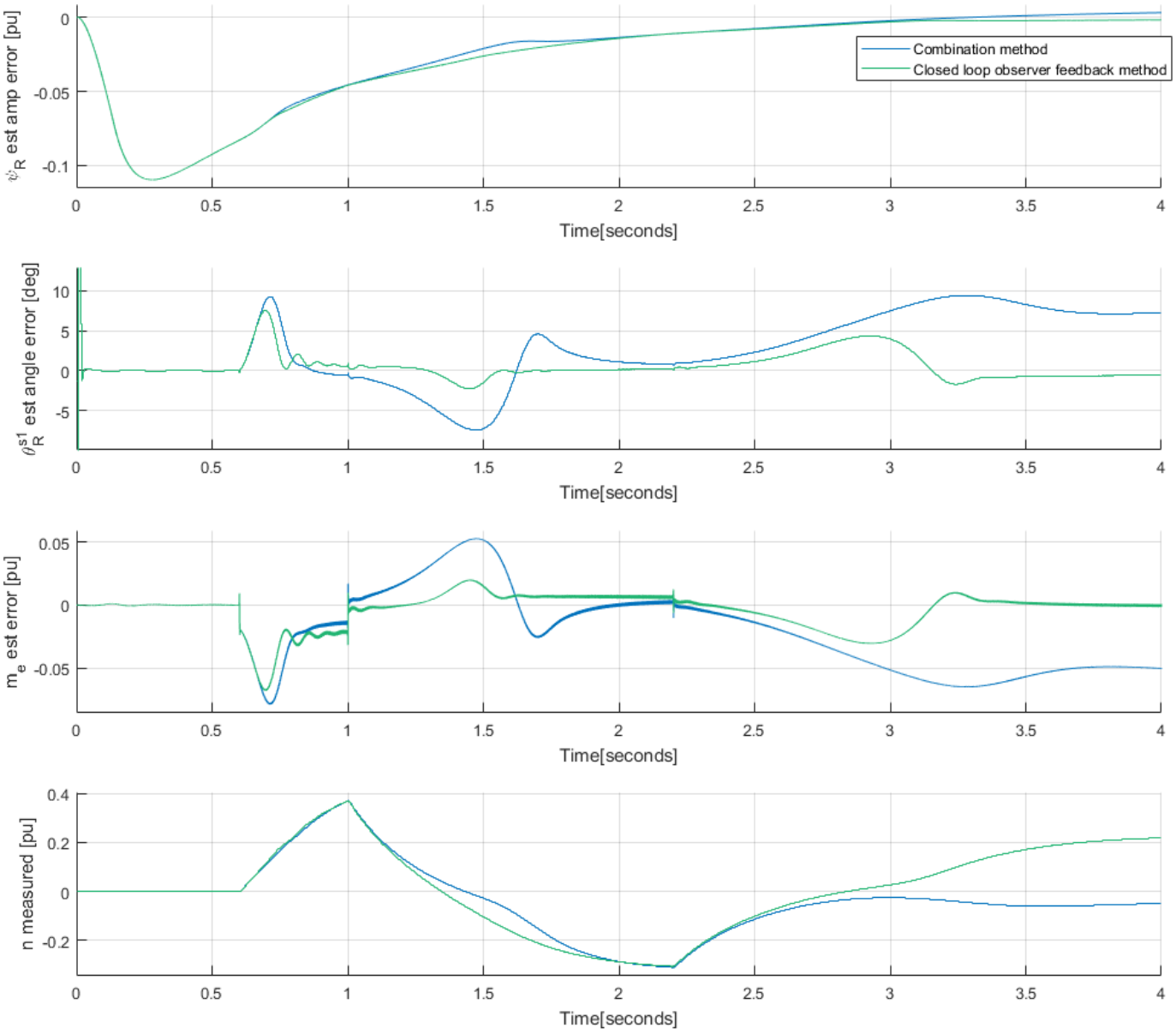

Figure 8.14: Closed loop feedback observer method vs Combination method with $\hat{r}_s = 1.2r_s$ and $\hat{r}_R = 1.2r_R$

8.3.2 Problems With The Closed Loop Observer Method

The stationary error in the estimated rotor flux linkage angle was the motivation for developing the closed loop observer feedback method but seems to be a more difficult challenge than expected. As seen in the simulations, the method experiences many of

the same problems as the correction method by Niemelä. In figure 8.13 it is observed that even though when the parameters are estimated correctly the model experiences disturbance during a change in the torque reference. In addition, as for the correction method, there are stationary errors in the estimated stator and rotor flux linkage's angle error. However, for some scenarios, like in figure 8.14, the stationary error in rotor flux linkage angle estimation is less using the closed loop observer feedback method. Besides, it was clear that the method was better for driving through zero speed.

A drawback with the method, compared to the classical voltage model with drifting correction, is that the model is sensitive to more parameters. In the voltage model, the critical parameter is the stator resistance. In the closed loop observer feedback method, one uses both the voltage model and the current model. Hence in addition to the parameters from the voltage model, the method is parameter sensitive to the rotor resistance and the main reactance. Then a possible scenario is correctly estimated resitances and a wrongly estimated main reactance. Then the standard voltage model estimates correctly, and the feedback serves only as an additional disturbance. Besides, since the closed loop observer feedback method is sensitive to more parameters, it is more technically demanding to estimate these. Hence, due to its more advanced structure, it is fair to assume that using the closed loop observer feedback method, the drive costs more.

8.4 Possible Improvements Not Investigated

There exist a lot of different strategies that can be used to improve the standard voltage model. As discussed earlier, the closed loop observer method works well. In addition to the feedback from the stator fluxes in the different models, one can use the rotor flux linkage or a current estimation. Another possibility is to estimate the current from the rotor flux linkage in the voltage model. Besides, it is possible to develop more advanced observers such as the sliding mode observer, adaptive gain for observer or use a PI as closed loop feedback control.[12][9]

In addition using a PLL (Phase-lock loop) slow enough to not follow the oscillations the estimated rotor flux linkage angle experiences driving through zero speed was proposed by supervisor Prof. Roy Nilsen, but simulating showed no success. Hence it was omitted in this thesis.

9 Summary

In section 6 the stationary parameter sensitivity of both the voltage model and the current model were analyzed. From the voltage model, it is clear that the low-speed operation is problematic if there is an estimation error in the stator resistance. The amplitude error of the stator flux linkage is in theory infinity at zero frequency because of a division by zero in equation 6.2. The estimation of the stator flux linkage angle is also problematic at low-speed operation because the voltage magnitude decreased at low speed that implies a more dominant stator resistance voltage drop in the equation 6.4. If the stator resistance was estimated wrong the estimated stator flux linkage SV is located 90 degrees lagging or leading of the current SV at the positive or negative limit of zero frequency depending if the estimated stator resistance is bigger or smaller than the real value. This was seen in figure 6.8. The estimation of the rotor flux linkage experiences the same problems as the stator flux linkage at low-speed operation with a wrongly estimated stator resistance. This occurs because the estimation of the rotor flux linkage is a function of the estimation of the stator flux linkage. Hence, both the estimation of angle and amplitude experiences problems in the low-speed region and likewise the estimated torque is also not reliable in this region.

For the current model, the critical parameters are the rotor resistance and the main reactance. The model does not experience the same problems during low-speed operation as the voltage model and hence is more reliable in this operational region. On the other hand, the model depends on the torque level in the machine for both angle and amplitude for the estimation of the rotor flux linkage. The problems with torque dependency would be the same for the estimated torque. In summary it can be concluded that the voltage model is a more reliable model without at low-speed operation where the current model is more reliable.

The dynamical parameter sensitivity analysis and the phenomenon of drifting in the voltage model is discussed in section 7. A wrongly estimated stator resistance is seen as the reason for the drifting of the origo for the estimated fluxes. This comes as a consequence of the use of the open integration in the voltage model and hence an error in the estimation is in theory a part of the estimation forever. The size of the drifting depends on different circumstances. Likewise, for the stationary parameter sensitivity analysis the frequency at the time when the transient occurred is important for scaling the size of the drifting. This is seen in section 7.3. Hence changing torque reference at low speed gives a more erroneous flux linkage estimation than changing at high speed. In addition, driving trough zero with a wrongly estimated stator resistance is shown very challenging.

Hence the drifting of the voltage model need to be corrected in some way. The correction method based on the square of the estimated stator flux linkage amplitude presented by Niemelä[5] and investigated by Fossen[11] is suggested as a solution. This filter solution is explained in section 7.6. Even though it removes the oscillating errors in estimated flux linkage amplitude and angle, it did not work ideally. In section 8.1 it is evident that the method seems noisy when the estimated stator resistance is correct, and it has stationary errors in both estimated flux linkage amplitude and angle when the estimated stator resistance is not correct. In most scenarios this will be negligible errors.

The rotor flux linkage estimated amplitude is improved using both the filter method and the combination method in section 8.2. This is motivated because the original rotor flux linkage amplitude from the voltage model has oscillations and ripple that made the flux regulator in the model unstable. The filter method uses the rotor time constant to low pass filter the estimated amplitude, removing ripple and oscillation. The combination method used the current model equation 8.2 but instead of measuring the speed and the estimating the rotor flux linkage SV angle one used directly the estimated rotor flux linkage angle from equation 4.4. The combination method was shown to be the better method, but a drawback was the new dependency of the rotor resistance and the main reactance estimation.

An alternative method to the correction method is introduced in section 8.3 using a new estimation of the stator flux linkage from equation 8.3 and 8.4 from the estimated rotor flux linkage from the combination method. The motivation that the combination method filtered some drifting and hence the new estimated stator flux linkage was assumed more correct than the original from the voltage model. Then the difference between the new estimation and the old from the voltage model was amplified by a feedback gain and used for correcting the voltage model and removing drifting. This was shown success full for some scenarios compared to using the correction method with the combined method for example. On the other hand it is suggested by the author to optimize this closed loop observer feedback method. The gain K is suggested adaptive and in addition it should be investigated if a Proportional integral feedback could remove the stationary errors seen in the model.

10 Conclusion and Further Work

In this thesis the parameter sensitivity analysis of the voltage model used for speed sensorless control of a six-phase induction machine was investigated thoroughly. Starting with the stationary parameter sensitivity analysis and the voltage model it was revealed a strong dependency on a correct estimation of the stator resistance driving at low speed. The most sensitive operational point was running on DC($f_\psi = 0$), where the stator flux linkage amplitude could in theory be estimated to infinity. In addition the stationary parameter sensitivity analysis for the current model was investigated. The current model was more reliable at low speed operation, but was parameter sensitive to the rotor resistance and the main inductance. If the parameters were not estimated sufficiently correct, the current model became unreliable.

The next section of the thesis investigated parameter sensitivity dynamically in MATLAB Simulink. The drifting phenomenon from the open integration in the voltage model was the primary attention and it was analyzed thoroughly. It became clear that some correction was absolutely necessary to have high performance of the control. The correction method introduced by Niemelä in 1999[5] was investigated and tested on the simulation model. The method improved the model, but had some drawbacks like stationary error in the angle estimation error of both the stator and rotor flux linkage. Hence, new improvements were necessary to increase the control performance.

Two methods to improve the rotor flux linkage amplitude estimation was tested and investigated. One of the methods was based on a filter and the other was based on a combination of the voltage and the current model. The combination method showed great promise and the rotor flux linkage became more stable.

Finally, an alternative method to Niemelä's correction block was developed and tested. The method was also a combination of the voltage and current model and corrected against drifting by a feedback mechanism. The voltage model was corrected by the current model that worked like a closed loop observer. The control method was still speed-sensorless since the input to the current model was earlier estimations from the voltage model. This method showed great promise and especially was more reliable driving through zero speed. A drawback with the method is that the model depends on more parameters compared to Niemelä's correction method.

The parameter sensitivity analysis done in this thesis was focused on the voltage model, which is a natural choice for a speed sensorless control method. On the other hand when the combined model was used in section 8.3 the parameter sensitivity

analysis done earlier lacked some content. The dynamical analysis did not include the current model and the combined model will in general be most sensitive for stator and rotor resistance estimation errors and estimation errors in the main inductance. A more thoroughly analysis of the combined model should be done as further work which can simplify the optimization of the feedback control based on the closed loop observer.

For further work the author suggest to try a proportional integral as feedback control instead of the simple gain used in this thesis for the closed loop observer. The hope for this adjustment is to remove the stationary error. Another suggestion is to make the feedback gain adaptive to frequency as drifting is very depending on the frequency.

Something that was tried without luck and has not been explained in this thesis was a PLL used for the rotor flux linkage angle estimate. The hope was to make the PLL too slow to follow the erroneous path of the estimated angle when the machine drove through zero speed. This was tried without success and hence skipped in this thesis. On the other hand with thoroughly analysis it can be tried in further work.

The correction method by Niemelä can hopefully be improved to give zero stationary errors in angle and amplitude flux linkage estimation in further work. It was experienced by my colleague Magnus Bolstad in his master thesis that for a synchronous motor there was no stationary error for the angle estimation. This may imply that the reason for the stationary angle estimation error comes from a current and a voltage not in phase as generally happens in an induction motor and not a synchronous motor.

Finally a topic that deserves a full thesis, is parameter estimation. There exist a dozen method both online and offline to estimate the resistances and inductances and improve the model. In this thesis this was not analyzed and is suggested for further work as it will improve the model.

References

[1] N. R. Klaes. *Parameter Identification of an Induction Machine with Regard to Dependencies on Saturation*
IEEE Transactions on Industry Applications, Vol. 29, no.6, Nov/Dec 1993, page 1135-1140

[2] Tom Nestli. *Modelling and Identification of Induction Machines*
Doctoral thesis, Dept. Electric Power Engineering, NTNU, Dec. 1995.

[3] Jun Hu and Bin Wu. *New Integration Algorithms for Estimating Motor Flux over a Wide Speed Range*
IEEE Transactions on Power Electronics, Vol. 13, No. 5, September 1998

[4] Kaukonen Jukka. *Salient Pole Synchronous Machine Modelling an Industrial Direct Torque Controlled Drive Application.*
Doctoral thesis, Lappeenranta University of Tecnology, 1999

[5] Markku Niemelä. *Position Sensorless Electrically Excited Synchronous Motor Drive For Industrial Use Based On Direct Flux Linkage and Torque Control*
Doctoral thesis, Lappeenranta University of Tecnology, 1999

[6] Joachim Holtz. *Sensorless control of Induction Motor Drives*
Invited paper, Proceedings of the IEEE, Vol. 90, No. 8, August 2002, page 1359-1394

[7] Julius Luukko, Markku Niemelä and Juha Pyrhönen. *Estimation of the Flux Linkage in a Direct-Torque-Controlled Drive*
IEEE Transacions on Industrial Electronics, Vol. 50, No. 2, April 2003, page 283-287

[8] Roy Nilsen. *Modelling of Multi-phase synchronous machines.*
Wärtsilä Norway AS, Ship Power Technology R/D, Trondheim, April 2009

[9] Mohamed S. Zaky. *A stable adaptive føux observer for a very low speed-sensorless induction motor drives insensitive to stator resistance varitations*
Ain Shams Engineering Journal, (2011) 2, 11-20

[10] Nebrom Berihu Araya. *Modelling and Control of Six-phase Induction Motor Drive.*
Master thesis, Dept. Elect. Power Eng., NTNU, July 2012.

[11] Bendik Fossen. *Modelling and Identification of Multi-phase Machines.*
Project thesis, Dept. Elect. Power Eng., NTNU, December 2016

[12] Armaghan Aliaskari and Seyed Alireza Davari. *A New Closed-Loop Voltage Model Flux Observer for Sensorless DTC Method*
Conference paper, 8th Power Electronics, Drive Systems and Technologies Conference (PEDSTC 2017) 14-16 Feb. 2017, Ferdowski University of Mashhad, Mashhad, Iran

[13] Kamal Nounou, Jean Frédéric Charpentier, Khoudir Marouani, Mohamed Benbouzid and Abdelaziz Kheloui. *Hardware-in-the-Loop Emulation of an Electric Naval Propulsion System based on a Multiphase Permanent Magnet Synchronous Machine*
IEEE Conference paper, Dec. 2017

[14] Bo Fan, Zhi-Xin Yang, Xian-Bo Wang, Lu Song and Shu-Zhong Song. *Model reference adaptive vector control for induction motor without speed sensor*
Special Issue Article, Advances in Mechanical Engineering, 2017, Vol. 9(I) 1-14

[15] Emil Mørkved. *Sensorless control of a 6-phase Induction Machine* Project thesis, Dept. Elect. Power Eng., NTNU, December 2017

[16] Magnus Bolstad *Sensorless control of synchronous machines used in adjustable speed hydro.* Master thesis, Dept. Elect. Power Eng., NTNU, June 2018.

A Machine Parameters

Parameter	**Explanation**	**Value**
U_{sN}	Nominal line to line stator voltage rms	230 V
I_{sN}	Nominal line current rms	25 A
p	Number of pole pairs	2
i_s max	Maximum current in pu	3.0
r_s	Stator resistance in pu	0.031
r_R	Rotor resistance experienced by stator in pu	0.0068
x_H	Magnetizing inductance in pu	0.93425
x_σ	Leakage inductance in pu	0.1646
$x_{s\sigma}$	Leakage inductance stator in pu	0.1117
T_{tri}	Triangular Carrier Period pu	$\frac{1}{3000}$
M_e max	Maximum Electrical Torque in pu	1.4
f_N	Nominal frequency in Hz	50
n	Nominal speed, rpm	1500

Table 1: Parameters

B Base values

Physical quantity	**Base quantity definition**
AC Voltage	$U_n = \sqrt{2} \cdot \frac{U_N}{\sqrt{3}}$
DC link voltage	$U_{dc,n} = 2 \cdot \sqrt{2} \cdot \frac{U_N}{\sqrt{3}}$
Current	$I_n = \sqrt{2} \cdot I_N$
Impedance	$Z_n = \frac{U_n}{I_n}$
Power	$S_n = 2 \cdot \sqrt{3} \cdot U_N \cdot I_N$
Frequency	$f_n = f_N$
Angular speed (electrical)	$\omega_n = 2 \cdot \pi \cdot f_N$
Speed (mechanical)	$n_n = 60 \cdot \frac{f_N}{p}$
Torque	$M_n = p \cdot \frac{S_N}{\omega_n}$
Flux linkage	$\Psi_n = \frac{U_n}{\omega_n}$

Table 2: Base values

C Control parameters

Parameter	**Value**
K_i Current controller	0.4615
T_i Current controller	0.0223
K_ψ Flux controller	4.681
T_ψ Flux controller	4.373
K_n Speed controller	5
T_n Speed controller	0.1

Table 3: Control Parameters

D Derivation of Error-Equations in Sensitivity Analysis

D.1 Voltage Model

D.1.1 Amplitude Error Stator Flux Linkage Estimate

The estimation of the stator flux linkage amplitude by phasor analysis:

$$\begin{aligned}\underline{\hat{\psi}}_{s1}^{s1} &= -\frac{\mathbf{j}}{f_\psi} \cdot (\underline{u}_{s1}^{s1} - \hat{r}_s \underline{i}_{s1}^{s1}) \\ &= -\frac{\mathbf{j}}{f_\psi}(u_{s1}\cos(\gamma_{s1}^{s1}) + \mathbf{j}u_{s1}\sin(\gamma_{s1}^{s1}) - \hat{r}_s(i_{s1}\cos(\varepsilon_{s1}^{s1}) + \mathbf{j}i_{s1}\sin(\varepsilon_{s1}^{s1}))) \\ &= \frac{1}{f_\psi} \cdot (u_{s1}\sin(\gamma_{s1}^{s1}) - \hat{r}_s i_{s1}\sin(\varepsilon_{s1}^{s1}) + \mathbf{j}(\hat{r}_s i_{s1}\cos(\varepsilon_{s1}^{s1}) - u_{s1}\cos(\gamma_{s1}^{s1})))\end{aligned} \tag{D.1}$$

Then the estimated amplitude will hence be:

$$\begin{aligned}\hat{\psi}_{s1} &= \frac{1}{f_\psi}\sqrt{(u_{s1}\sin(\gamma_{s1}^{s1}) - \hat{r}_s i_{s1}\sin(\varepsilon_{s1}^{s1}))^2 + (\hat{r}_s i_{s1}\cos(\varepsilon_{s1}^{s1}) - u_{s1}\cos(\gamma_{s1}^{s1}))^2} \\ &= \frac{1}{f_\psi}\sqrt{u_{s1}^2 + \hat{r}_s^2 i_{s1}^2 - 2u_{s1}\hat{r}_s i_{s1}(\sin(\gamma_{s1}^{s1})\sin(\varepsilon_{s1}^{s1}) + \cos(\gamma_{s1}^{s1})\cos(\varepsilon_{s1}^{s1}))} \\ &= \frac{1}{f_\psi}\sqrt{u_{s1}^2 + \hat{r}_s^2 i_{s1}^2 - 2u_{s1}\hat{r}_s i_{s1}\cos(\gamma_{s1}^{s1} - \varepsilon_{s1}^{s1})}\end{aligned} \tag{D.2}$$

This means that also the real stator flux linkage amplitude will be:

$$\psi_{s1} = \frac{1}{f_\psi}\sqrt{u_{s1}^2 + r_s^2 i_{s1}^2 - 2u_{s1}r_s i_{s1}\cos(\gamma_{s1}^{s1} - \varepsilon_{s1}^{s1})} \tag{D.3}$$

And the amplitude error will be:

$$\begin{aligned}\hat{\psi}_{s1} - \psi_{s1} = \frac{1}{f_\psi}(&\sqrt{u_{s1}^2 + \hat{r}_s^2 i_{s1}^2 - 2u_{s1}\hat{r}_s i_{s1}\cos(\gamma_{s1}^{s1} - \varepsilon_{s1}^{s1})} \\ &- \sqrt{u_{s1}^2 + r_s^2 i_{s1}^2 - 2u_{s1}r_s i_{s1}\cos(\gamma_{s1}^{s1} - \varepsilon_{s1}^{s1})})\end{aligned} \tag{D.4}$$

To get zero error $\hat{r}_s = r_s$ or:

$$\begin{aligned}
\sqrt{u_{s1}^2 + r_s^2 i_{s1}^2 - 2u_{s1} r_s i_{s1} \cos(\gamma_{s1}^{s1} - \varepsilon_{s1}^{s1})} &= \sqrt{u_{s1}^2 + \hat{r}_s^2 i_{s1}^2 - 2u_{s1} \hat{r}_s i_{s1} \cos(\gamma_{s1}^{s1} - \varepsilon_{s1}^{s1})} \\
u_{s1}^2 + r_s^2 i_{s1}^2 - 2u_{s1} r_s i_{s1} \cos(\gamma_{s1}^{s1} - \varepsilon_{s1}^{s1}) &= u_{s1}^2 + \hat{r}_s^2 i_{s1}^2 - 2u_{s1} \hat{r}_s i_{s1} \cos(\gamma_{s1}^{s1} - \varepsilon_{s1}^{s1}) \\
r_s^2 i_{s1}^2 - 2u_{s1} r_s i_{s1} \cos(\gamma_{s1}^{s1} - \varepsilon_{s1}^{s1}) &= \hat{r}_s^2 i_{s1}^2 - 2u_{s1} \hat{r}_s i_{s1} \cos(\gamma_{s1}^{s1} - \varepsilon_{s1}^{s1}) \\
r_s^2 i_{s1} - 2u_{s1} r_s \cos(\gamma_{s1}^{s1} - \varepsilon_{s1}^{s1}) &= \hat{r}_s^2 i_{s1} - 2u_{s1} \hat{r}_s \cos(\gamma_{s1}^{s1} - \varepsilon_{s1}^{s1}) \\
i_{s1}(r_s^2 - \hat{r}_s^2) &= 2u_{s1} \cos(\gamma_{s1}^{s1} - \varepsilon_{s1}^{s1})(r_s - \hat{r}_s) \\
i_{s1}(r_s + \hat{r}_s)(r_s - \hat{r}_s) &= 2u_{s1} \cos(\gamma_{s1}^{s1} - \varepsilon_{s1}^{s1})(r_s - \hat{r}_s) \\
i_{s1}(r_s + \hat{r}_s) &= 2u_{s1} \cos(\gamma_{s1}^{s1} - \varepsilon_{s1}^{s1}) \\
\\
\Rightarrow \qquad i_{s1} &= \frac{2u_{s1} \cos(\gamma_{s1}^{s1} - \varepsilon_{s1}^{s1}}{r_s + \hat{r}_s}
\end{aligned} \tag{D.5}$$

D.1.2 Angle Error Stator Flux Linkage Estimate

From equation D.1 we can write the estimated stator flux linkage angle:

$$\hat{\xi}_{s1}^{s1} = \arctan\left(\frac{\hat{r}_s i_{s1} \cos(\varepsilon_{s1}^{s1}) - u_{s1} \cos(\gamma_{s1}^{s1})}{u_{s1} \sin(\gamma_{s1}^{s1}) - \hat{r}_s i_{s1} \sin(\varepsilon_{s1}^{s1})}\right) \tag{D.6}$$

Then the correct measured angle will be:

$$\xi_{s1}^{s1} = \arctan\left(\frac{r_s i_{s1} \cos(\varepsilon_{s1}^{s1}) - u_{s1} \cos(\gamma_{s1}^{s1})}{u_{s1} \sin(\gamma_{s1}^{s1}) - r_s i_{s1} \sin(\varepsilon_{s1}^{s1})}\right) \tag{D.7}$$

Hence the error will be:

$$\hat{\xi}_{s1,err}^{s1} = \arctan\left(\frac{\hat{r}_s i_{s1} \cos(\varepsilon_{s1}^{s1}) - u_{s1} \cos(\gamma_{s1}^{s1})}{u_{s1} \sin(\gamma_{s1}^{s1}) - \hat{r}_s i_{s1} \sin(\varepsilon_{s1}^{s1})}\right) - \arctan\left(\frac{r_s i_{s1} \cos(\varepsilon_{s1}^{s1}) - u_{s1} \cos(\gamma_{s1}^{s1})}{u_{s1} \sin(\gamma_{s1}^{s1}) - r_s i_{s1} \sin(\varepsilon_{s1}^{s1})}\right) \tag{D.8}$$

Since the arctan-function only has a range between $[-\frac{\pi}{2}, \frac{\pi}{2}]$ one has to use the arctan2-function which gives a range between $[-\pi, \pi]$

$$\hat{\xi}_{s1,error}^{s1} = \begin{cases}
\arctan\frac{y}{x} - \arctan\frac{\psi_{sq1}^{s1}}{\psi_{sd1}^{s1}}, & \text{if } x > 0 \\
\arctan\frac{y}{x} + \pi - \arctan\frac{\psi_{sq1}^{s1}}{\psi_{sd1}^{s1}}, & \text{if } x < 0 \text{ and } y \geq 0 \\
\arctan\frac{y}{x} - \pi - \arctan\frac{\psi_{sq1}^{s1}}{\psi_{sd1}^{s1}}, & \text{if } x < 0 \text{ and } y < 0 \\
\frac{\pi}{2} - \arctan\frac{\psi_{sq1}^{s1}}{\psi_{sd1}^{s1}}, & \text{if } x = 0 \text{ and } y > 0 \\
-\frac{\pi}{2} - \arctan\frac{\psi_{sq1}^{s1}}{\psi_{sd1}^{s1}}, & \text{if } x = 0 \text{ and } y < 0 \\
\text{undefined}, & \text{if } x = 0 \text{ and } y = 0
\end{cases} \tag{D.9}$$

where

$$y = \hat{r}_s i_{s1} \cos(\varepsilon_{s1}^{s1}) - u_{s1} \cos(\gamma_{s1}^{s1}), \qquad x = u_{s1} \sin(\gamma_{s1}^{s1}) - \hat{r}_s i_{s1} \sin(\varepsilon_{s1}^{s1}) \tag{D.10}$$

D.1.3 Amplitude Error Rotor Flux Linkage Estimate

The estimation of the rotor flux linkage amplitude is written in the rotor flux oriented system:

$$\hat{\psi}_R = \hat{\psi}_{sd1} - \hat{x}_\sigma \hat{i}_{sd1} - (\hat{x}_\sigma - \hat{x}_{s\sigma}) \hat{i}_{sd2} \tag{D.11}$$

Here:

$$\begin{aligned} \hat{i}_{sd1} &= \hat{i}_{sd2} \\ \hat{i}_{sd1} &= i_{s1} \cos(\hat{\varepsilon}_{s1}^R) = i_{s1} \cos(\varepsilon_{s1}^{s1} - \hat{\theta}_{s1}^R) \\ \hat{\psi}_{sd1} &= \hat{\psi}_{s1} \cos(\xi_{s1}^R) \end{aligned} \tag{D.12}$$

Then:

$$\hat{\psi}_R = \hat{\psi}_{s1} \cdot \cos(\hat{\xi}_{s1}^R) - 2 \cdot \hat{x}_\sigma \cdot i_{s1} \cdot \cos(\hat{\varepsilon}_{s1}^R) + \hat{x}_{s\sigma} \cdot i_{s1} \cdot \cos(\hat{\varepsilon}_{s1}^R) \tag{D.13}$$

Hence the error function will be:

$$\hat{\psi}_{R,err} = (\psi_{s1} \cos \xi_{s1}^R - \hat{\psi}_{s1} \cos \hat{\xi}_{s1}^R) - i_{s1}(\cos \varepsilon_{s1}^R (2x_\sigma - x_{s\sigma}) - \cos \hat{\varepsilon}_{s1}^R (2\hat{x}_\sigma - \hat{x}_{s\sigma})) \tag{D.14}$$

D.2 Current Model

D.2.1 Angle Error Rotor Flux Linkage Estimate

Now the speed of the rotor is measured and we know the synchronous frequency by measurements. Hence:

$$\hat{f}_s = \hat{f}_r + n, \qquad f_s = f_r + n \tag{D.15}$$

If $i_{sq1} = i_{sq2}$ and

$$\hat{f}_s = f_s \Rightarrow \quad \hat{f}_r = f_r \tag{D.16}$$

Hence

$$\begin{aligned} \frac{2\hat{r}_R \hat{i}_{sq1}}{\hat{\psi}_R} &= \frac{2 r_R i_{sq1}}{\psi_R} \\ \frac{\hat{r}_R \hat{i}_{sq1}}{\hat{x}_H \hat{i}_{sd1}} &= \frac{r_R i_{sq1}}{x_H i_{sd1}} \end{aligned} \tag{D.17}$$

We put in

$$\tan \hat{\varepsilon}_{s1}^R = \frac{\hat{i}_{sq1}}{\hat{i}_{sd1}} \tag{D.18}$$

Hence

$$\begin{aligned}\tan\hat{\varepsilon}_{s1}^{R} &= \frac{\hat{x}_H r_R i_{sq1}}{\hat{r}_R x_H i_{sd1}} \\ \hat{\varepsilon}_{s1}^{R} &= \arctan(\frac{\hat{x}_H r_R i_{sq1}}{\hat{r}_R x_H i_{sd1}})\end{aligned} \tag{D.19}$$

The error of the rotor flux linkage angle estimation can be written:

$$\begin{aligned}\hat{\theta}_R^{s1} - \theta_R^{s1} =& (\varepsilon_{s1}^{s1} - \hat{\varepsilon}_{s1}^{R}) - (\varepsilon_{s1}^{s1} - \varepsilon_{s1}^{R}) = \varepsilon_{s1}^{R} - \hat{\varepsilon}_{s1}^{R} \\ =& \arctan(\frac{i_{sq1}}{i_{sd1}}) - \arctan(\frac{\hat{x}_H r_R i_{sq1}}{\hat{r}_R x_H i_{sd1}})\end{aligned} \tag{D.20}$$

The most sensitive torque operational point can be investigated by derivating the equation. The generated electrical torque can be written like:

$$m_e = 2\psi_R i_{sq1} = 4x_H i_{sd1} i_{sq1} \Rightarrow i_{sq1} = \frac{m_e}{4x_H i_{sd1}} \tag{D.21}$$

Hence:

$$\hat{\theta}_R^{s1} - \theta_R^{s1} = \hat{\theta}_{R,err}^{s1} = \arctan(\frac{m_e}{4x_H i_{sd1}^2}) - \arctan(\frac{\hat{x}_H r_R m_e}{4\hat{r}_R x_H^2 i_{sd1}^2}) \tag{D.22}$$

Using the trigonometric property:

$$\frac{d}{dx}\arctan x = \frac{1}{1+x^2} \tag{D.23}$$

Then:

$$\frac{d}{dm_e}\hat{\theta}_{R,err}^{s1} = \frac{\frac{1}{4x_H i_{sd1}^2}}{1 + (\frac{m_e}{4x_H i_{sd1}^2})^2} - \frac{\frac{\hat{x}_H r_R}{4\hat{r}_R x_H^2 i_{sd1}^2}}{1 + (\frac{\hat{x}_H r_R m_e}{4\hat{r}_R x_H^2 i_{sd1}^2})^2} \tag{D.24}$$

Setting this to zero and solving a second degree equation for m_e gives:

$$m_e = \pm 4x_H i_{sd1}^2 \sqrt{\frac{\hat{r}_R x_H}{r_R \hat{x}_H}} \tag{D.25}$$

E Modelling from Project thesis [15]

E.1 Introduction

An induction machine is an AC machine where the stator windings get feeded by alternating current. The rotor can be of two types; wound-rotor type or squirrel cage type. A wound-rotor is a rotor made up of windings, and a squirrel cage rotor is a rotor made up of short-circuited conducting bars formed as a squirrel cage. The AC current in the stator produces a rotating flux linkage which rotates at synchronous speed. By electromagnetic induction the rotor will get induced some voltage and current will also flow in the rotor. This alternating current will again result in a rotating rotor flux linkage space vector which will try to align itself with the rotating stator flux linkage space vector. Though it will never completely do so, because of slacking. Hence in steady state the rotor's rotating flux linkage and the stator's rotating flux linkage will both rotate in synchronous speed.

In this thesis the focus will be at a six-phase induction motor with a non specified rotor type. The six-phase windings consists of two groups of three-phase windings seperated by 30 electrical degrees with isolated neutrals. The phase groups are star connected and each phase is seperated by 120 electrical degrees. The stator phase windings have a sinusoidal distribution and hence it is assumed that it will make a synchronously rotating sinusoidal magnetic field around the air gap between the stator and the rotor.

There exist different modelling approaches depending on the choice of control used for the induction machine. One of the types is called stationary frame control and is done in coordinates fixed to the stator. Another one, which will be used in this project is the synchronously frame control where the reference frame is rotating synchronously. The synchronous frame control can be divided in single and double synchronous frame control (DSFC) and in this thesis the double synchronous frame control is used.

In the modelling some assumptions are made[10][8]:

1. The stator windings produce a sinusoidally distributed magnetic field around the air-gap in the machine, hence only the fundamental component of the field will be modelled.
2. The stator windings are equal, but are oriented in different directions of winding axes.
3. Resistances and inductances are independent of temperature and frequency and are known.

4. Magnetic saturation, hysteresis and eddy currents are neglected.

5. The rotor can be modelled as a wound rotor.

E.2 Modelling in Double Synchronus Reference Frame

By modelling in the double synchronous reference frame the modelling of the rotor consist of three phase windings seperated by 120 electrical degrees. This is shown in figure E.1. At first it will be modelled physically and then the equations will be transformed to a synchronously rotating d-q-0 reference frame. Finally the per unit equations will be executed. This modelling was done in [10] and only some of the results are found here. For more thoroughly investigation one should look in the reference.

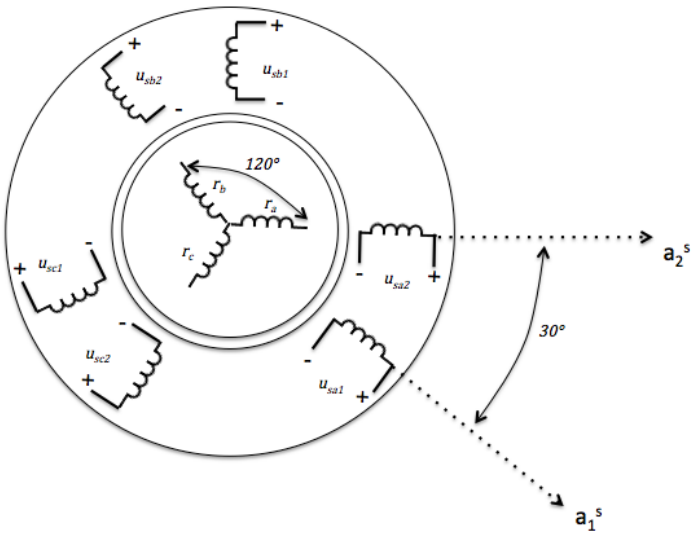

Figure E.1: Double Synchronous Frame Modelling

Starting with the equations:[3]

$$\underline{U}^{SR} = \mathbf{R}^{SR} \cdot \underline{I}^{SR} + \frac{d\underline{\Psi}^{SR}}{dt} \tag{E.1}$$

$$\underline{\Psi}^{SR} = \mathbf{L}^{SR} \cdot \underline{I}^{SR} \tag{E.2}$$

Here the vectors will be described as:

$$\underline{U}^{SR} = \begin{bmatrix} U_{sa1} \\ U_{sb1} \\ U_{sc1} \\ U_{sa2} \\ U_{sb2} \\ U_{sc2} \\ U_{ra} \\ U_{rb} \\ U_{rc} \end{bmatrix} \quad \underline{I}^{SR} = \begin{bmatrix} I_{sa1} \\ I_{sb1} \\ I_{sc1} \\ I_{sa2} \\ I_{sb2} \\ I_{sc2} \\ I_{ra} \\ I_{rb} \\ I_{rc} \end{bmatrix} \quad \underline{\Psi}^{SR} = \begin{bmatrix} \Psi_{sa1} \\ \Psi_{sb1} \\ \Psi_{sc1} \\ \Psi_{sa2} \\ \Psi_{sb2} \\ \Psi_{sc2} \\ \Psi_{ra} \\ \Psi_{rb} \\ \Psi_{rc} \end{bmatrix} \tag{E.3}$$

The resistance matrix is described as:

$$\mathbf{R}^{SR} = diag[R_s \ R_s \ R_s \ R_s \ R_s \ R_s \ R_r \ R_r \ R_r]^T \tag{E.4}$$

The inductance matrix is described as:

$$\mathbf{L}^{SR} = \begin{bmatrix} \mathbf{L}^S_{ss} & \mathbf{L}^S_{sr}(\theta) \\ \mathbf{L}^R_{rs}(\theta) & \mathbf{L}^R_{rr} \end{bmatrix} \tag{E.5}$$

where:

$$\mathbf{L}^S_{ss} = \begin{bmatrix} L_{sa1} & L_{sa1,sb1} & L_{sa1,sc1} & L_{sa1,sa2} & L_{sa1,sb2} & L_{sa1,sc2} \\ L_{sb1,sa1} & L_{sb1} & L_{sb1,sc1} & L_{sb1,sa2} & L_{sb1,sb2} & L_{sb1,sc2} \\ L_{sc1,sa1} & L_{sc1,sb1} & L_{sc1} & L_{sc1,sa2} & L_{sc1,sb2} & L_{sc1,sc2} \\ L_{sa2,sa1} & L_{sa2,sb1} & L_{sa2,sc1} & L_{sa2} & L_{sa2,sb2} & L_{sa2,sc2} \\ L_{sb2,sa1} & L_{sb2,sb1} & L_{sb2,sc1} & L_{sb2,sa2} & L_{sb2} & L_{sb2,sc2} \\ L_{sc2,sa1} & L_{sc2,sb1} & L_{sc2,sc1} & L_{sc2,sa2} & L_{sc2,sb2} & L_{sc2} \end{bmatrix} = L_{s\sigma} \cdot \mathbf{I} + \mathbf{L}^S_{sh} \tag{E.6}$$

$$\mathbf{L}^S_{sh} = L_{sh} \cdot \begin{bmatrix} 1 & -\frac{1}{2} & -\frac{1}{2} & \frac{\sqrt{3}}{2} & -\frac{\sqrt{3}}{2} & 0 \\ -\frac{1}{2} & 1 & \frac{1}{2} & 0 & \frac{\sqrt{3}}{2} & -\frac{\sqrt{3}}{2} \\ -\frac{1}{2} & -\frac{1}{2} & 1 & -\frac{\sqrt{3}}{2} & 0 & \frac{\sqrt{3}}{2} \\ \frac{\sqrt{3}}{2} & 0 & -\frac{\sqrt{3}}{2} & 1 & -\frac{1}{2} & -\frac{1}{2} \\ -\frac{\sqrt{3}}{2} & \frac{\sqrt{3}}{2} & 0 & -\frac{1}{2} & 1 & -\frac{1}{2} \\ 0 & -\frac{\sqrt{3}}{2} & \frac{\sqrt{3}}{2} & -\frac{1}{2} & -\frac{1}{2} & 1 \end{bmatrix} \tag{E.7}$$

$$\mathbf{L}^R_{rr} = \begin{bmatrix} L_{ra} & L_{ra,rb} & L_{ra,rc} \\ L_{rb,ra} & L_{rb} & L_{rb,rc} \\ L_{rc,ra} & L_{rc,rb} & L_{rc} \end{bmatrix} = L_{r\sigma} \cdot \mathbf{I} + \mathbf{L}^R_{rh} \tag{E.8}$$

$$\mathbf{L}_{rh}^{R} = L_{rh} \cdot \begin{bmatrix} 1 & -\frac{1}{2} & -\frac{1}{2} \\ -\frac{1}{2} & 1 & -\frac{1}{2} \\ -\frac{1}{2} & -\frac{1}{2} & 1 \end{bmatrix} \tag{E.9}$$

$$\mathbf{L}_{sr}^{S}(\theta) = (\mathbf{L}_{rs}^{R}(\theta))^{T} = \begin{bmatrix} L_{sa1,ra} & L_{sa1,rb} & L_{sa1,rc} \\ L_{sb1,ra} & L_{sb1,rb} & L_{sb1,rc} \\ L_{sc1,ra} & L_{sc1,rb} & L_{sc1,rc} \\ L_{sa2,ra} & L_{sa2,rb} & L_{sa2,rc} \\ L_{sb2,ra} & L_{sb2,rb} & L_{sb2,rc} \\ L_{sc2,ra} & L_{sc2,rb} & L_{sc2,rc} \end{bmatrix} \tag{E.10}$$

$$= L_{srh} \cdot \begin{bmatrix} cos\theta & cos(\theta + \frac{2\pi}{3}) & cos(\theta + \frac{4\pi}{3}) \\ cos(\theta - \frac{2\pi}{3}) & cos\theta & cos(\theta + \frac{2\pi}{3}) \\ cos(\theta - \frac{4\pi}{3}) & cos(\theta - \frac{2\pi}{3}) & cos\theta \\ cos(\theta - \frac{\pi}{6}) & cos(\theta + \frac{\pi}{2}) & cos(\theta + \frac{7\pi}{6}) \\ cos(\theta - \frac{5\pi}{6}) & cos(\theta - \frac{\pi}{6}) & cos(\theta - \frac{2\pi}{3}) \\ cos(\theta - \frac{3\pi}{2}) & cos(\theta - \frac{5\pi}{6}) & cos(\theta - \frac{\pi}{6}) \end{bmatrix}$$

The equations for the mechanical system:

$$J \cdot \frac{d\Omega}{dt} = M_e - M_L, \quad \frac{d\theta_{mech}}{dt} = \Omega, \quad \theta = p \cdot \theta_{mech} \tag{E.11}$$

$$M_e = \frac{p}{2}(\underline{I}^S)^T \cdot \frac{\partial \mathbf{L}_{ss}^{S}(\theta)}{\partial \theta} \cdot \underline{I}^S \tag{E.12}$$

One of the motivations for making use of the transformation to the d-q-0 reference frame is to remove the dependency of angle for the inductances. Hence the expressions for the mutual inductances will not depend on the angle. In addition the AC qunatities will be described as stationary DC quantities which make the control less complex. The stator quantities will be transformed into the coordinate sets, (d_1, q_1, 0_1) and (d_2, q_2, 0_2). The rotor quantities will be transformed into the coordinate set (d, q, 0).

The transformation matrix is described as:

$$\mathbf{T}^{k} = \begin{bmatrix} \mathbf{T}_{SS}^{k} & \mathbf{0} \\ \mathbf{0} & \mathbf{T}_{RR}^{k} \end{bmatrix} \tag{E.13}$$

Where:

$$\mathbf{T}^k_{SS} = \frac{2}{3}\cdot\begin{bmatrix} cos\theta_k & cos(\theta_k - \frac{2\pi}{3}) & cos(\theta_k - \frac{4\pi}{3}) & 0 & 0 & 0 \\ -sin\theta_k & -sin(\theta_k - \frac{2\pi}{3}) & -sin(\theta_k - \frac{4\pi}{3}) & 0 & 0 & 0 \\ \frac{1}{2} & \frac{1}{2} & \frac{1}{2} & 0 & 0 & 0 \\ 0 & 0 & 0 & cos(\theta_k - \frac{\pi}{6}) & cos(\theta_k - \frac{5\pi}{6}) & cos(\theta_k - \frac{3\pi}{2}) \\ 0 & 0 & 0 & -sin(\theta_k - \frac{\pi}{6}) & -sin(\theta_k - \frac{5\pi}{6}) & -sin(\theta_k - \frac{3\pi}{2}) \\ 0 & 0 & 0 & \frac{1}{2} & \frac{1}{2} & \frac{1}{2} \end{bmatrix} \tag{E.14}$$

$$\mathbf{T}^k_{RR} = \frac{2}{3}\cdot\begin{bmatrix} cos\theta_r & cos(\theta_r - \frac{2\pi}{3}) & cos(\theta_r - \frac{4\pi}{3}) \\ -sin\theta_r & -sin(\theta_r - \frac{2\pi}{3}) & -sin(\theta_r - \frac{4\pi}{3}) \\ \frac{1}{2} & \frac{1}{2} & \frac{1}{2} \end{bmatrix} \tag{E.15}$$

θ_k is the angle between the synchronously rotating d-axis and the a1 stator axis. θ_r is the angle between the synchronoulsy rotating d-axis and the rotor a axis. Their correlation is given by:

$$\theta_k = \theta + \theta_r \tag{E.16}$$

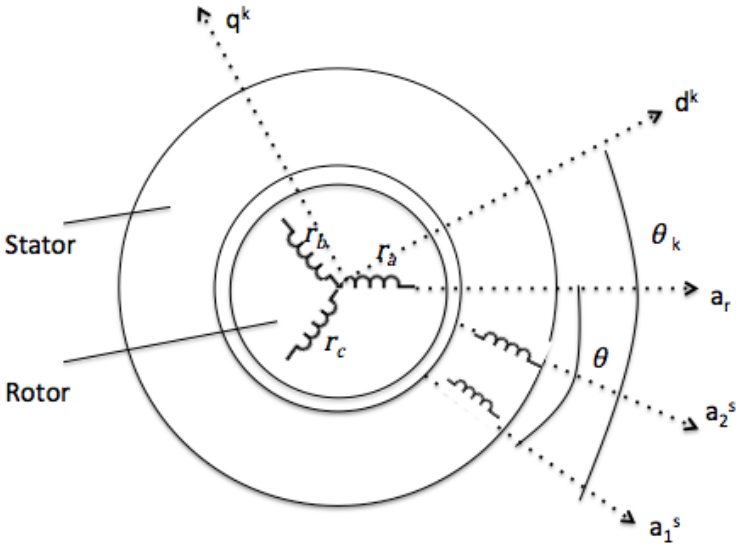

Figure E.2: Transforming to the d-q-0 rotating reference frame

Applying eq. (E.13) to eq. (E.1) yields:

$$\underline{U}^k = \mathbf{R}^k \cdot \underline{I}^k + \frac{d\underline{\Psi}^k}{dt} + \omega_n \cdot f_x \cdot \mathbf{J} \cdot \underline{\Psi}^k \tag{E.17}$$

Where:

$$\mathbf{J} = \begin{bmatrix} 0 & -1 & 0 & 0 & 0 & 0 & 0 & 0 & 0 \\ 1 & 0 & 0 & 0 & 0 & 0 & 0 & 0 & 0 \\ 0 & 0 & 0 & 0 & 0 & 0 & 0 & 0 & 0 \\ 0 & 0 & 0 & 0 & -1 & 0 & 0 & 0 & 0 \\ 0 & 0 & 0 & 1 & 0 & 0 & 0 & 0 & 0 \\ 0 & 0 & 0 & 0 & 0 & 0 & 0 & 0 & 0 \\ 0 & 0 & 0 & 0 & 0 & 0 & 0 & -1 & 0 \\ 0 & 0 & 0 & 0 & 0 & 0 & 1 & 0 & 0 \\ 0 & 0 & 0 & 0 & 0 & 0 & 0 & 0 & 0 \end{bmatrix} \tag{E.18}$$

$$\mathbf{R}^k = diag[R_s \ R_s \ R_s \ R_s \ R_s \ R_r \ R_r \ R_r] \tag{E.19}$$

And regarding the f_x, x is k in stator terms and r in rotor terms.

Applying eq. (E.13) to eq. (E.2) yields:

$$\underline{\Psi}^k = \mathbf{L}^k \cdot \underline{I}^k \tag{E.20}$$

Where

$$\mathbf{L}^k = \begin{bmatrix} L_s & 0 & 0 & L_h & 0 & 0 & L_h & 0 & 0 \\ 0 & L_s & 0 & 0 & L_h & 0 & 0 & L_h & 0 \\ 0 & 0 & L_{s\sigma} & 0 & 0 & 0 & 0 & 0 & 0 \\ L_h & 0 & 0 & L_s & 0 & 0 & L_h & 0 & 0 \\ 0 & L_h & 0 & 0 & L_s & 0 & 0 & L_h & 0 \\ 0 & 0 & 0 & 0 & 0 & L_{s\sigma} & 0 & 0 & 0 \\ L_h & 0 & 0 & L_h & 0 & 0 & L_{rd} & 0 & 0 \\ 0 & L_h & 0 & 0 & L_h & 0 & 0 & L_{rq} & 0 \\ 0 & 0 & 0 & 0 & 0 & 0 & 0 & 0 & L_{r\sigma} \end{bmatrix} \tag{E.21}$$

and

$$L_s = L_{s\sigma} + \frac{3}{2}L_{sh}, \quad L_r = L_{r\sigma} + \frac{3}{2}L_{srh} \quad L_h = \frac{3}{2}L_{srh} = \frac{3}{2}L_{sh} \tag{E.22}$$

Applying eq. (E.13) to eq. (E.12) yields:

$$M_e = \frac{p}{2} \cdot 3 \cdot (\Psi_{rq} \cdot I_{rd} - \Psi_{rd} \cdot I_{rq}) \tag{E.23}$$

Now the scaling to the per unit system will be done. The equations will be divided

by the base quantities defined in the appendix. Here only the result will be showed:

$$
\begin{aligned}
u_{sd1} &= r_s \cdot i_{sd1} + \frac{1}{\omega_n} \cdot \frac{d\psi_{sd1}}{dt} - f_k \cdot \psi_{sq1}, \quad & u_{sq1} &= r_s \cdot i_{sq1} + \frac{1}{\omega_n} \cdot \frac{d\psi_{sq1}}{dt} + f_k \cdot \psi_{sd1} \\
u_{sd2} &= r_s \cdot i_{sd2} + \frac{1}{\omega_n} \cdot \frac{d\psi_{sd2}}{dt} - f_k \cdot \psi_{sq2}, \quad & u_{sq2} &= r_s \cdot i_{sq2} + \frac{1}{\omega_n} \cdot \frac{d\psi_{sq2}}{dt} + f_k \cdot \psi_{sd2} \\
0 &= r_r \cdot i_{rd} + \frac{1}{\omega_n} \cdot \frac{d\psi_{rd}}{dt} - f_r \cdot \psi_{rq}, \quad & 0 &= r_r \cdot i_{rq} + \frac{1}{\omega_n} \cdot \frac{d\psi_{rq}}{dt} + f_r \cdot \psi_{rd}
\end{aligned}
\tag{E.24}
$$

$$
\begin{aligned}
\psi_{sd1} &= x_s \cdot i_{sd1} + x_h \cdot i_{sd2} + x_h \cdot i_{rd}, \quad & \psi_{sq1} &= x_s \cdot i_{sq1} + x_h \cdot i_{sq2} + x_h \cdot i_{rq} \\
\psi_{sd2} &= x_h \cdot i_{sd1} + x_s \cdot i_{sd2} + x_h \cdot i_{rd}, \quad & \psi_{sq2} &= x_h \cdot i_{sq1} + x_s \cdot i_{sq2} + x_h \cdot i_{rq} \\
\psi_{rd} &= x_h \cdot i_{sd1} + x_h \cdot i_{sd2} + x_r \cdot i_{rd}, \quad & \psi_{rq} &= x_h \cdot i_{sq1} + x_h \cdot i_{sq2} + x_r \cdot i_{rq}
\end{aligned}
\tag{E.25}
$$

$$
\begin{aligned}
m_e &= \frac{\psi_{rq} \cdot i_{rd} - \psi_{rd} \cdot i_{rq}}{2}, \quad & T_m \cdot \frac{dn}{dt} &= m_e - m_L, \quad & T_m &= \frac{J \cdot \Omega_N^2}{S_N} \\
f_r &= f_k - n, & f_k &= \frac{\omega_k}{\omega_n}, & f_r &= \frac{\omega_r}{\omega_n}
\end{aligned}
\tag{E.26}
$$

The zero subspace will not be excited in this model and hence is omitted from the equations[10].

The equivalent circuit of the d- and the q-axis can be seen in fig. E.3 and E.4.

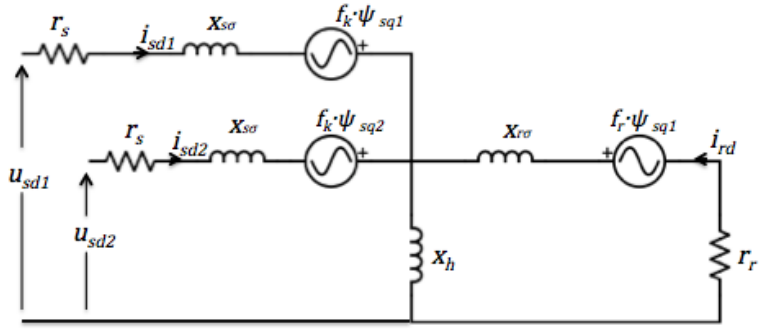

Figure E.3: d axis equivalent circuit in per unit

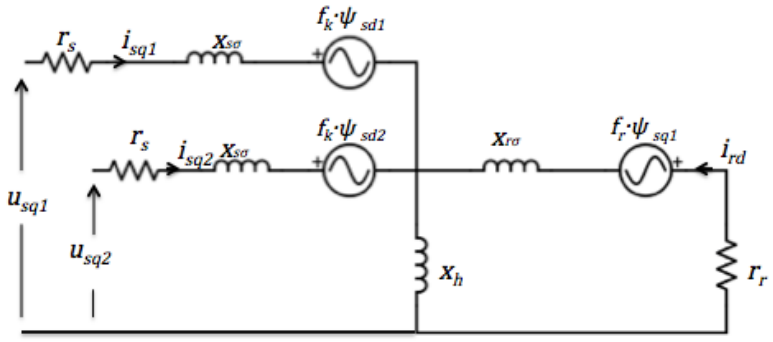

Figure E.4: q axis equivalent circuit in per unit

F Estimating the Rotor Flux Linkage Angle θ

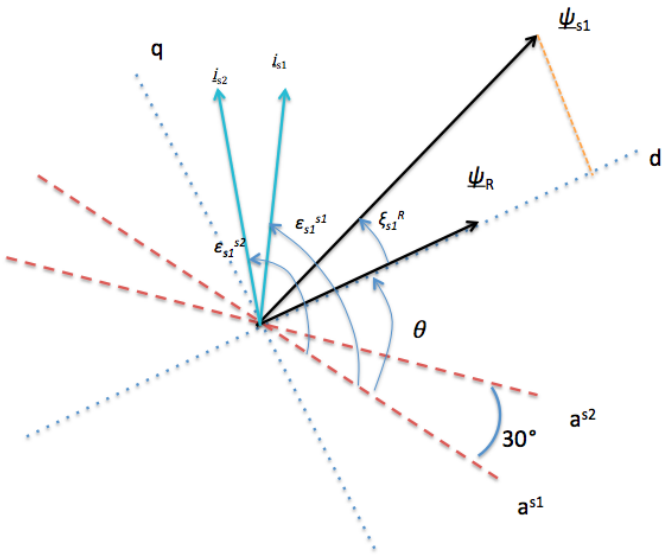

Figure F.1: Obtaining the rotor flux linkage space vector

There exists different method for obtaining the angle θ. One of them is by first calculating the angle between the stator flux linkage space vector and the rotor flux linkage space vector. This angle is referred here as ξ_{s1}^{r}. The strategy is to first find this angle and then calculate the θ from the fact that:

$$\theta = \xi_{s1}^{s1} - \xi_{s1}^{r} \tag{F.1}$$

Using eq. (3.4) and by trigonometry from figure F.1 one can see that:

$$\psi_{s1} \cdot sin\xi_{s1}^{r} = x_\sigma \cdot i_{sq1} + (x_\sigma - x_{s\sigma}) \cdot i_{sq2} \tag{F.2}$$

The task now is to find expressions for the i_{sq1} and i_{sq2}. By looking at the figure F.1 it can be seen that:

$$i_{sq1} = i_{s1} \cdot sin(\xi_{s1}^{r} + \varepsilon_{s1}^{\psi_{s1}}), \quad i_{sq2} = i_{s2} \cdot sin(\xi_{s2}^{r} + \varepsilon_{s2}^{\psi_{s1}}) \tag{F.3}$$

Where $\varepsilon_{s1}^{\psi_r}$ is equal to the angle between the stator flux linkage space vector and the stator 1 current space vector and $\varepsilon_{s2}^{\psi_r}$ is the angle between the stator flux linkage space vector and the stator 2 current space vector.

Using the trigonometric identity:

$$sin(x \pm y) = sinx \cdot cosy \pm cosx \cdot siny \tag{F.4}$$

One obtain the equation for obtaining the angle:

$$tan\xi_{s1}^{r} = \frac{x_\sigma \cdot i_{s1} \cdot sin\varepsilon_{s1}^{\psi_{s1}} + (x_\sigma - x_{s\sigma}) \cdot i_{s2} \cdot sin\varepsilon_{s2}^{\psi_{s1}}}{\psi_{s1} - x_\sigma \cdot i_{s1} \cdot cos\varepsilon_{s1}^{\psi_{s1}} - (x_\sigma - x_{s\sigma}) \cdot i_{s2} \cdot cos\varepsilon_{s2}^{\psi_{s1}}} \tag{F.5}$$

G Additional Simulations

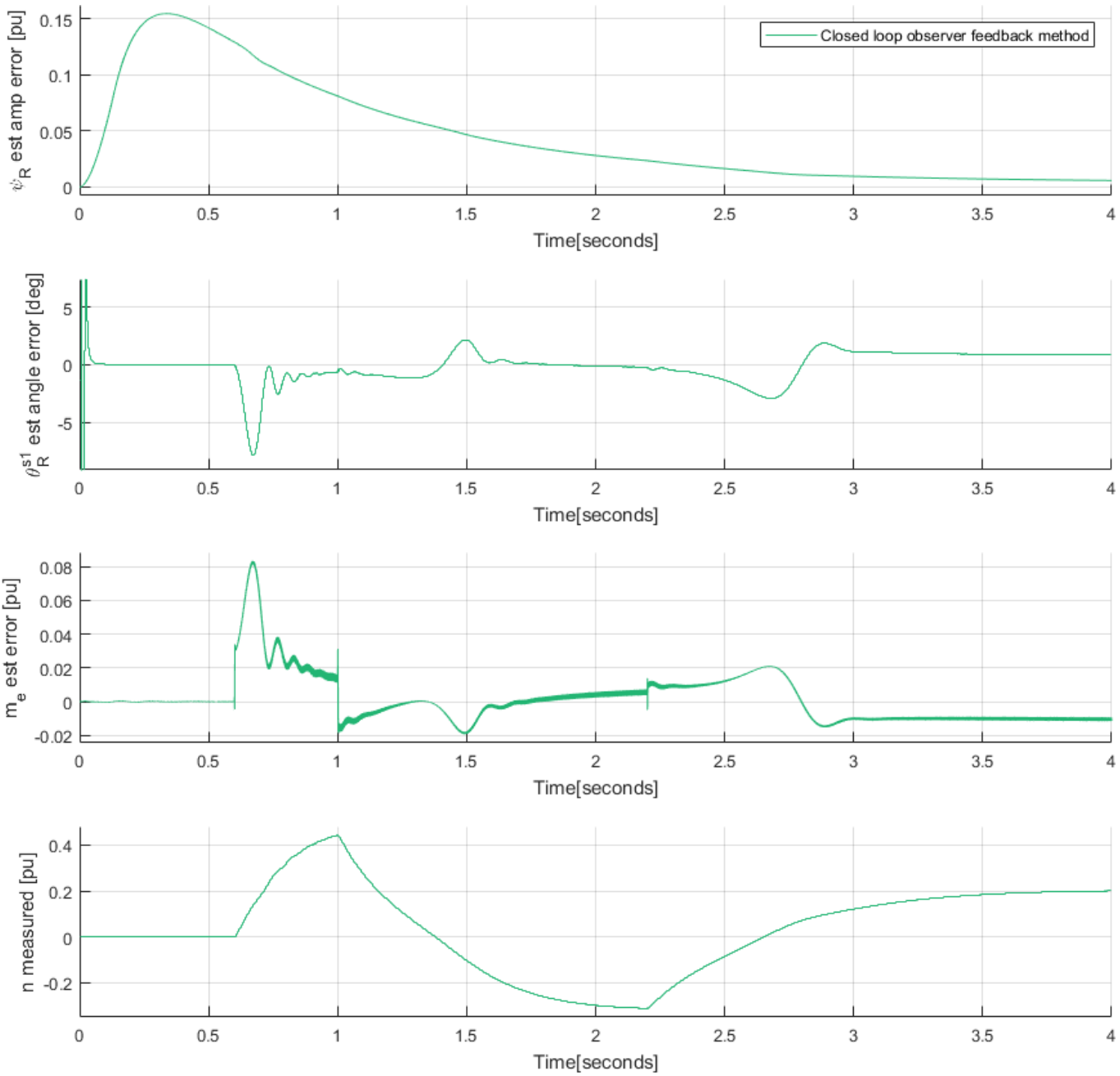

Figure G.1: Closed loop feedback observer method with $\hat{r}_s = 0.8r_s$ and $\hat{r}_R = 0.8r_R$

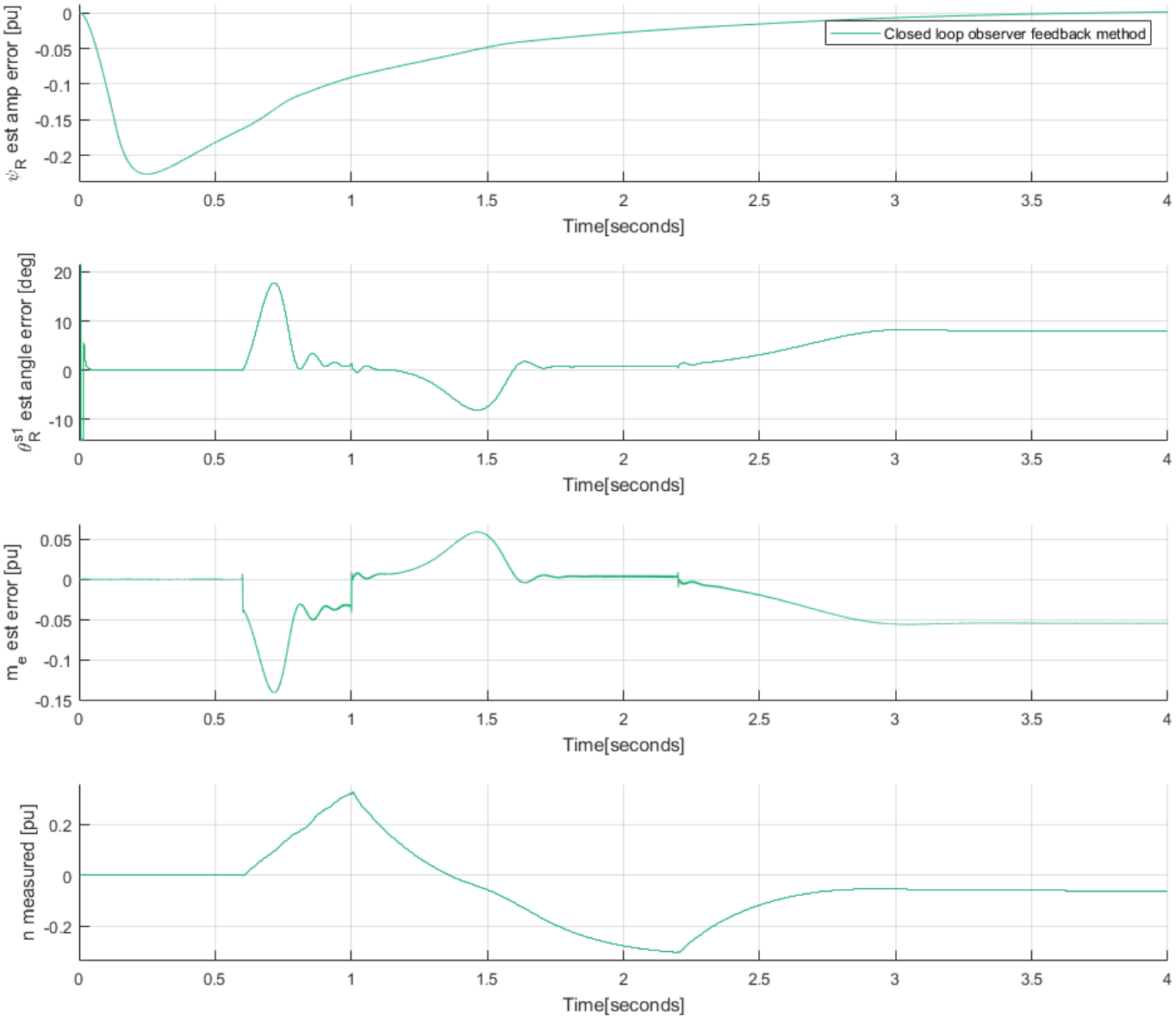

Figure G.2: Closed loop feedback observer method with $\hat{r}_s = 1.5r_s$ and $\hat{r}_R = 1.5r_R$

H Matlab Code Stationary Parameter Sensitivity Analysis

```
%% MATLAB CODE STATIONARY PARAMETER SENSITIVITY ANALYSIS %%

%% CALCULATING REAL VALUES %%%%%%%%%%%%%%%%

% Initial
t_e=[-1:0.005:1];
n=transpose([-2:0.002:2]);
omega_n = 2*pi*50;
Psi_R0 = 0.95;
u_max = 1.0;
i_max = 1.0;
n_max = 1.0; % without field weakening
m = 401; % for loop help
l = 2001; % for loop help

% parameters
x_H = 1.8685*0.5;
r_R = 0.0068*0.5;
r_s = 0.031;
x_sigma = 0.756595484*0.2175;
x_ssigma = 0.1117;

% calculating time constants

T_r = x_H/(r_R*omega_n);

for k=1:l

    for i=1:m

    Psi_R(k,i) = 0.95;

    % calculating currents

    epsilon_s1_s1(k,i)= atan2(t_e(1,i)*x_H,Psi_R(k,i)^2);
    epsilon_s2_s1(k,i) = epsilon_s1_s1(k,i);
```

```
37      i_s_amp(k,i) = sqrt((t_e(1,i)/Psi_R(k,i))^2+(Psi_R(k,i)/
            x_H)^2)/2;
38
39      [i_sd1(k,i) i_sq1(k,i)] = pol2cart(epsilon_s1_s1(k,i),
            i_s_amp(k,i));
40      i_s1(k,i) = i_sd1(k,i) + 1j*i_sq1(k,i);
41
42      [i_sd2(k,i) i_sq2(k,i)] = pol2cart(epsilon_s2_s1(k,i),
            i_s_amp(k,i));
43      i_s2(k,i) = i_sd2(k,i) + 1j*i_sq2(k,i);
44
45      % calculating stator flux linkage
46
47      Psi_sd1 = x_sigma*real(i_s1(k,i))+(x_sigma-x_ssigma)*real
            (i_s2(k,i))+Psi_R(k,i);
48      Psi_sq1 = x_sigma*imag(i_s1(k,i))+(x_sigma-x_ssigma)*imag
            (i_s2(k,i));
49      Psi_s1(k,i) = Psi_sd1 + 1j*Psi_sq1;
50
51
52      xi_s1_s1(k,i) = angle(Psi_s1(k,i));
53      Psi_s1_amp(k,i) = sqrt(Psi_sd1^2+Psi_sq1^2);
54
55
56
57      % calculating angles
58
59      epsilon_s1_PsiS1(k,i) = epsilon_s1_s1(k,i) - xi_s1_s1(k,i
            );
60      epsilon_s2_PsiS1(k,i) = epsilon_s2_s1(k,i) - xi_s1_s1(k,i
            );
61
62
63      % calculating slip
64
65      f_r(k,i) = r_R*(imag(i_s1(k,i))+imag(i_s2(k,i)))/Psi_R(k,
            i);
66
67      % speed rotor flux linkage space vector
68
```

```
69      f_psi(k,i) = n(k,1) + f_r(k,i);
70
71      % calculating voltages:
72
73      u_sd1 = r_s*real(i_s1(k,i))-f_psi(k,i)*Psi_sq1;
74      u_sq1 = r_s*imag(i_s1(k,i))+f_psi(k,i)*Psi_sd1;
75      u_s1(k,i) = u_sd1 + 1j*u_sq1;
76
77      u_amp(k,i) = abs(u_s1(k,i));
78      gamma(k,i) = atan2(u_sq1,u_sd1);
79      % enabling theta
80
81      theta(k,i) = 0;
82
83      % Field weakening region
84
85      if  abs(n(k,1)) > n_max
86
87          Psi_R(k,i) = abs(Psi_R0/(n(k,1)));
88
89          % Calculating currents
90
91          epsilon_s1_s1(k,i)= atan2(t_e(1,i)*x_H,Psi_R(k,i)^2);
92          epsilon_s2_s1(k,i) = epsilon_s1_s1(k,i);
93          i_s_amp(k,i) = sqrt((t_e(1,i)/Psi_R(k,i))^2+(Psi_R(k,
                i)/x_H)^2)/2;
94
95          [i_sd1(k,i) i_sq1(k,i)] = pol2cart(epsilon_s1_s1(k,i)
                ,i_s_amp(k,i));
96          i_s1(k,i) = i_sd1(k,i) + 1j*i_sq1(k,i);
97
98          [i_sd2(k,i) i_sq2(k,i)] = pol2cart(epsilon_s2_s1(k,i)
                ,i_s_amp(k,i));
99          i_s2(k,i) = i_sd2(k,i) + 1j*i_sq2(k,i);
100
101         % calculating stator flux linkage
102
103         Psi_sd1 = x_sigma*real(i_s1(k,i))+(x_sigma-x_ssigma)*
                real(i_s2(k,i))+Psi_R(k,i);
```

```
104         Psi_sq1 = x_sigma*imag(i_s1(k,i))+(x_sigma-x_ssigma)*
                imag(i_s2(k,i));
105         Psi_s1(k,i) = Psi_sd1 + 1j*Psi_sq1;
106
107         xi_s1_s1(k,i) = angle(Psi_s1(k,i));
108         Psi_s1_amp(k,i) = sqrt(Psi_sd1^2+Psi_sq1^2);
109
110         % calculating angles
111
112         epsilon_s1_PsiS1(k,i) = epsilon_s1_s1(k,i) - xi_s1_s1
                (k,i);
113         epsilon_s2_PsiS1(k,i) = epsilon_s2_s1(k,i) - xi_s1_s1
                (k,i);
114
115         theta(k,i) = 0;
116
117         % calculating slip
118
119         f_r(k,i) = r_R*(imag(i_s1(k,i))+imag(i_s2(k,i)))/
                Psi_R(k,i);
120
121         % speed rotor flux linkage space vector
122
123         f_psi(k,i) = n(k,1) + f_r(k,i);
124
125         % calculating voltages:
126
127         u_sd1 = r_s*real(i_s1(k,i))-f_psi(k,i)*Psi_sq1;
128         u_sq1 = r_s*imag(i_s1(k,i))+f_psi(k,i)*Psi_sd1;
129         u_s1(k,i) = u_sd1 + 1j*u_sq1;
130
131         u_amp(k,i) = sqrt(u_sd1^2+u_sq1^2);
132
133         if abs(n(k,1)) > 1 && abs(t_e(1,i)) > abs(1/n(k,1))
134
135         Psi_R(k,i) = 0;
136         epsilon_s1_s1(k,i) = 0;
137         epsilon_s2_s1(k,i) = epsilon_s1_s1(k,i);
138         i_s_amp(k,i) = 0;
139         i_s1(k,i) = 0;
```

```
140             i_s2(k,i) = 0;
141             i_sd1(k,i) = 0;
142             u_s1(k,i) = 0;
143             xi_s1_s1(k,i) = 0;
144             Psi_s1(k,i) = 0;
145             end
146
147
148
149         end
150         i = i +1;
151
152         end
153
154     k = k+1;
155
156 end
157
158 %% Changing the parameters
159 x_H_M = x_H*1.0;
160 r_R_M = r_R*1.0;
161 r_s_M = r_s*1.0;
162 x_sigma_M = x_sigma*1.1;
163 x_ssigma_M = x_ssigma*1.0;
164 %% ESTIMATING USING THE VOLTAGE MODEL %%
165
166 for k=1:l
167
168         for i=1:m
169
170
171         Psi_s1_est_Mv(k,i) = -1j*(u_s1(k,i)-r_s_M*i_s1(k,i))/
                f_psi(k,i);
172         xi_s1_s1_est_Mv(k,i) = angle(Psi_s1_est_Mv(k,i));
173
174         y_Mv(k,i) = abs(i_s1(k,i))*abs(u_s1(k,i))*sin(
                epsilon_s1_s1(k,i)-gamma(k,i))*(r_s-r_s_M);
175         x_Mv(k,i) = abs(u_s1(k,i))^2+r_s_M*r_s*abs(i_s1(k,i))^2-
                abs(i_s1(k,i))*abs(u_s1(k,i))*cos(epsilon_s1_s1(k,i)-
                gamma(k,i))*(r_s+r_s_M);
```

```
176         xi_s1_s1_est_Mv_test(k,i) = atan2(y_Mv(k,i),x_Mv(k,i));
177
178         Psi_s1_amp_est_Mv(k,i) = abs(Psi_s1_est_Mv(k,i));
179
180         epsilon_s1_PsiS1_est_Mv(k,i) = epsilon_s1_s1(k,i)-
                xi_s1_s1_est_Mv(k,i);
181         epsilon_s2_PsiS1_est_Mv(k,i) = epsilon_s2_s1(k,i)-
                xi_s1_s1_est_Mv(k,i);
182
183         xi_s1_R_est_Mv(k,i)=atan2(x_sigma_M*i_s_amp(k,i)*sin(
                epsilon_s1_PsiS1_est_Mv(k,i))+(x_sigma_M-x_ssigma_M)*
                i_s_amp(k,i)*sin(epsilon_s2_PsiS1_est_Mv(k,i)),
                Psi_s1_amp_est_Mv(k,i)-x_sigma_M*i_s_amp(k,i)*cos(
                epsilon_s1_PsiS1_est_Mv(k,i))-(x_sigma_M-x_ssigma_M)*
                i_s_amp(k,i)*cos(epsilon_s2_PsiS1_est_Mv(k,i)));
184
185         theta_est_Mv(k,i) = xi_s1_s1_est_Mv(k,i) - xi_s1_R_est_Mv
                (k,i);
186         Psi_R_est_Mv(k,i) = abs(Psi_s1_est_Mv(k,i)*cos(
                xi_s1_R_est_Mv(k,i)))- abs(x_sigma_M*i_s1(k,i)*cos(
                epsilon_s1_s1(k,i)-theta_est_Mv(k,i)))-abs((x_sigma_M-
                x_ssigma_M)*i_s2(k,i)*cos(epsilon_s1_s1(k,i)-
                theta_est_Mv(k,i)));
187
188         f_slip_est_Mv(k,i) = r_R_M*(imag(i_s1(k,i))+imag(i_s2(k,i
                )))/Psi_R_est_Mv(k,i);
189
190         t_e_est_Mv(k,i) = Psi_R_est_Mv(k,i)*2*abs(i_s1(k,i))*sin(
                epsilon_s1_s1(k,i)-theta_est_Mv(k,i));
191
192
193         i = i + 1;
194         end
195
196         k = 1 + k;
197
198 end
199
200 %% ESTIMATING USING THE CURRENT MODEL
201
```

```
202 for k=1:l
203     for i=1:m
204         epsilon_s1_R_est(k,i) = atan2(x_H_M*r_R*i_sq1(k,i),
                r_R_M*x_H*i_sd1(k,i));
205         theta_est_Mc(k,i) = epsilon_s1_s1(k,i)-
                epsilon_s1_R_est(k,i);
206
207         Psi_R_est_Mc(k,i) =2*x_H_M*abs(i_s1(k,i))*cos(
                epsilon_s1_R_est(k,i));
208
209         Psi_sd1_est_Mc(k,i) = x_sigma_M*abs(i_s1(k,i))*cos(
                epsilon_s1_R_est(k,i))+(x_sigma_M-x_ssigma_M)*abs(
                i_s1(k,i))*cos(epsilon_s1_R_est(k,i))+Psi_R_est_Mc
                (k,i);
210         Psi_sq1_est_Mc(k,i) = x_sigma_M*abs(i_s1(k,i))*sin(
                epsilon_s1_R_est(k,i))+(x_sigma_M-x_ssigma_M)*abs(
                i_s1(k,i))*sin(epsilon_s1_R_est(k,i));
211         Psi_s1_est_Mc(k,i) = Psi_sd1_est_Mc(k,i) + 1j*
                Psi_sq1_est_Mc(k,i);
212         Psi_s1_amp_est_Mc(k,i) = abs(Psi_s1_est_Mc(k,i));
213         xi_s1_s1_est_Mc(k,i) = angle(Psi_s1_est_Mc(k,i))+
                theta_est_Mc(k,i);
214
215         t_e_est_Mc(k,i) = Psi_R_est_Mc(k,i)*abs(i_s1(k,i))*
                sin(epsilon_s1_R_est(k,i))*2;
216
217         i = i + 1;
218     end
219     k = k +1;
220 end
221
222
223 %% FINDING ERROR MATRIX FOR VOLTAGE MODEL %%%%%
224
225 for k=1:l
226
227     for i=1:m
228
229         Psi_s1_amp_error_Mv(k,i) = Psi_s1_amp_est_Mv(k,i) -
                Psi_s1_amp(k,i);
```

```
230             if abs(Psi_s1_amp_error_Mv(k,i)) < 0.0001
231                 Psi_s1_amp_error_Mv(k,i) = 0;
232             end
233             xi_s1_s1_error_Mv(k,i) = (xi_s1_s1_est_Mv(k,i) -
                    xi_s1_s1(k,i))/pi*180;
234             if abs(xi_s1_s1_error_Mv(k,i)) < 0.0001
235                 xi_s1_s1_error_Mv(k,i) = 0;
236             end
237             Psi_R_est_error_Mv(k,i) = (Psi_R_est_Mv(k,i)-Psi_R(k,
                    i));
238             if abs(Psi_R_est_error_Mv(k,i)) < 0.0001
239                 Psi_R_est_error_Mv(k,i) = 0;
240             end
241             theta_error_Mv(k,i) = (theta_est_Mv(k,i)-theta(k,i))/
                    pi*180;
242             if abs(theta_error_Mv(k,i)) < 0.0001
243                 theta_error_Mv(k,i) = 0;
244             end
245             t_e_est_error_Mv(k,i) = t_e_est_Mv(k,i)-t_e(1,i);
246             if abs(t_e_est_error_Mv(k,i)) < 0.0001
247                 t_e_est_error_Mv(k,i) = 0;
248             end
249             if abs(n(k,1)) > 1 && abs(t_e(1,i)) > abs(1/n(k,1))
250                 Psi_s1_amp_error_Mv(k,i) = 0/0;
251                 xi_s1_s1_error_Mv(k,i) = 0/0;
252                 Psi_R_est_error_Mv(k,i) = 0/0;
253                 theta_error_Mv(k,i) = 0/0;
254                 t_e_est_error_Mv(k,i) = 0/0;
255             end
256
257         i = i + 1;
258         end
259         k = k + 1;
260 end
261
262 %% FINDING ERROR MATRIX FOR CURRENT MODEL %%%%%
263
264 for k=1:l
265
266         for i=1:m
```

```
267
268         theta_error_Mc(k,i) = (theta_est_Mc(k,i)-theta(k,i))/
                pi*180;
269         Psi_s1_amp_error_Mc(k,i) = Psi_s1_amp_est_Mc(k,i) -
                Psi_s1_amp(k,i);
270         if abs(Psi_s1_amp_error_Mc(k,i)) < 0.0001
271             Psi_s1_amp_error_Mc(k,i) = 0;
272         end
273         xi_s1_s1_error_Mc(k,i) = (xi_s1_s1_est_Mc(k,i) -
                xi_s1_s1(k,i))/pi*180;
274         if abs(xi_s1_s1_error_Mc(k,i)) < 0.0001
275             xi_s1_s1_error_Mc(k,i) = 0;
276         end
277         Psi_R_est_error_Mc(k,i) = (Psi_R_est_Mc(k,i)-Psi_R(k,
                i));
278         if abs(Psi_R_est_error_Mc(k,i)) < 0.0001
279             Psi_R_est_error_Mc(k,i) = 0;
280         end
281         theta_error_Mc(k,i) = (theta_est_Mc(k,i)-theta(k,i))/
                pi*180;
282         if abs(theta_error_Mc(k,i)) < 0.0001
283             theta_error_Mc(k,i) = 0;
284         end
285         t_e_est_error_Mc(k,i) = t_e_est_Mc(k,i)-t_e(1,i);
286         if abs(t_e_est_error_Mc(k,i)) < 0.0001
287             t_e_est_error_Mc(k,i) = 0;
288         end
289
290         Psi_s1_amp_error_Mc(k,i) = Psi_s1_amp_est_Mc(k,i) -
                Psi_s1_amp(k,i);
291         if abs(Psi_s1_amp_error_Mc(k,i)) < 0.0001
292             Psi_s1_amp_error_Mv(k,i) = 0;
293         end
294         if abs(n(k,1)) > 1 && abs(t_e(1,i)) > abs(1/n(k,1))
295             Psi_s1_amp_error_Mc(k,i) = 0/0;
296             xi_s1_s1_error_Mc(k,i) = 0/0;
297             Psi_R_est_error_Mc(k,i) = 0/0;
298             theta_error_Mc(k,i) = 0/0;
299             t_e_est_error_Mc(k,i) = 0/0;
300         end
```

```
301         i = i + 1;
302         end
303         k = k + 1;
304 end
305
306
307 %% Plot the matrixes
308
309 X = t_e;
310 lX = length (X)
311 Y = n;
312 lY = length(Y)
313 Z = Psi_s1_amp_error_Mv;
314 lZ = length(Z)
315
316 figure(1)
317
318 [XI YI ZI] = griddata(X,Y,Z,linspace(-2,2),linspace(-2,2)');
319
320 subplot(1,2,1);
321 surf(XI,YI,ZI);
322 xlabel('m_e [pu]');
323 ylabel('n [pu]');
324 z = zlabel('$\hat{\psi}_{s1}^{s1}$ error [pu]');
325 set(z,'Interpreter','latex');
326 set(z,'Fontsize',18);
327
328 Z = xi_s1_s1_error_Mv;
329
330 [XI YI ZI] = griddata(X,Y,Z,linspace(-2,2),linspace(-2,2)');
331 subplot(1,2,2);
332 surf(XI,YI,ZI);
333
334 xlabel('m_e [pu]');
335 ylabel('n [pu]');
336 z = zlabel('$\hat{\xi}_{s1}^{s1}$ error [deg]');
337 set(z,'Interpreter','latex');
338 set(z,'Fontsize',18);
339
340
```

```
341 figure(2)
342
343 Z = Psi_R_est_error_Mv;
344
345 [XI YI ZI] = griddata(X,Y,Z,linspace(-2,2),linspace(-2,2)');
346 subplot(1,2,1);
347 surf(XI,YI,ZI);
348
349 xlabel('m_e [pu]');
350 ylabel('n [pu]');
351 z = zlabel('$\hat{\psi}_R$ error [pu]');
352 set(z,'Interpreter','latex');
353 set(z,'Fontsize',18);
354
355 Z  = theta_error_Mv;
356
357 [XI YI ZI] = griddata(X,Y,Z,linspace(-2,2),linspace(-2,2)');
358 subplot(1,2,2);
359 surf(XI,YI,ZI);
360
361 xlabel('m_e [pu]');
362 ylabel('n [pu]');
363 z = zlabel('$\hat{\theta}_R^{s1}$ error [deg]');
364 set(z,'Interpreter','latex');
365 set(z,'Fontsize',18);
366
367
368 %figure(9)
369 figure(3)
370 Z = t_e_est_error_Mc;
371
372 [XI YI ZI] = griddata(X,Y,Z,linspace(-2,2),linspace(-2,2)');
373 surf(XI,YI,ZI);
374
375 xlabel('m_e [pu]');
376 ylabel('n [pu]');
377 z = zlabel('$\hat{m}_e$ error [pu]');
378 set(z,'Interpreter','latex');
379 set(z,'Fontsize',18)
380 tit = title('$\hat{x}_H=1.2x_H$');
```

```
381 set(tit,'Interpreter','latex');
382 set(tit,'Fontsize',15);
383
384 figure(4)
385
386 Z = Psi_s1_amp_error_Mc;
387
388 [XI YI ZI] = griddata(X,Y,Z,linspace(-2,2),linspace(-2,2)');
389 subplot(1,2,1);
390 surf(XI,YI,ZI);
391
392 xlabel('m_e [pu]');
393 ylabel('n [pu]');
394 z = zlabel('$\hat{\psi}_{s1}$ error [pu]');
395 set(z,'Interpreter','latex');
396 set(z,'Fontsize',18);
397
398 Z = xi_s1_s1_error_Mc;
399
400 [XI YI ZI] = griddata(X,Y,Z,linspace(-2,2),linspace(-2,2)');
401 subplot(1,2,2);
402 surf(XI,YI,ZI);
403
404 xlabel('m_e [pu]');
405 ylabel('n [pu]');
406 z = zlabel('$\hat{\xi}_{s1}^{s1}$ error [deg]');
407 set(z,'Interpreter','latex');
408 set(z,'Fontsize',18);
```